2016

THE DESIGN AND SYNTHESIS OF SMALL MOLECULE DRUGS TO INHIBIT EPIGENETIC ALTERATIONS CAUSED BY DNA METHYLTRANSFERASE 1

Patrick Anthony Barney
The University of Montana

THE DESIGN AND SYNTHESIS OF SMALL MOLECULE DRUGS TO INHIBIT EPIGENETIC

ALTERATIONS CAUSED BY DNA METHYLTRANSFERASE 1

By

PATRICK ANTHONY BARNEY

B.S. Chemistry, Truman State University, Kirksville, MO, 2011

Dissertation

Presented in partial fulfillment of the requirements
for the degree of

Doctor of Philosophy
in Organic Chemistry

The University of Montana
Missoula, MT

July 2016

Approved by:

Scott Whittenburg, Dean of the Graduate School
Graduate School

Dr. Nigel Priestley, Committee Chair
Department of Chemistry

Dr. Orion Berryman, Committee Member
Department of Chemistry

Dr. Kent Sugden, Committee Member
Department of Chemistry

Dr. Christopher Palmer, Committee Member
Department of Chemistry

Dr. Stephen Lodmell, Committee Member
Division of Biological Sciences

Barney, Patrick, PhD, July 2016   Organic Chemistry

The design and synthesis of small molecule drugs to inhibit epigenetic alterations caused by DNA methyltransferase 1

Chairperson: Dr. Nigel Priestley, Department of Chemistry

The acquisition of genomic alterations is a defining feature of human cancers. Many cancer chemotherapies rely upon an apoptotic pathway to eradicate cells containing those alterations. One such alteration is the epigenetic methylation of cytosine in DNA, which occurs at CpG sites in dense clusters of CpG dinucleotide repeats within the gene promoter region. The maintenance of appropriate methylation levels of DNA is necessary during normal DNA replication. Disruption of correct and appropriate methylation patterns leads to DNA associated with transcriptional silencing. Cytosine methylation is catalyzed by DNA methyltransferase enzymes (DNMTs), which transfer a methyl group from S-adenosylmethionine to the 5-position of cytosine to yield 5-methylcytosine. While there are four main classes of DNMTs, DNMT1 is the most abundant methylase responsible for maintaining gene expression patterns following cell division. Therapeutics that can inhibit DNMT1 can reactivate genes silenced by hypermethylation, therefore, the design and development of novel DNMT1 inhibitors is a worthy goal, especially since the silenced genes remain intact and functional. This dissertation outlines a systematic approach taken to the successful design and testing of isoindolinone-based DNMT1 inhibitors. Three synthetic routes were employed to create the inhibitors, the routes include an Ugi-IMDAF reaction, a multiple step scheme using homothallic acid as a starting point, and utilizing convertible isocyanides. The best compound synthesized and tested was **78**, which has a % DNMT1 activity of 7.31 ± 0.98 and a calculated K_i' value of 18 ± 3 μM.

ACKNOWLEDGEMENTS

TABLE OF CONTENTS

LIST OF FIGURES

LIST OF TABLES

LIST OF ABBREVIATIONS

^{13}C NMR	carbon nuclear magnetic resonance spectrum
^{1}H NMR	proton nuclear magnetic resonance spectrum
^{3}H	tritium
bs	broad singlet
BSA	bovine serum albumin
BP1	buffer preparation 1
calcd.	calculated
Ci	curie
CDI	1,1'-carbonyldiimidazole
d	doublet
DCC	*N,N'*-dicyclohexylcarbodiimide
DCM	dichloromethane
dd	doublet of doublets
ddd	doublet of doublets of doublets
DI H$_2$O	deionized water
DMAP	4-dimethylaminopyridine
DNMT1	DNA methyltransferase 1
DNA	deoxyribonucleic acid
dpm	disintegrations per minute
dt	doublet of triplets
eq	equivalent
GC/MS	gas chromatography/mass spectroscopy
IC$_{50}$	drug concentration which inhibits activity (or growth) by 50 percent
kg	kilogram(s)
mg	milligram(s)
mL	milliliter(s)
mmol	millimolar
n-BuLi	*n*-butyllithium
poly dI-dC	poly(deoxyinosinic-deoxycytidylic) acid sodium salt
SAH	*S*-adenosyl homocysteine
SAM	*S*-adenosyl methionine
Sat.	saturated
sex	sextet
td	Triplet of doublets
TEA	triethylamine
tris	tris(hydroxymethyl)aminomethane
μg	microgram(s)
μM	micromolar

Chapter 1 THE USE OF SMALL MOLECULE DRUGS TO INHIBIT EPIGENETIC ALTERATIONS OF DNA.

1.1 Epigenetics

The term epigenetics was initially conceived to describe the causal mechanisms that bring about different phenotypes in fruit flies.[1] Today, this classification is expanding to include a variety of biological processes that includes heritable changes in gene expression that occur independent of alterations of DNA bases. The recent publications by Holliday, Jablonka *et al.* describe the mechanism by which epigenetic modifications occur including chromatin remodeling, DNA methylation, RNA transcription, microRNA synthesis, and prion formation.[2,3] The modulation of epigenetic modification involving DNA methylation is the major focus of this dissertation.

1.2 Chromatin and DNA Methylation

The major function of chromatin is to tightly package eukaryotic DNA into a small enough bundle to fit within the confines of the nucleus.[4] The dense packaging is vital to preserve an entire genome within one cell; however, this compactness can also be an obstacle. If the DNA is packaged too tightly, it is not readily accessible and vital functions including transcription, replication, repair, and recombination are no longer feasible. Consequently, there must be a balance between genome packaging and genome accessibility. This concept is the basis for either enabling transcription factors to bind to a targeted DNA sequence, or altogether preventing access to that particular sequence. In this way, epigenetic information is regulated by chromatin packaging and chromatin modifications that involve histones and DNA.

Histones and nonhistone proteins are the major structural units of chromatin. Histones are abundant within the cell and five distinct histones are recognized as structurally vital to

chromatin composition: H1, H2A, H2B, H3, and H4.[5] All five are positively charged, arginine or lysine rich proteins that interact via ionic bonds with the negatively charged phosphate backbone of DNA. Two copies of each histone protein H2A, H2B, H3, and H4 assemble to form octameric core structures, and the DNA helix winds itself about these core octamers, creating nucleosomes. Luger *et al.* deduced the structure of this DNA wrapped histone core (Figure 1.1 and **Figure 1.2**).[5] The core octamer of each histone has landmarks that guide 147 base pairs of DNA in a left-handed superhelical conformation that makes 1.6 turns about the core. The fifth histone protein, H1, is a linker protein that binds nucleosomes together resulting in 29-43 base pairs of DNA between each nucleosome.
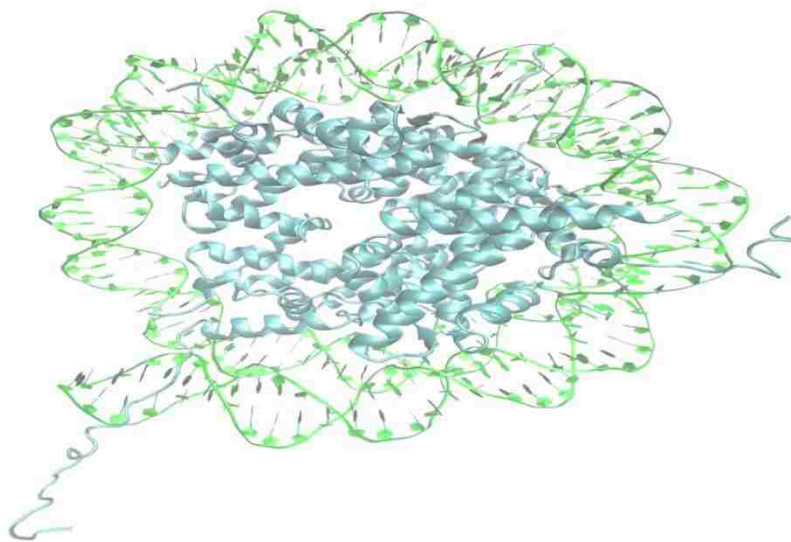
Figure 1.1. Head-on view of DNA wrapped around a histone core. Image adapted from work by Luger *et al.*[5]
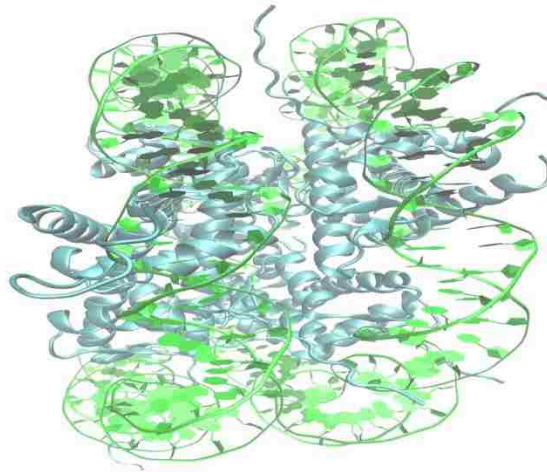
Figure 1.2. Side view of DNA wrapped around a histone core. Image adapted from work by Luger *et al*.[5]

DNA is often targeted for epigenetic modifications, which includes methylation.[6,7] This DNA methylation is an epigenetic marker that occurs at the 5-position of cytosine in a CpG dinucleotide (Figure 1.3).[8] DNA methylation is associated with transcriptional silencing of genes linked in pathogenesis of many diseases including cancer.[9-11] Methylation is catalyzed by DNA methyltransferases (DNMTs) and the majority of CpG dinucleotides are located in CpG islands, which occupy about 50% - 60% of gene promoters.[12,13]
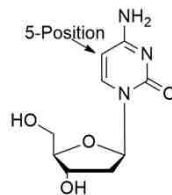
Figure 1.3. The Cytosine 5-position is the site where DNA methylation occurs.

DNA methylation is vital for regulating embryonic development and is required for chromosomal stability.[14] When the promotor regions are subjected to methylation, the corresponding gene is repressed, because they are not recognized by transcription factors.[15] A failure to maintain the epigenetic markers and DNA methylation patterns is associated with under and over expression of certain proteins, which can lead to cancer.[16] As a whole, the epigenetic modifications have been associated with virtually all types of cancer.[17-23] Unlike genetic mutations, epigenetic modifications are reversible and the DNA sequence never changed.[24,25] For these reasons, DNA methylation is an exciting target for therapeutics.

1.3   DNA methyltransferases (DNMTs)

DNMTs are divided into two classes based on their preferred substrate and function (Figure 1.4).[26,27] In *Homo sapiens*, DNMTs share common features, specifically a regulating N-terminal domain and a catalytic C-terminal domain.[28] There are ten sequence motifs in the catalytic domain (I to X) that act as binding sites for the substrate *S*-adenosyl-L-methionine (SAM) (Figure 1.4).[29] The *N*-terminal region of DNMTs binds DNA and has protein recognition domains to guide the DNMTs to the nucleus and chromatin , thus creating a link between

chromatin and DNA methylation.[28]
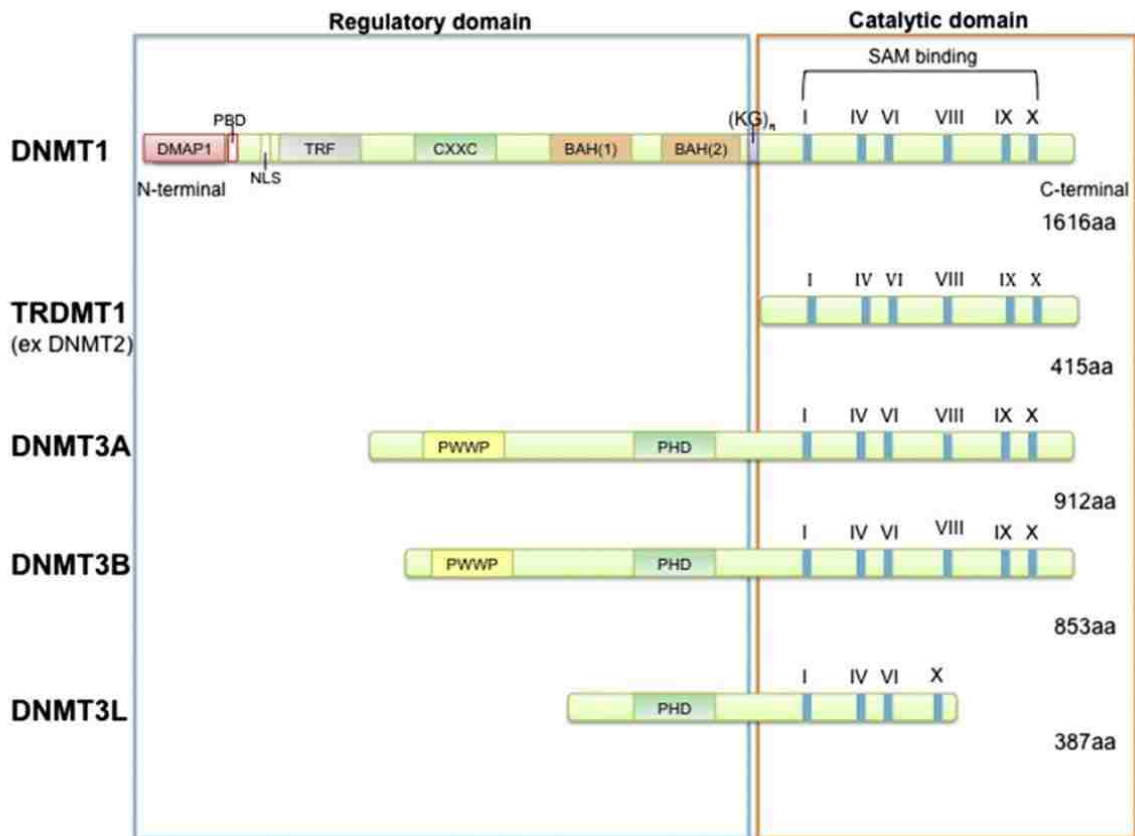
Figure 1.4. Schematic representations of the human DNMT1, TRDMT1, and DNMT3s.[29]

DNMT1 is the most abundant of the DNMTs, and has a higher affinity for hemimethylated DNA than unmethylated DNA compared to other DNA methyltransferases.[30-32] DNMT1 typically intercedes after DNA replication to methylate the newly formed strand and achieves methylation via two mechanisms: (i) through direct interaction with the replication fork and (ii) as a partner of ubiquitin with PHD and ring finger domains 1 (UHRF1), which recognizes and binds hemimethylated DNA and recruits DNMT1 to help propagate DNA methylation patterns (Figure 1.5).[33,34] DNMT1's main function is to copy patterns of CG

methylation onto the newly synthesized DNA strand.[35-37] The cytosine to be methylated is flipped out into the catalytic pocket and the methyl group of SAM is transferred to the 5-position (Figure 1.6).[28] After the CpG is fully methylated, DNMT1 moves along the newly synthesized DNA strand and methylates where needed.
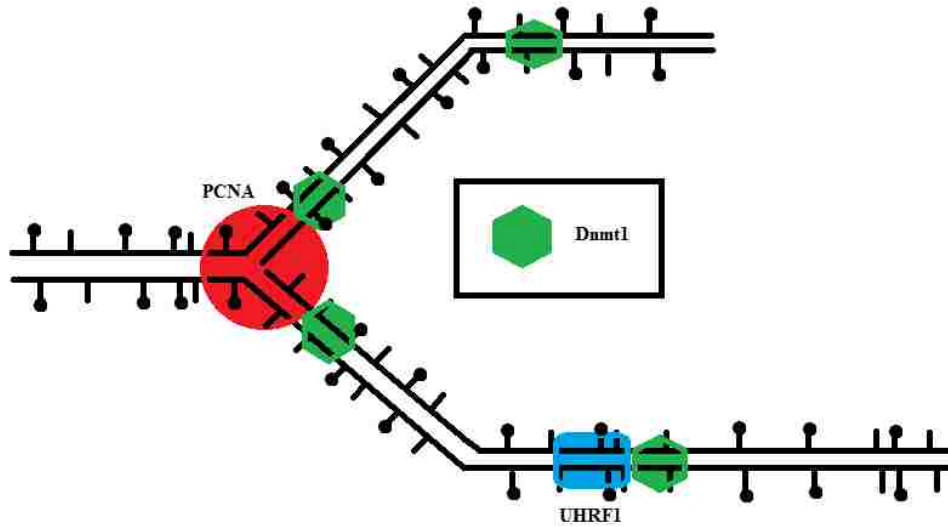
Figure 1.5. DNMT1 interacting with the replication fork of DNA synthesis.

Figure 1.6. Schematic representation of the catalytic site of the DNMTs showing the targeted cytidine (blue), the SAM substrate (red), and catalytic thiolate (green).

The general mechanism of DNA methylation is uniform for all methylating enzymes; the enzymes catalyze the transfer of a methyl group from SAM to the targeted cytosine.[38] The 5-position of the cytosine is poorly reactive, and prevents direct methylation, for this reason, DNMTs undergo a covalent catalytic reaction (Figure 1.7).[39] The targeted cytosine enters the catalytic site, the thiolate of the cysteine performs a nucleophilic attack on the 6-position of the cytosine. This reaction leads to the formation of an enamine. A nucleophilic attack of the enamine on the SAM is followed by deprotonation of the C5 by a base, releasing a molecule of S-adenosyl-L-homocysteine (SAH). The new methyl group causes a steric hindrance in favor of a

8

β-elimination allowing the enzyme to be reused. The newly methylated DNA strand is then

released from the catalytic pocket along with SAH. [40]
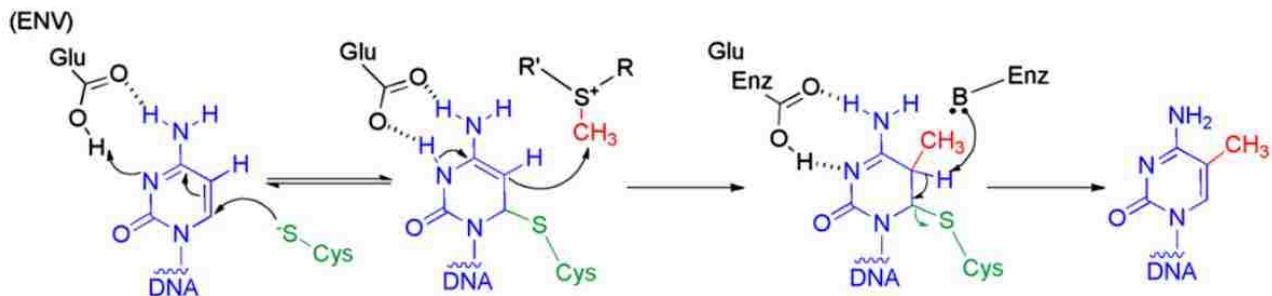
Figure 1.7. Catalytic mechanism of C5-DNA methylation showing the targeted cytidine (blue), the methyl group (red), and the catalytic thiolate (green).

The preservation of DNA methylation patterns is not always correct and possesses an

error frequency of around 5% per CpG, allowing cells some flexibility for changing methylation

patterns.[41] DNMT3a and DNMT3b are frequently utilized to assist DNMT1 in the maintenance

of methylation profiles during replication.[42] Both DNMT3a and DNMT3b are present in smaller

quantities in human cells, and bind to both unmethylated and hemimethylated CpG sites.[43] The

roles of these two enzymes are *de novo* methylation. DNMT3L is a cofactor for DNMT3a, as

DNMT3L possesses no catalytic motif.[44]

Aberrant DNA methylation patterns are extensively observed in numerous cancers

(Figure 1.8).[45,46] Hypermethylation of gene promoter regions silences those particular segments

of DNA, causing that strand to be completely unrecognizable by RNA polymerase II. The ability

to reverse DNA methylation offers interesting opportunities in the realm of treatment options.

By creating targeted inhibitors of DNMT (DNMTi), there is significant potential to allow the

9

transcription factors to work unhindered, inducing the reprogramming of cancerous cells within the body.[47]
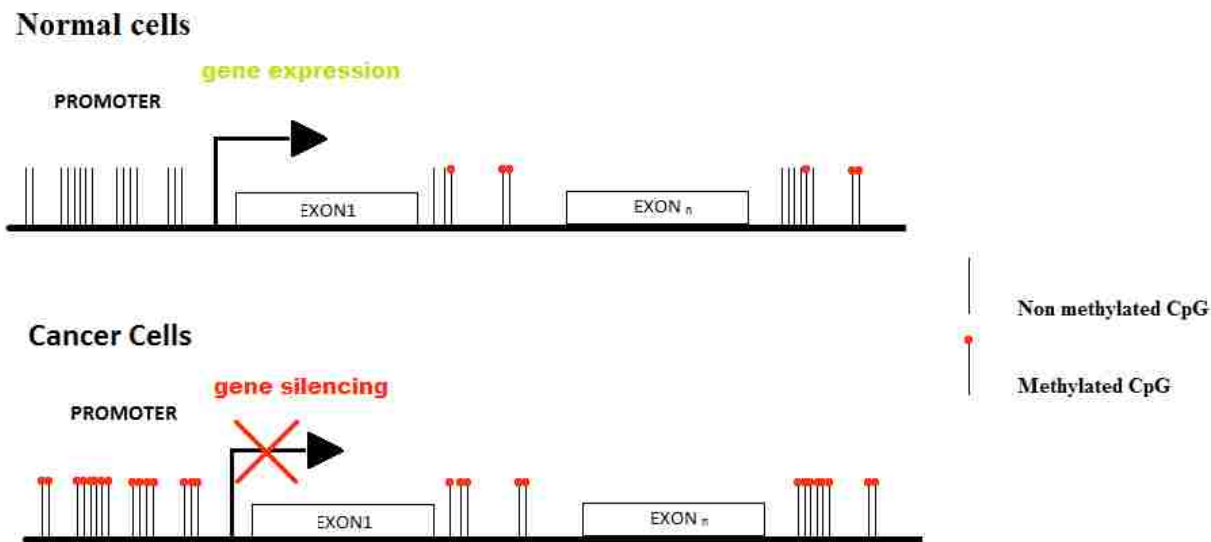
Figure 1.8. Representation of methylation patterns found in normal and cancerous cells.

1.4 DNMT inhibitors

Given the importance of DNMT1 in various diseases including cancer, a number of inhibitors were designed and are continually being optimized to exploit the mechanism of methylation within the conserved residues of the catalytic pocket of DNMT1. Two classes of inhibitors will be discussed further: nucleoside-like inhibitors and non-nucleoside inhibitors.

Nucleoside-like inhibitors are cytosine analogs that cannot inhibit DNMT1 directly, but instead become incorporated into the DNA (Figure 1.9).[48] Once in the DNA, the cytosine analogs are recognized by the DNMTs and undergo similar reactions as normal cytosines, specifically a covalent intermediate forms between the catalytic cysteine of the enzyme and the 6-postion of

the cytosine analogs. From this juncture the reaction deviates from real cytosine interactions, since the β-elimination reaction cannot occur due to the presence of a nitrogen atom in the 5-position of the analogs.[49] As a result, a covalent irreversible complex, known as a "suicide inhibitor" remains. The disadvantage of using these types of inhibitors is that most need to be chemically modified within the body to be incorporated in to DNA.

5-Azacytidine, **4**, was described more than 50 years ago, but its demethylation activity was discovered in 1980 as the result of its ability to influence cellular differentiation.[50,51] 5-Azacytidine is an antitumor agent for the treatment of myelodysplastic syndrome.[52] 5-Azacytidine is a ribose nucleoside and thus needs to be modified to a deoxyribonucleotide to be incorporated into DNA. However, before all 5-azacytidine is converted, a small portion of it is incorporated into RNA, which affects a variety of RNA functions including ribosome biogenesis.[53] 5-Aza-2'-deoxycytidine (Decitabine, **5**), is a deoxyribose analogue that does not need to be modified and can be more directly incorporated into DNA. Therefore, Decitabine shows greater inhibition of DNA methylation and antitumor activity in experimental models.[54] Decitabine has activity in myeloid malignancies including myelodysplastic syndrome, acute myelogenous leukemia, and chronic myelogenous leukemia. [55,56] However, decitabine has substantial toxic effects, in particular myelosuppression.[57]   A study performed by Cheng *et al.* showed that orally administered 2-Pyrimidone-1-β-D-riboside (Zebularine, **6**) caused detectable demethylation and inhibits tumor growth in mice. [58,59]

The use of nucleoside-like drugs is associated with increased incidence of bone marrow suppression, including neutropenia and thrombocytopenia.[25,60-62] Because nucleoside-like

inhibitors are inherently cytotoxic, interest has been on the rise to find non-nucleoside inhibitors, whose mechanism does not include incorporation into DNA. Non-nucleoside inhibitors interact with DNMTs directly, and can be reversible. The reversibility feature lowers the toxic effects associated with nucleoside-like inhibitors.[63]

Discovering therapies that selectively inhibit DNMT1, reverse hypermethylated phenotypes, revitalize the normal cell cycle, and reactivate the apoptosis mechanism, are vital research targets. Advancement in therapies is a necessity due to the stubborn nature and poor prognosis of cancer caused by hypermethylation and epigenetic silencing of tumor suppressor genes.[64] Synthesizing small molecule drugs that both target and modify epigenetic responses in cancer cells have significant advantages over classical chemotherapy as the target genes remain intact and are simply silenced due to an epigenetic modification.[65]
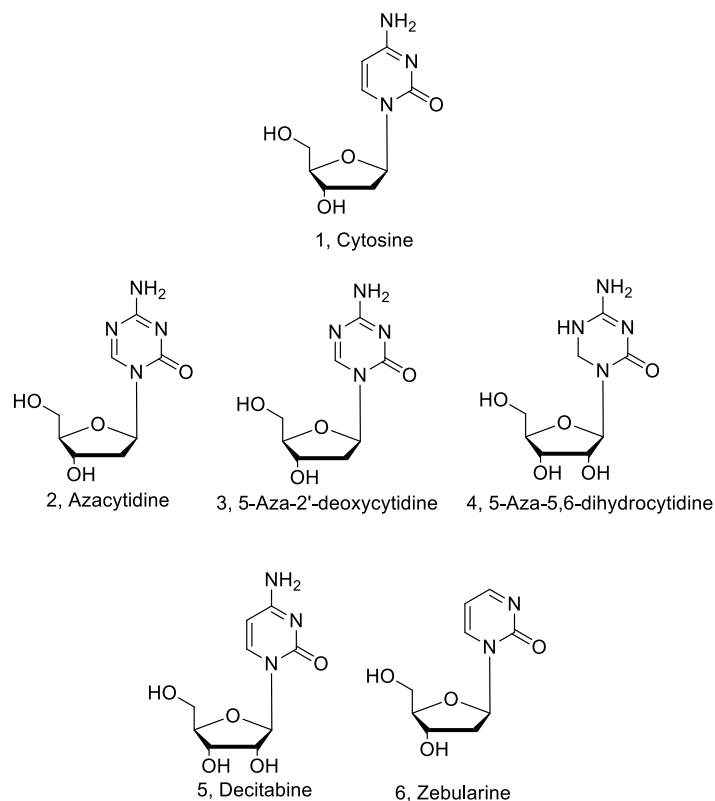
Figure 1.9. Nucleoside-like inhibitors of DNMTs. This type of inhibitor creates an irreversible complex with DNA.

At present, several drugs have made it through clinical trials and are permitted for human use.[52] Unfortunately, most of the active compounds currently in use are nucleoside-like inhibitors that incorporate into the DNA and covalently bind DNMT1, thereby lowering the active concentration of DNMT1 in the cell. Reducing the availability of DNMT consequently lowers gene methylation, reactivates tumor suppressor genes, and returns normal apoptotic responses.[62,66] These inhibitors are non-specific, thus affecting healthy cells as well. The high levels of toxicity and short half-lives of these drugs have seriously hindered their utility.[67]

Non-nucleoside inhibitors have been investigated in an attempt to overcome the problems with cytosine analogs (Figure 1.10). These studies highlight a number of approaches to identify new lead compounds.[68-73] Epigallocatechin-3-gallate, **7**, is a natural product isolated from green tea. Epigallocatechin-3-gallate has been shown to inhibit methyltransferase activity in protein extracts and human cancer cell lines.[74] Yoo *et al.* showed that epigallocatechin-3-gallate degrades in the body to form hydrogen peroxide and the oxidation of DNA methyltransferases might contribute to the inhibition of DNA methylation and to its cytotoxicity in human cell lines. [25,75] Psammaplin A, **11**, is a natural products isolated from a marine sponge.[76] Although it has been shown that psammaplin exerts strong cytotoxic effects in human tumor cell lines and limits grow rates, DNMT inhibition was not followed by DNA demethylation and re-expression of tumor suppressor genes. [77] Procainamide, **10**, and hydralazine, **9**, are drugs recently used that are being repurposed in an attempt to generate clinically useful DNMT inhibitors.[77] Hydralazine is currently in phase II trials for breast cancer and phase III trials for cervical and ovarian cancer. The phthalimide protected tryptophan derivative RG108, **8**, was identified in a fragment-based virtual screening campaign and represents a success of rational drug design.[78-80] A major pitfall for these compounds remains the toxicity and lack of potency when tested in animal models.[81,82]
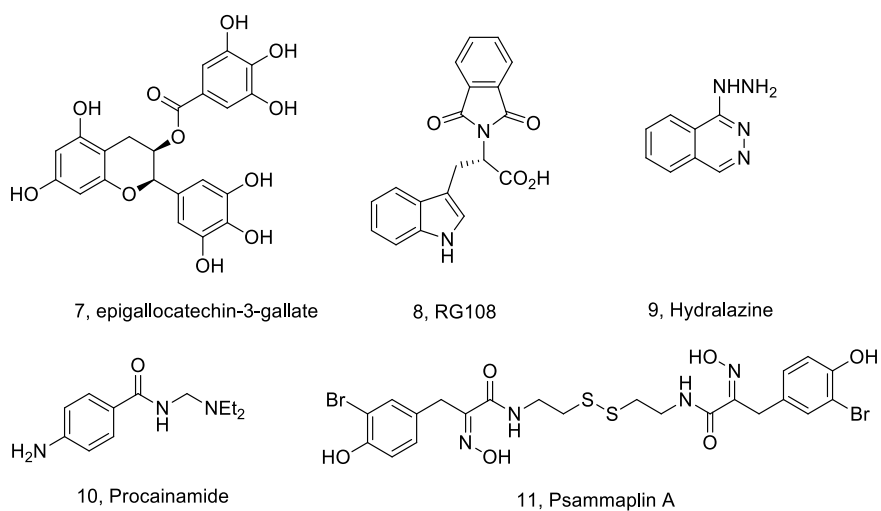
Figure 1.10. Non-nucleoside analogs that are used as inhibitors of epigenetic methylation catalyzed by DNMT1.

In summary, there are several DNMT inhibitors known, but the high levels of toxicity, lack of specificity, and chemical instability hinder the use of them.[81] Therefore, it is of great need to design and synthesize novel drugs that can specifically target DNMTs.

Chapter 2 BIOLOGICAL EVALUATION OF INHIBITORS USING A RADIOACTIVITY-BASED ASSAY

2.1 Introduction

Recent studies have shown DNMT1 as a therapeutic target in diagnosis and treatment of various types of cancer since aberrant DNMT1 activity usually occurs before other signs of malignancy.[83-87] The activity of DNMT1, at a cellular level, has to be screened in order to gain an insight into the regulation of methylation and determine therapeutic strategies.[88-90] Conventional assays used to screen global methylation include enzyme-linked immunosorbent assay (ELISA), fluorescence-based, and radioactivity-based. Even though all three techniques prove to be useful, they are not without limitations. The following sections will give examples and explain each assay.

2.2 Enzyme-linked immunosorbent assays (ELISA)

There are several commercially available kits, all enzyme-linked immunosorbent assay (ELISA) based, that provide a way to assess DNA methylation levels. ELISA procedures are typically uniform for all kits (Figure 2.1). Briefly, the DNA is captured on a ELISA plate, and the methylated DNA is detected through sequential incubation steps of: a primary antibody raised against 5-methylcytosine, a labelled secondary antibody, and a colorimetric/fluorometric detection method.[91] ELISA allows for the evaluation of major changes in global methylation levels, meaning region-specific DNA methylation cannot be analyzed.
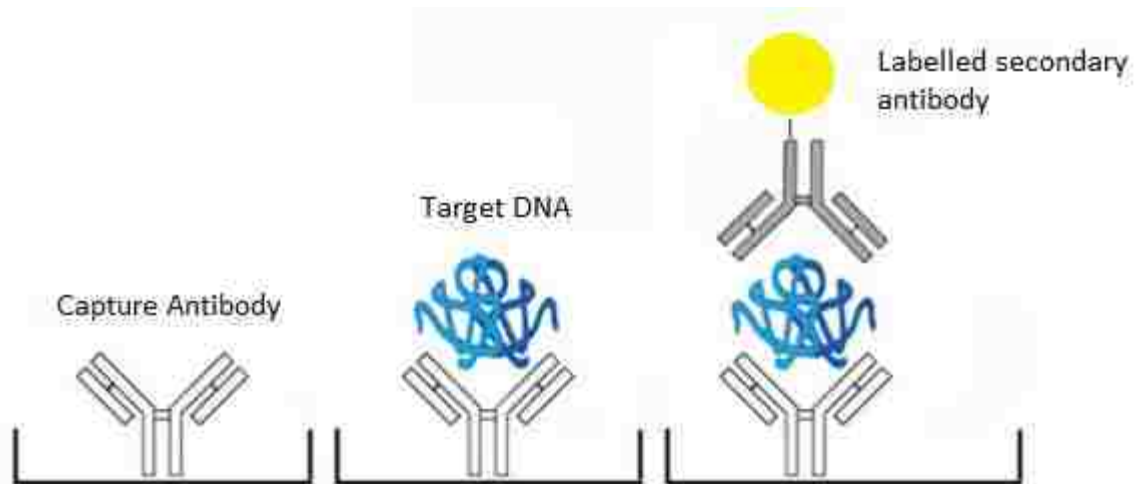
Figure 2.1. Schematic of ELISA procedure.

An example of this type of assay is seen in the work produced by Kremer *et al*. in which they quantify genome-wide DNA methylation patterns.[92] In Kremer's work, DNA was applied to a microtiter plate and incubated overnight. The plate wells were then washed twice with 200 µL of TBS followed by anti-5-methylcytosine mouse antibody and incubated for 1 h. The plate was then washed and incubated with a conjugated goat anti-mouse polyclonal antibody for 1 h. After three more washing steps, substrate reagent was added and incubated for 20 minutes and the reaction stopped by the addition of H_2SO_4. The finished assay plate was then loaded onto a plate reader and the absorption read at 450 nm.

A second example of implementing this assay type is seen in the work of Karaca *et al*.[93] Total DNMT activity was measured using an EpiQuik DNA Methyltransferase activity assay. Karaca added 3 µL of isolated DNA extract to each well of an ELISA plate. The plate was washed and incubated with primary and secondary antibodies followed by a developing solution. The finished assay plate was then loaded onto a plate reader and absorption read at 450 nm.

It is easy to see that this assay type requires great attention to detail. There is a large number of time-consuming steps making this assay slow. In addition, attention needs to be given to the amount of freeze thaw cycles the cells undergo because it has been shown over periods of time that significant variability of signal arises.[94,95] Overall, this assay was not chosen to assess the DNMT1 activity with our inhibitors because of the time consuming procedures.

2.3   Fluorescence-based assays

2.3.1   Direct florescent-based assay

In this assay a fluorophore and quencher are attached to either single-stranded DNA or double-stranded DNA which organize into hairpin probes.[96] Typically, the fluorophores get energy from light and when the quenchers are in close proximity, the quenchers absorb the energy and emit as heat, thus preventing the fluorophores from fluorescing.[97] The basic form of this assay type is shown in detail by Wood *et al* (Figure 2.2).[98]

Wood's assay couples the use of a methylation sensitive restriction endonuclease with the protection of cleavage of a break light oligonucleotide. A break light is a single-stranded oligonucleotide, that forms a hairpin loop consisting of a fluorophore at the 5' terminus and a quencher at the 3' terminus.[99] This structure places the fluorophore and quencher close in space, promoting efficient quenching (Figure 2.2). Once the hairpin probe is methylated by DNMT1, the restriction endonuclease *GlaI* cleaves the probe at the methylated sites, creating single-stranded DNA and a short double-stranded DNA segment. The cleavage causes the

melting of short double-stranded DNA segment and separation of the fluorophore and

quencher resulting in increased fluorescence.
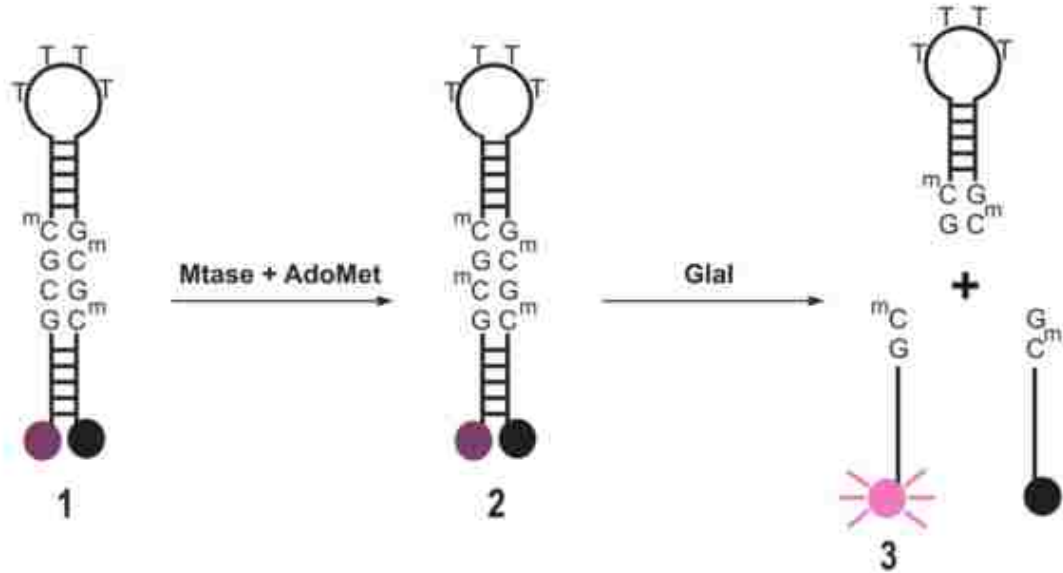
Figure 2.2. Fluorescent-based assay detailed by Wood *et al.*[98] The fluorescence of the hemimethylated oligonucleotide **1** is quenched by a dabcyl group (black dot). DNMT1 methylates the oligonucleotide to yield **2**, which is then cleaved by *GlaI*, separating the fluorophore (pink dot) from the quencher and leading to an increased fluorescence **3**.

When the assay described by *Wood et al.*[98] was investigated as a potential screening

technique for inhibitory drugs, *GlaI* was sensitive to the antitumor drugs concentrations at 100

µM, resulting in the methylated sequence remaining whole. This drawback limits the versatility

of the assay in clinical settings. In addition, GlaI is expensive to use, and large quantities are

needed per assay.

2.3.2 Amplified fluorescent-based assay

Xing *et al.* reported a way of detecting DNA methylation by using substrate hairpin

probes with methylation sequences in the stems and the fluorophore (FAM)/quencher (BHQ)

labelled hairpin, reporting probes (FQ), and utilizing exonuclease III (Exo III). [100] The signal is amplified by Exo III-assisted recycling (Figure 2.3).[101] Figure 2.3Once the DNA has successfully been methylated and cleaved by *Dpn* 1, single-stranded DNA is released. The released DNA strands then hybridize to the 3' terminus of the FQ probe. Exo III then binds to the blunt 3' terminus of FQ and degrades the probe, releasing FAM. The benefit of using Exo III is that it only digests from the 3' terminus of double-stranded DNA with blunt or receding ends.[102] The single-stranded DNA produced from the substrate hairpin probes is unaffected during Exo III treatment. Consequently, the single-stranded DNA is available for the next step of hybridization and digestion, thus creating a recycling mechanism.   Fluorescence from FAM is amplified after several rounds of incubation with Exo III, thus allowing for sensitive detection of DNA methylation activity. The detection sensitivity is much better than direct fluorescent-based assays, and can detect as low as 0.01 U.mL^{-1}.[96,100] The procedure outlined by Xing *et al*. is a labor intensive, multistep fluorescent assay that requires expensive reagents making this technique not ideal for every laboratory.
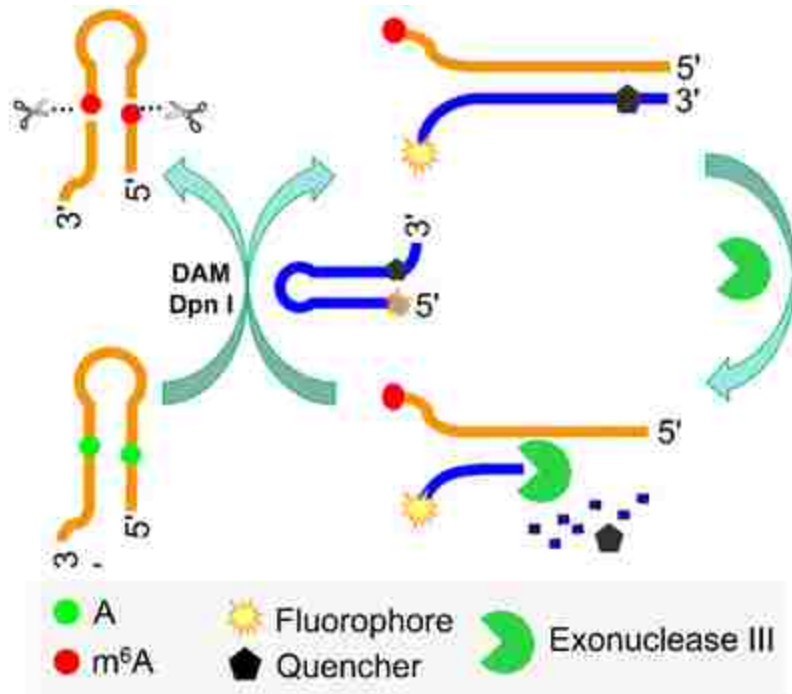
Figure 2.3 Schematic representation of assay for methylation activity based on exonuclease recycling. Adenine (green dot) methylated adenine (red dot).

2.3.3   Conclusion

Fluorescence-based assays involve the absorption of light that excites fluorophores to promote electrons from ground states to excited states. The advantages to fluorescent-based assays are their straightforwardness in the detection process and high sensitivity.[103] The disadvantage of this technique is neither DNA nor methylated DNA is intrinsically fluorescent. The fluorescence-based assays require a fluorescence generation mechanism so that the methylation event can be detected by a fluorimeter. The high cost associated with specific instrumentation and specific antibodies makes this assay type not ideal for every laboratory. Fluorescence-based assays can be broadly classified into direct and amplified assays. Generally, the amplified assay out performs its unamplified counterpart. The downside to the amplified

assay is the high cost and time-consuming procedures. Due to the high cost and time intensive procedures, this assay type was not chosen to assess the DNMT1 activity with our inhibitors.

2.4   Radioactivity-based assays

The aim of this type of assay is to monitor the incorporation of [^{3}H]-methyl groups into DNA. Briefly, DNMT1 transfers from [methyl-^{3}H] SAM the radiolabeled methyl group into the DNA. Any unreacted [methyl-^{3}H] SAM can be separated from the radiolabeled DNA using gel filtration,[104] filter-binding,[105] or thin layer chromatography.[106] The DNA, now with radiolabeled methyl groups can be quantified by liquid scintillation.

An example of this type of assay is seen in the work produced by Gros *et al*. when utilizing a [methyl-^{3}H] SAM along with a scintillation proximity assay (SPA).[107] In SPA, the scintillant is fixed onto microplate,[108] or incorporated into beads.[109] The methylation step of the assay was done in homogeneous phase and incorporated tritiated methyl groups into a biotinylated DNA substrate. The reaction was then transferred and quenched in a streptavidin-coated microplate containing streptavidin-coated beads (Figure 2.4). The problem with this type of radioactivity assay is there are many steps that need to be followed. The large amounts of incubation, and wash steps make this technique time consuming.
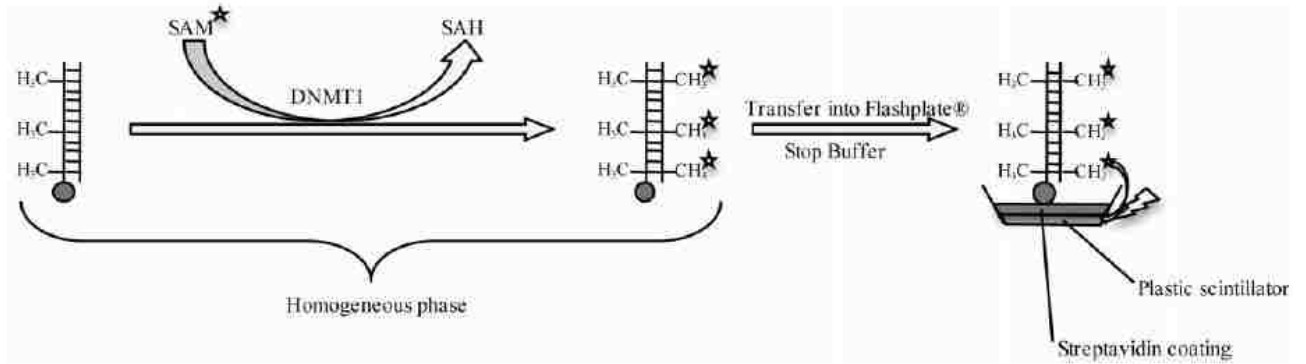
Figure 2.4 DNMT radioactivity-based assay detailed in work by Gros *et al*. Biotin (gray circle), tritium atoms (stars) lightning bolt represents ability for tritium atoms to excite scintillator.

The assay used to analyze the DNMT1 activity in this dissertation utilized a radioactivity-based gel filtration assay (Figure 2.5). Briefly, the radioactive gel filtration assay was performed in triplicate 50 μL total reaction volumes. The reaction was incubated at 37 °C for 1 h, then the unreacted [methyl-^{3}H] SAM and enzyme were separated from the ^{3}H-DNA by passing through a Micro Bio-Spin® P-30 size exclusion column. Both negative and positive controls were also tested in triplicate, utilizing 10 μM *S*-adenosylhomocysteine as a positive control for enzyme inhibition. The negative control contained the DMSO carrier without inhibitor present. The column flow through was transferred to scintillation vials, and 5 mL of Ultima Gold liquid scintillation cocktail was added. After thorough mixing, the samples were read on a Beckman 1500 scintillation counter, with a maximum time limit of counting fixed to 1 h. All counts were reported in disintegrations per minute (dpm).
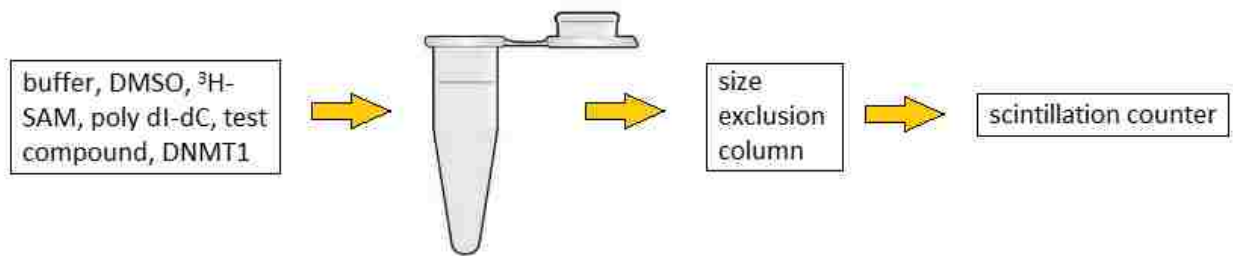
Figure 2.5 Schematic representation of radioactivity-based gel filtration assay.

Radioactivity-based assays have advantages over other types of assays because they are inexpensive to use. The radioactivity-based assays also give complete coverage of CpG sites allowing for global methylation analysis. The radioactivity-based gel filtration assay was chosen to test the DNMT1 inhibitors because of its ease of use, and the limited amount of time needed to complete a test.

2.5   Michaelis-Menten Kinetics

The Michaelis-Menten model is one of the simplest and best-known approaches to enzyme kinetics (Figure 2.6).[110] In the model, substrate (S) binds reversibly to an enzyme (E) for form an enzyme-substrate complex (ES), which then reacts irreversibly to generate a product (P) and regeneration of E.

$$E + S \xrightleftharpoons{K_m} ES \xrightarrow{K_{cat}} E + P$$

Figure 2.6. The interaction between enzyme (E) and substrate (S) and the conversion of the enzyme/substrate (ES) complex enzyme and product (P).

Leonor Michaelis and Maud Menten derived an equation that described the kinetics of

enzyme and substrate interactions (Equation 1). As substrate concentration is increased, a

point is reached when all the available enzyme molecules are involved in enzyme substrate

complexes (ES). Plotting reaction rate (V) versus substrate concentration [s] results in a

Michaelis-Menten plot (Figure 2.7). Enzyme saturation can be seen on the graph as a plateau

and represents the maximum velocity (V_{max}). The point at which the concentration of substrate

is equal to half V_{max} can be used to approximate the affinity (K_m) of an enzyme for that

particular substrate. The size of the K_m indicates some unique properties of the enzyme. A small

K_m indicates that the enzyme only requires a small amount of substrate to become saturated.

This would mean that the maximum velocity would be reached at a low substrate concentration

and that the enzyme had high affinity for the substrate.

$$V = \frac{V_{max} * [S]}{K_m + [S]}$$

Equation 1. Michaelis-Menten equation for enzyme kinetics.
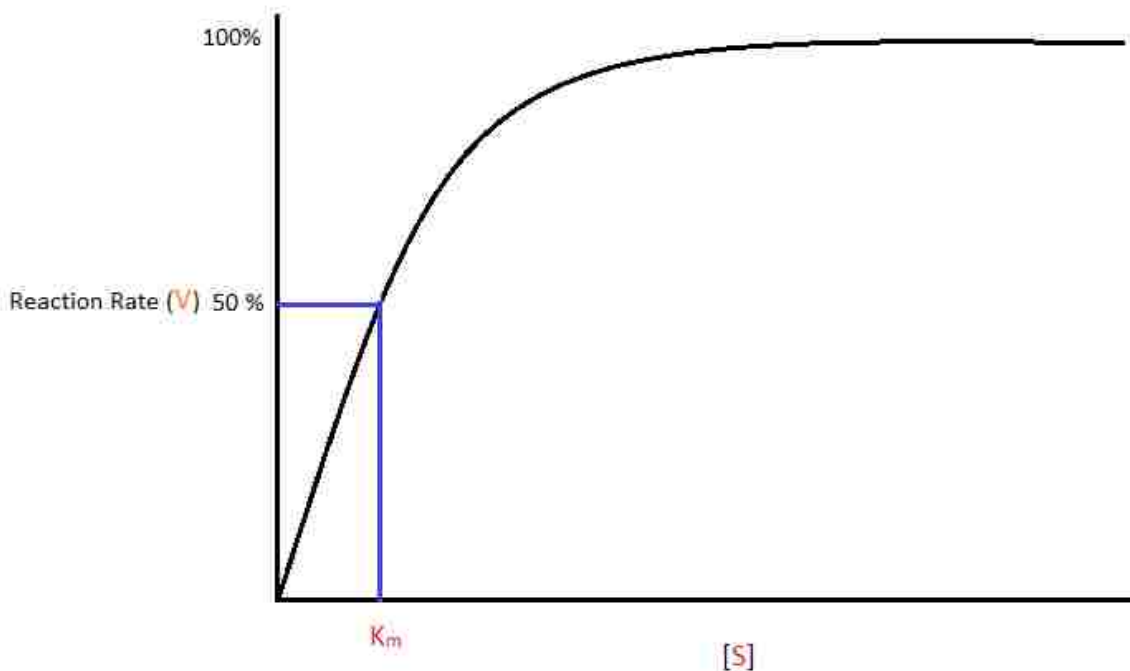
Figure 2.7. Michaelis-Menten plot. V is reaction rate. [S] is substrate concentration.

Enzyme inhibitors interact with enzymes in several different ways to decrease the rate of the reaction. For each inhibition type, a dissociation constant, K_i', can be calculated for the inhibitor that reflects the strength of interaction between the enzyme and the inhibitor. A small K_i' value means the enzyme and inhibitor bind tightly together, while a large K_i' indicates a weak binding between the pair.

In competitive inhibition, the inhibitor competes with the substrate for an active site on the enzyme. The rate of catalysis depends on the concentration of the inhibitor and the substrate.[111] The conventional form of the rate equation to calculate the rate of the reaction with a competitive inhibitor present is shown below where [I] is the inhibitor concentration (Equation 2).

$$V_o = \frac{V_{max}[S]}{K_m \left(1 + \frac{[I]}{K_i}\right) + [S]}$$

Equation 2. Rate equation to calculate the rate of reaction when a competitive inhibitor is present.

In order to normalize assays run on different days and using different isoindolinone

samples a fractional rate V_f is reported. This fractional rate can then be compared to other rates

found on different days.

$$V_f = \frac{rate\ (with\ inhibition)}{rate\ (no\ inhibition)} = \frac{V_{max}\ [S]}{K_M \left(1 + \frac{[I]}{K_i}\right) + [S]} * \frac{K_m + [S]}{V_{max}\ [S]}$$

Equation 3. Fractional rate equation.

Equation 3 can be simplified to equation 4.

$$V_f = \frac{K_m + [S]}{K_m \left(1 + \frac{[I]}{K_i}\right) + [S]}$$

Equation 4. Simplified fractional rate equation.

Equation 4 can be rearranged to give $K_i^{'}$ (equation 5).

$$K_i{'} = \frac{[I]\ V_f K_m}{(1 - V_f)(K_m + [S])}$$

Equation 5. Equation used to calculate binding affinity of inhibitors.

Equation 5 is an important equation, because it tells us how well our novel inhibitors bind to

the target enzyme based on V_f and parameters set in the radioactivity-based assay.

Chapter 3 SYNTHESIS OF DNA METHYLTRANSFERASE 1 INHIBITORS

Computational tools help to elucidate the basic structural requirements of inhibitors for activity against DNMTs. DNMT1 is the most targeted to search for inhibitors as its high enzyme activity is greatest among DNMTs.[112] The increase in the number of available crystallographic DNMTs has brought about the use of computational molecular docking and structure based approaches for searching for DNMT inhibitors.[113-115] Computational screenings of compounds have helped identify many promising leads for DNMT1 inhibitors.[116]

SGI-1027 is one of these promising leads that was synthesized by Datta *et al*.[117] and modeled in DNMT1 by Yoo *et al*. (Figure 3.1).[118] For the docking study, the crystal structure of DNMT1 with sinefungin bound (PDB id: 3SWR) was prepared to be docked by adding hydrogen atoms and removing water molecules within 5 Å of the crystalized sinefungin. The chemical structure of SGI-1027 was built using Maestro 9.2. The crystalized sinefungin was removed before the docking of the ligands began. The results of the study show that SGI-1027 occupies the binding site at the same location of the known inhibitor SAH (Figure 3.1). The same approach to docking studies was used for the work presented in this dissertation.
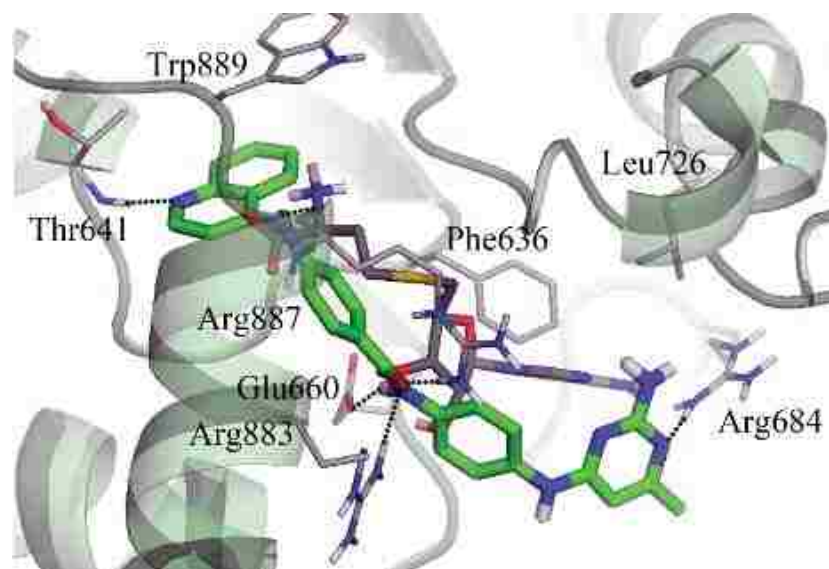
Figure 3.1 Docking image produced by Yoo *et al*. showing SGI-1027 (green) and SAH (black) bound to crystal structure of DNMT1.[118]

A previous colleague of mine, Dr. Ofuka Ichire, began his graduate career, with Dr. Nigel Priestley's help, by utilizing the same crystallographic structure of DNMT1 in a virtual docking study in order to find non-nucleoside inhibitors of DNMT1. The DNMT1 crystal structure 3SWR was downloaded from the Protein Data Bank and prepared using AutoDockTools.[119] The process consisted of removing water molecules, adding hydrogens, and removing the bound sinefungin. Ligands structures were obtained from the Promiliad Biopharma Incorporated library of compounds. The docking calculations were performed with AutoDock Vina[119] and the results visually displayed using Pymol (Figure 3.2).[120] Briefly, calculations were performed in an established cube area centered on the co-crystalized sinefungin ligand. The area covered both the catalytic and SAM binding sites. AutoDock Vina calculated binding energies for all ligands and is plotted below (Figure 3.3).

31
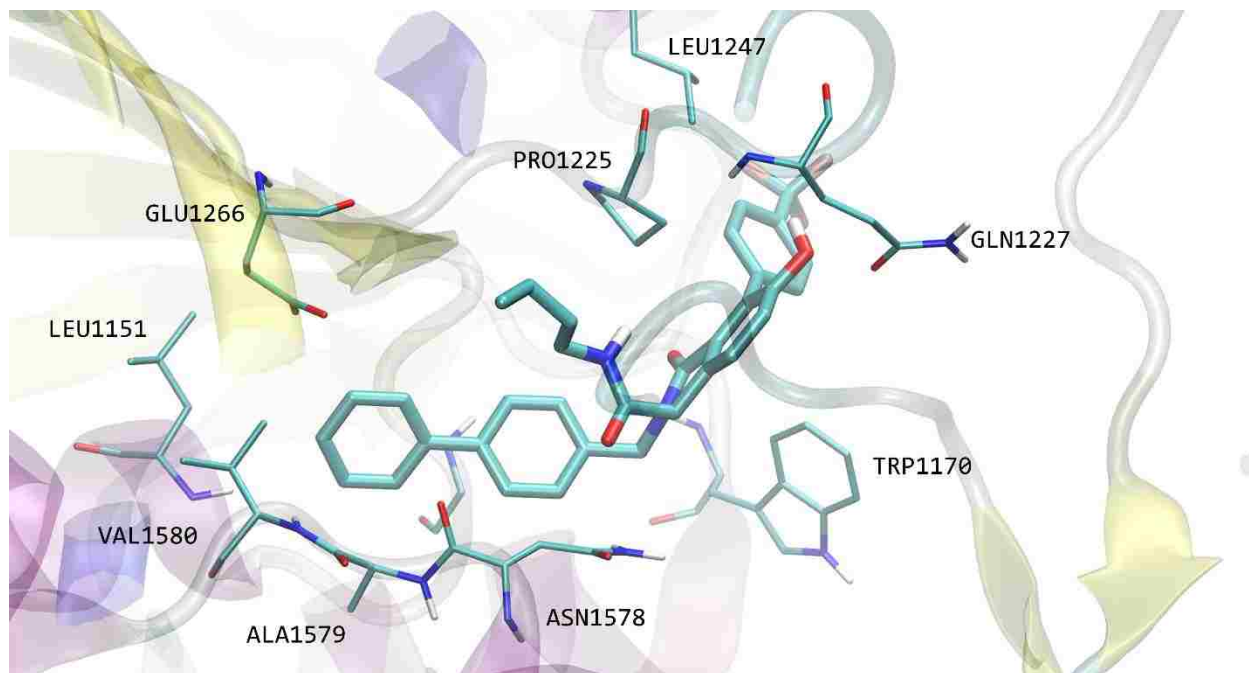
Figure 3.2. Docking study showing a novel inhibitor inside the active site of DNMT1.
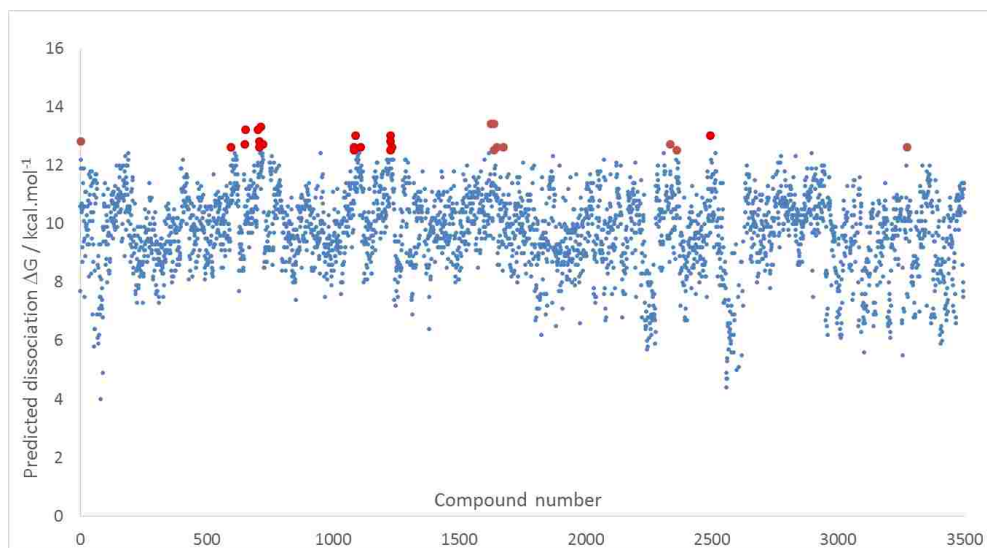
Figure 3.3 Predicted binding affinity of Promiliad Biopharma Incorporated library database. The blue dots represent the predicted dissociation energy for each compound tested. The red dots represent the top one percent of hits. Of the 26 top hits, 17 were isoindolinone compounds.

Testing our group's already existing library of compounds uncovered that a group of isoindolinone product analogs were predicted to bind with high affinity to DNMT1. Predicted binding energies for members of the library ranged from –4 to –13 kcal.mol^{-1}. Twenty-six small molecules with binding energies stronger than -12.5 kcal.mol^{-1} comprised the top one percent of hits. Of these, 17 out of the 26 (65 %) were isoindolinone derivatives. The isoidolinone scaffold, was of interest because it is found in pharmacologically active phytotoxins (such as porritoxin [121] and stachybotramide [122]), compound NU8231[123], and the alkaloid nuevamine (Figure 3.4).[124]
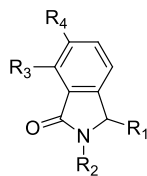
Figure 3.4 Isoindolinone scaffold.

In an effort to study this class of compounds further, Dr. Ichire synthesized analogs of isoindolinones using the Ugi-IMDAF reaction (Figure 3.5). By varying the amine and the isocyanide components of the reaction, a diverse library of isoindolinones were synthesized.
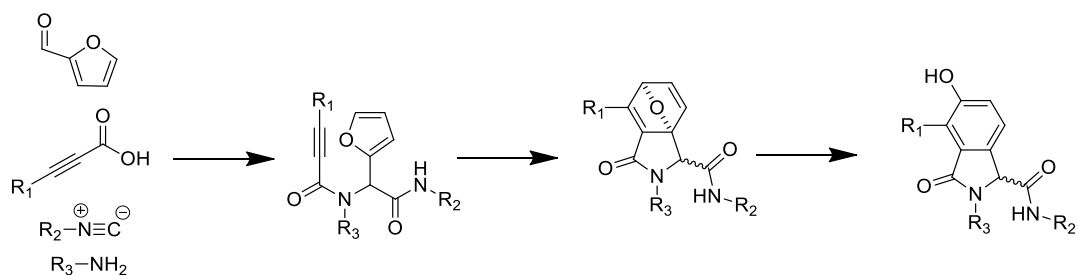
Figure 3.5. Synthetic route of Ugi-IMDAF reaction.

The synthesis was divided into two separate sets of compounds: 1) isoindolinones with a phenol group and 2) substitution of an acetate group for the phenol 3). Each set of compounds was tested in a radioactivity-based assay, with the best results shown below (Figure 3.6). The results of the assay show slight inhibition of DNMT1 at 100 µM. The goal of creating this second group of isoindolinones was to see the importance of the phenolic OH group. The results for the second set of compounds were similar to that of the first set.

% DNMT1 Activity
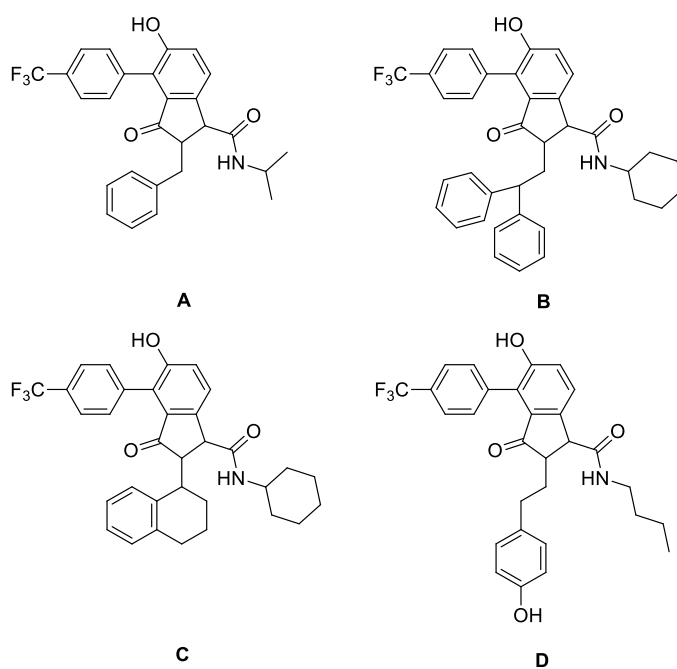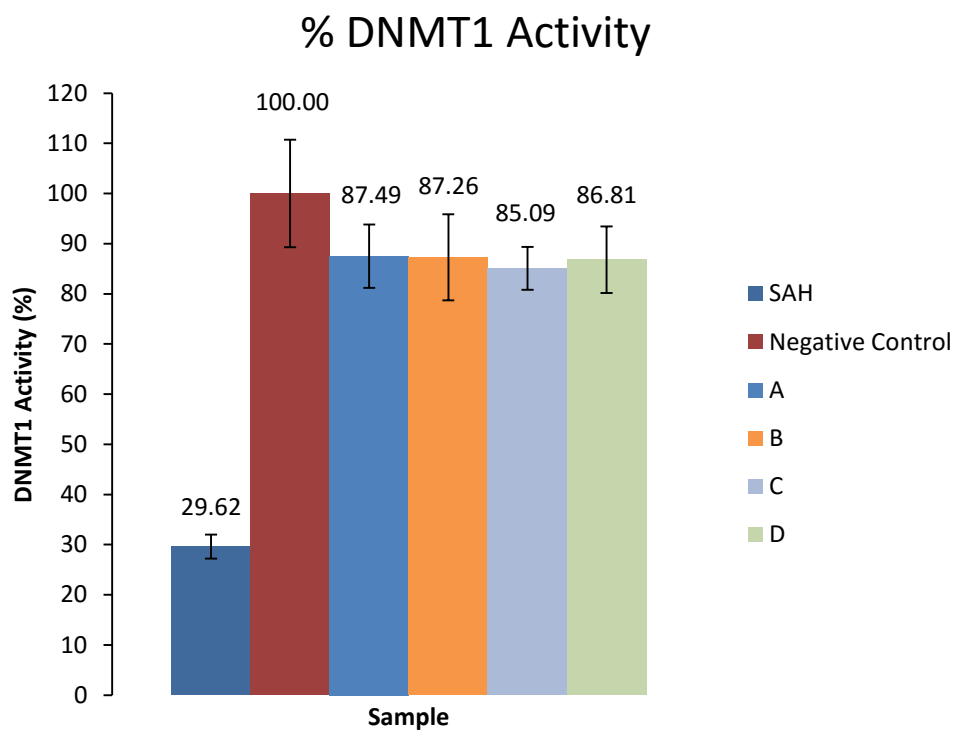
Figure 3.6. *In vitro* radioactivity assay showing top isoindolinone analogs from Dr. Ichire's dissertation. The error bars are ± S.E.M.

The work done for this dissertation begins where Dr. Ichire left off. The primary

approach to produce isoindolinones is the Ugi-IMDAF reaction. However, the one-pot Ugi-

IMDAF reactions are difficult to manage due to the number of by-products produced. The

IMDAF part of the reaction is reversible, so at the end of the reaction, multiple compounds are

mixed together, making isolation of the desired product difficult and a time consuming process.

A second issue with this reaction is a lack of commercially available isocyanides. This limits the

number of isoindolinone derivatives that can be produced.

An alternative synthetic route was developed that utilized homophthalic acid as a

starting point to successfully synthesize isoindolinones (Figure 3.7). The homophthalic acid

route proved much easier to work with. The addition of various primary amines was all that

was needed to successfully synthesize a large library of diverse isoindolinones. The downside

to this route is that it takes multiple steps to reach the desired product. The added steps meant

multiple days were needed per product generated.
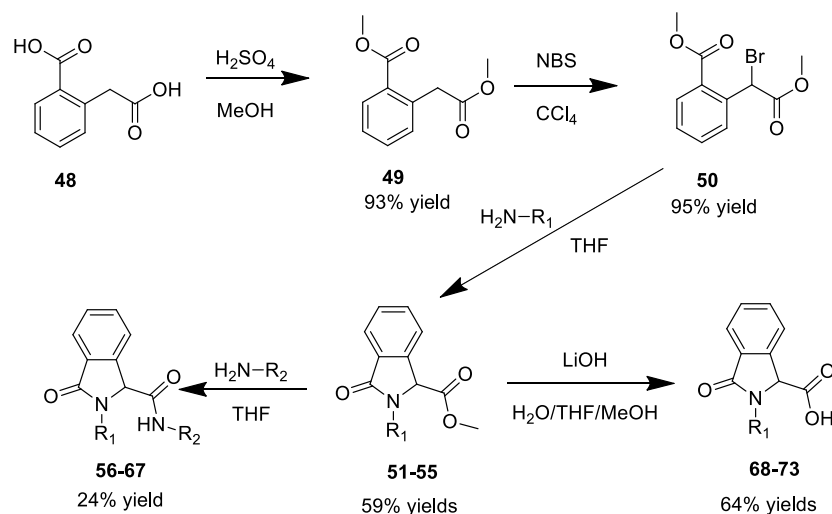
Figure 3.7. Homophthalic acid synthetic route.

Ugi *et al.* showcased a reaction scheme to produce convertible isocyanides from (β-isocyan-ethyl)-alkyl-carbonates (Figure 3.8).[125] A convertible isocyanide is an isocyanide functionality that can easy be converted into a series of other functional groups. This route proved to be the best of both previous routes, allowing us to create our own isocyanide groups to be used in the one pot Ugi-IMDAF reaction. These improvements to the process of producing isoindolinones are discussed in the following chapters, as well as biological methods for analyzing the effectiveness of each new compound against DNMT1.
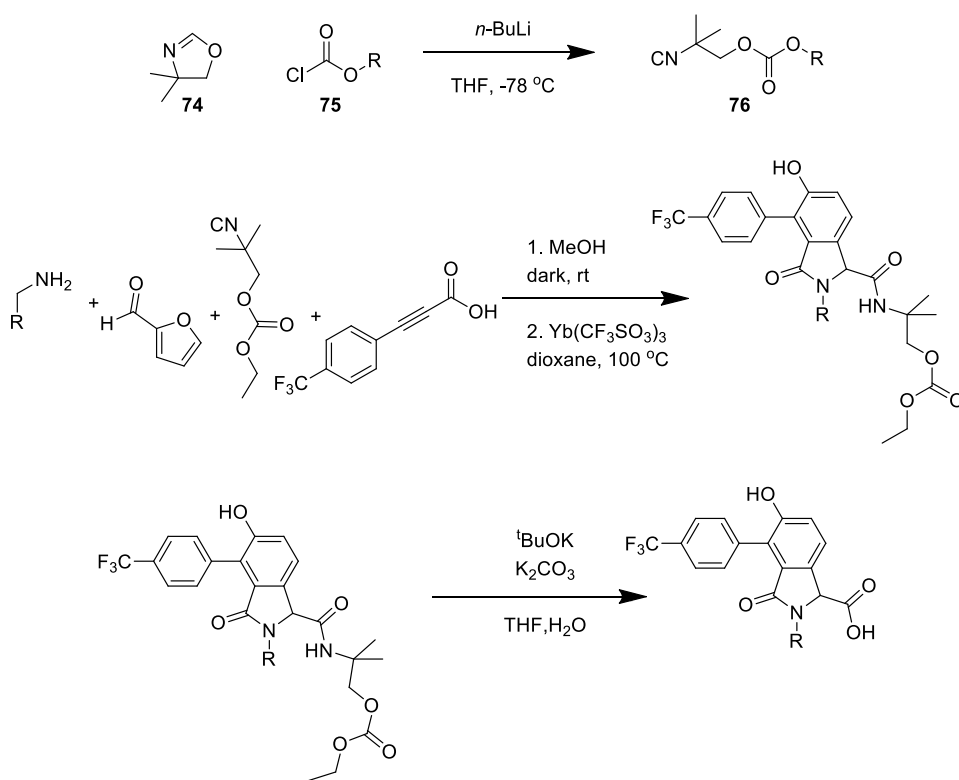
Figure 3.8. Reaction scheme for Ugi-IMDAF reaction using convertible isocyanides.

3.1 Ugi-IMDAF reaction to isoindolinone derivative

In an effort to study the isoindolinone class of compounds, additional analogs were synthesized using the Ugi-IMDAF reaction. By varying the amine (R_3) and the isocyanide (R_2) components of the reaction a diverse library of isoindolinones was synthesized (Figure 3.9).

24

25

26

27

28

29

30

31

32

33

34

35

36

37

38
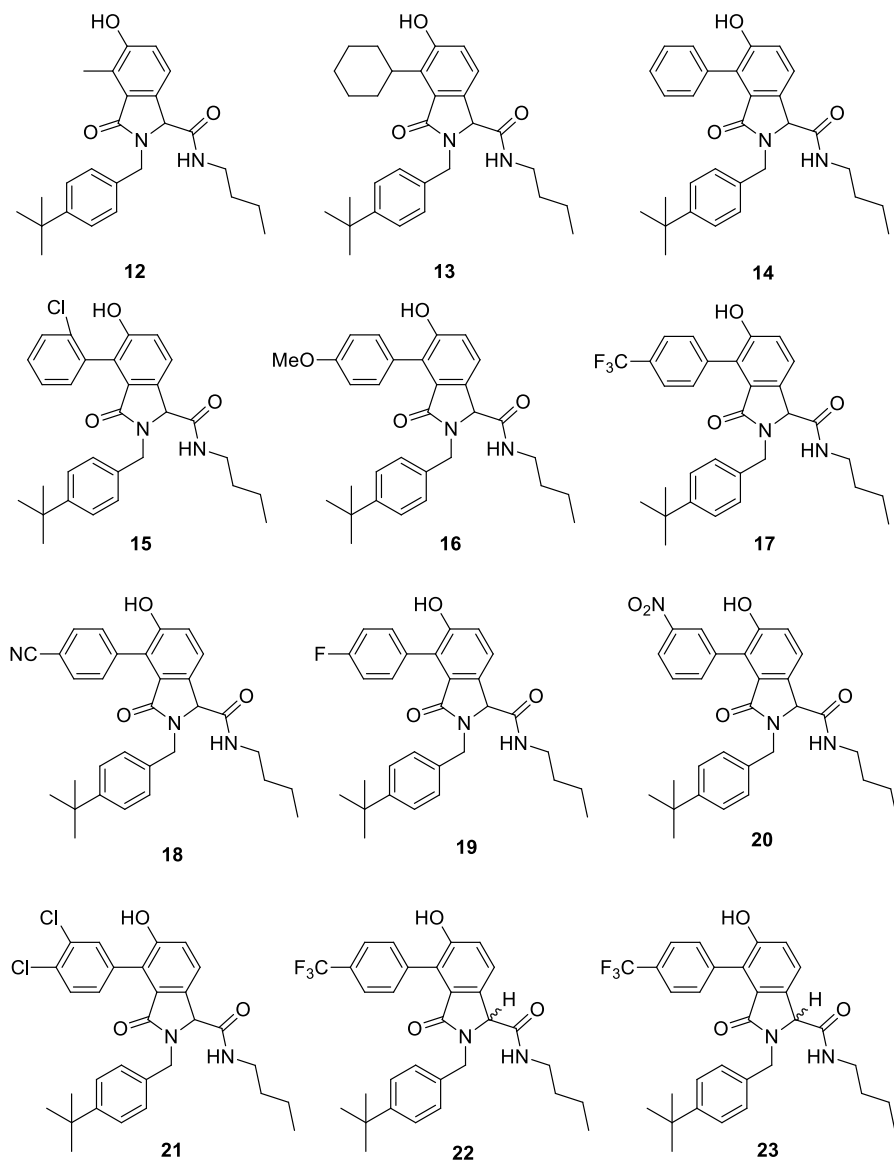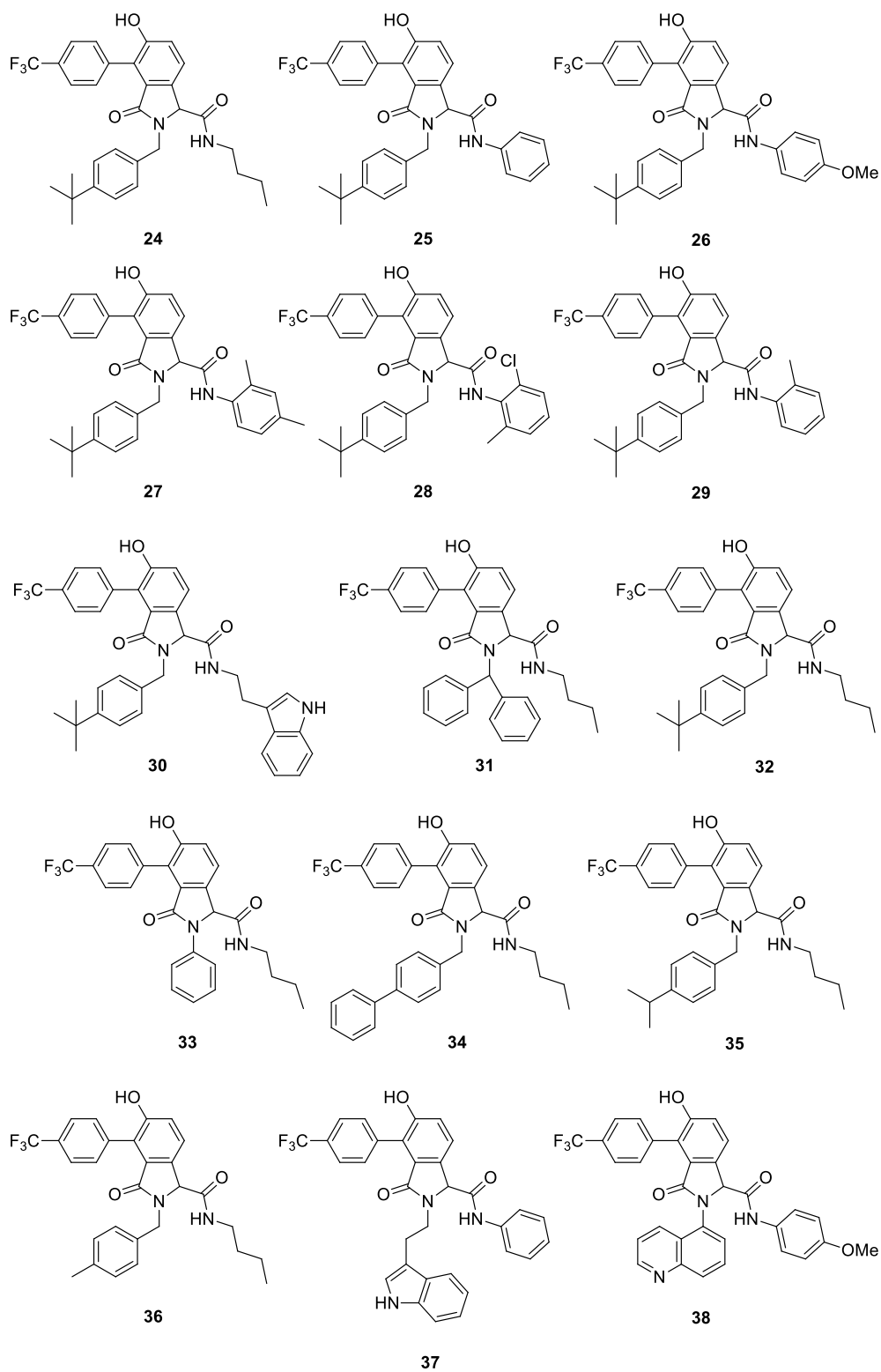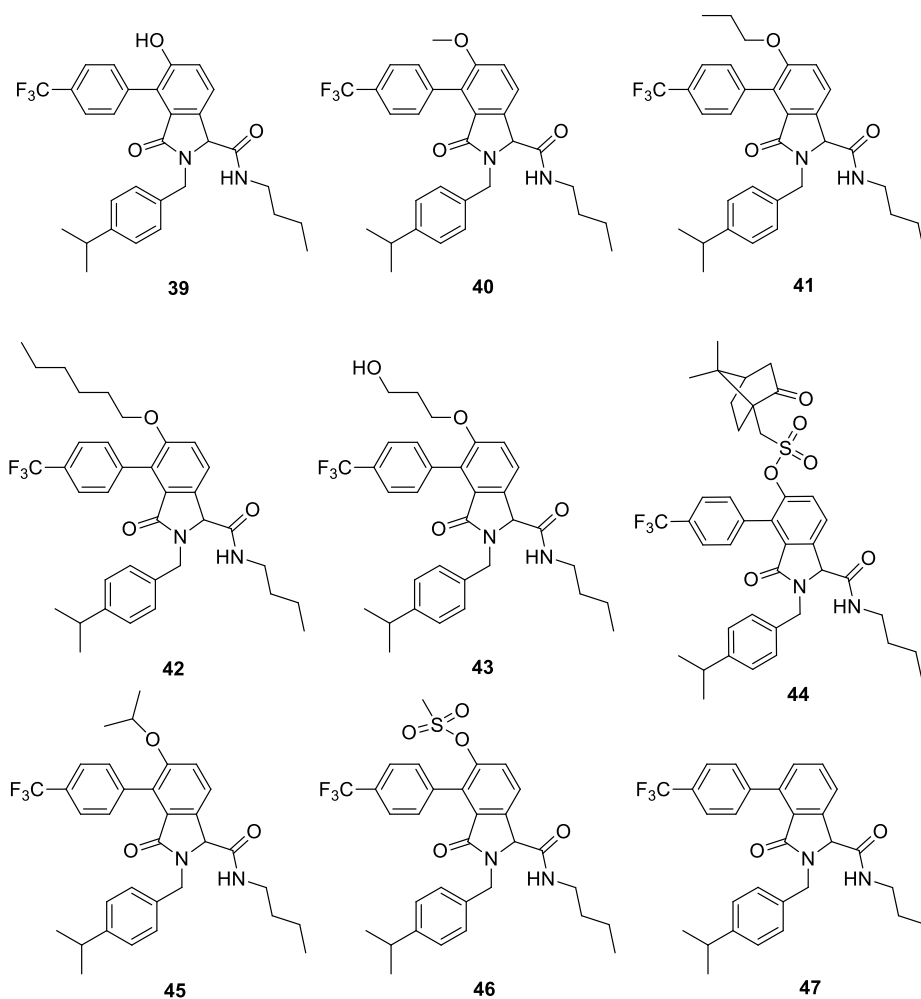
Figure 3.9. Structures of Ugi-IMDAF compounds made via scheme shown in Figure 3.5.

3.2   Results and discussion

The following tables show the Ugi-IMDAF compounds tested in the radioactivity-based assay. Each table shows which functional group was altered as well as the calculated binding affinity ($K_i^{'}$). For all the compounds tested, the results are compared to RG108 (**8**), since it's a current successful drug candidate. The hope is to see is a DNMT1 activity lower than 51.4% and a $K_i^{'}$ lower than 242 μM.
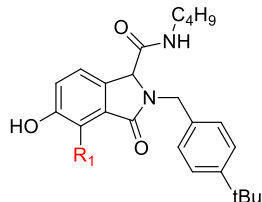
Compound	R$_1$	% DNMT1 Activity		K$_i^{'}$ (µM)
15	-Ph(2-Cl)	39.8 ± 1.7		151 ± 11
12	CH$_3$	40.0 ± 1.1		153 ± 7
16	-Ph(4-OCH$_3$)	40.3 ± 1.3		155 ± 8
13	Cyclohexane	41.7 ± 0.2		164 ± 1
23	-(+)-Ph(4-CF$_3$)	42.7 ± 4.7		171 ± 33
8 (RG108)		51.4 ± 5.7		242 ± 55
18	-Ph(4-CN)	54.4 ± 1.8		273 ± 19
22	-(-)-Ph(4-CF$_3$)	57.4 ± 1.3		309 ± 16
19	-Ph(4-F)	64.2 ± 2.2		410 ± 39
20	-Ph(3-NO$_2$)	64.5 ± 4.0		416 ± 73
17	-Ph(4-CF$_3$)	68.1 ± 0.9		487 ± 21
21	-Ph(3,4-Cl$_2$)	77.8 ± 4.7		801 ± 220
14	Ph	77.9 ± 1.7		807 ± 78

Table 3.1. Ugi-IMDAF products with variability in the propiolic acid position.
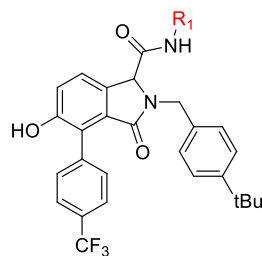
Compound	R$_1$	% DNMT1 Activity		K$_i^{'}$ (µM)
28	-Ph(2-Cl,6-Me)	39.9 ± 0.2		152 ± 1
8 (RG108)		51.4 ± 5.7		242 ± 55
25	-Bn	54.8 ± 1.2		277 ± 13
29	-Ph(2-Me)	62.3 ± 1.8		378 ± 29
24	-^{n}Bu	68.1 ± 0.9		487 ± 21
26	-Ph(4-OMe)	88.5 ± 1.9		1800 ± 300
30	-CH$_2$CH$_2$(3-indolyl)	90.7 ± 3.0		2200 ± 800
27 *	-Ph(2,6-Me$_2$)	no significant inhibition		-

Table 3.2. Ugi-IMDAF products with variability in the isocyanide position. '*' next to number indicates no significant inhibition.
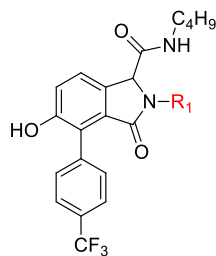
Compound	R$_1$	% DNMT1 Activity		K$_i'$ (µM)
34	-CH$_2$Ph(4-Ph)	31.3 ± 0.6		104 ± 3
8 (RG108)		51.4 ± 5.7		242 ± 55
38	-(5-quinolonyl)	53.6 ± 0.9		264 ± 10
37	-CH$_2$CH$_2$-(3-indolyl)	58.0 ± 1.2		315 ± 15
36	-CH$_2$Ph(4-Me)	62.3 ± 2.6		378 ± 42
32	-CH$_2$Ph(4-^{t}Bu)	68.1 ± 0.9		490 ± 20
35	-CH$_2$Ph(4-^{i}Pr)	68.9 ± 1.7		508 ± 41
31	-CHPh$_2$	87.2 ± 1.2		1600 ± 200
33	-Bn	88.4 ± 2.7		1800 ± 500

Table 3.3. Ugi-IMDAF products with variability in the amine position.
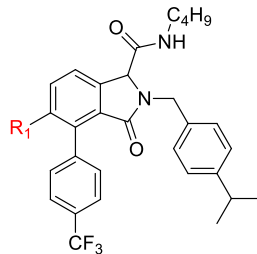
Compound	R₁	% DNMT1 Activity		K_i' (μM)
8 (RG108)		51.4 ± 5.7		242 ± 55
45	$-O^iPr$	59.3 ± 1.9		333 ± 26
47	-H	66.8 ± 5.6		461 ± 117
39	-OH	68.9 ± 1.7		507 ± 41
46	$-OSO_2Me$	70.6 ± 3.0		550 ± 78
40	-OMe	83.6 ± 5.1		1200 ± 450
44	-OCamphSulf	88.8 ± .07		1800 ± 130
41 *	$-O^nPr$	no significant inhibition		-
42 *	$-O^nC_6H_{11}$	no significant inhibition		-
43 *	$-OCH_2CH_2CH_2OH$	no significant inhibition		-

Table 3.4. Ugi-IMDAF products with variability in the hydroxyl group position. '*' next to number indicates no significant inhibition.

Varieties of isoindolinone compounds have been tested in this study. Each set of compounds were carefully designed as an SAR approach to arrive at the best possible isoindolinone. The goal of this study is to find a novel inhibitor that creates a lower DNMT1 activity and K_i' than RG108 (**8**). Each of the first series of products contains the amines n-butylamine and tert-butylamineuamine and has a phenolic OH group present while having variability in the propiolic acid position (Table 3.1).

The results show several compounds that exhibit more potent DNMT1 inhibition as compared to RG108. Compound **12** has a methyl group at the R_1 site. This compound has a DNMT1 activity of 40.0 ± 1.1. This is an 11.4 % decrease from RG108. The calculated K_i' value for compound **12** is 153 ± 7 μM, which is 89 μM lower than RG108. Next, we see compound **13** with a cyclohexane present at the R_1 site. This compound has a DNMT1 activity of 41.7 ± 0.2. Compound **13** showed a 9.7 % decrease from RG108. The calculated K_i' value for compound **13** is 164 ± 1μM, which is 78 μM lower than RG108.

Compound **15** contains a 2-chlorobenzene group at the R_1 site. Compound **15** has a DNMT1 activity of 39.8 ± 1.7. When comparing this to RG108, we a see an 11.6 % decrease in activity. The calculated K_i' value for **15** is 151 ± 11, which is 91 μM less than RG108. Compound **16** has a –Ph(4-OCH$_3$) group at the R1 site. Compound **16** has a DNMT1 activity of 40.3 ± 1.3. When comparing this to RG108, we a see an 11.1 % decrease in activity. . The calculated K_i value for **16** is 155 ± 8, which is 87 μM less than RG108. The final compound that showed improvement on RG108 in this series is number **23**. Compound **23** has a Ph(4-CF3) group in the R_1 site and a DNMT1 activity of 42.7 ± 4.7. This value is a 8.7 % decrease when compared to the

activity of RG108. The calculated $K_i^{'}$ for compound **23** is 171 ± 33, which is 71 µM lower than

RG108.

The next series of compounds has variability in the isocyanide position (Table 3.2). As

mentioned above, there is a limited number of commercially available isocyanides, making this

series of compounds smaller in number than most. Each of the compounds made in the series

contains the amine ^{t}butylamine, has a 4-CF$_3$ phenyl group, and has a phenolic OH group

present. Of the seven compounds tested in this series one compound, **28,** showed an

improvement when compared to RG108. Compound **28** has a –Ph(2-Cl,6-Me) group present.

This compound gave a DNMT1 activity of 39.9 ± 0.2, which is an 11.5 % decrease from RG108.

The calculated $K_i^{'}$ value for compound **28** is 152 ± 1 µM, which is 90 µM lower than RG108. This

series of compounds tells us there is a need for some sort of electron donating group in the R$_1$

position.

The next series of compounds are Ugi-IMDAF reaction products with variability in the

amine position (Table 3.3). Each of the compounds made in the series contains the *n*-butyl

amine, has a 4-CF3 phenyl group, and has a phenolic OH group present. Of the eight

compounds tested, only compound **34** showed an improvement when compared to RG108.

Compound **34** has a –CH$_2$Ph(4-Ph) group at the R$_1$ site. The DNMT1 activity for compound **34**

was 31.3 ± 0.6. This value is 20.1 % lower in activity than RG108. The calculated $K_i^{'}$ value for

this compound is 104 ± 3 µM, which is 138 µM less than RG108.

In Table 3.4, we show the results for a series of Ugi-IMDAF products generated with

variability in the hydroxyl group position. Each of the compounds made in the series contains

the amines n-butyl isocyanide, 4-isopropylbenzyl amine, has a 4-CF$_3$ phenyl group. Of the nine

compounds tested, none of them showed improvement on the DNMT1 activity or the

calculated binding affinity when compared to RG108. These results tell us that leaving a

hydroxyl group on the ring would give us the desired lower DNMT1 activity.

Of all the Ugi-IMDAF products tested so far compound **34** has the best improvement in

DNMT1 inhibition when compared to RG108. Next, we decided to create a new series of

compounds that would get around the issues presented in the Ugi-IMDAF synthetic route. The

route created utilizes homophthalic acid as a starting material and creates the desired

isoindolinone structures. The results for these series of compounds are seen in tables 4.1 – 4.3.

Chapter 4 HOMOPHTHALIC ACID SYNTHETIC ROUTE TO PRODUCE ISOINDOLINONES

4.1   Introduction

The one-pot Ugi-IMDAF reaction generated the desired isoindolinone structures with overall yields between 54% and 89%. The use of the reaction in a true combinatorial sense is limited as each reaction required individual optimization. Difficulties were observed with the initial Ugi condensation and particularly with the reversibility of the Diels-Alder reaction. This, along with a limited number of commercially available isocyanides makes that synthetic route not as useful as at first. Here we discuss an approach to synthesize novel isoindolinones using a multi-step synthesis scheme (Figure 4.1). Briefly, homophthalic acid, **48**, is dissolved in methanol with 5% v/v H_2SO_4 to create the Fischer esterification product **49**. **49** undergoes a benzylic bromination reaction to produce compound **50**, which then undergoes a S_N2 reaction followed by an intramolecular cyclization by the addition of a primary amine, to produce compounds **51-55**. The methyl esters in compounds **51-55** go through hydrolysis to produce the carboxylic acids, compounds **68-71**. The carboxylic acids are then activated and undergo a reductive amination reaction to produce compounds **56-67**. The structures of products generated via this route are show below (Figure 4.2).
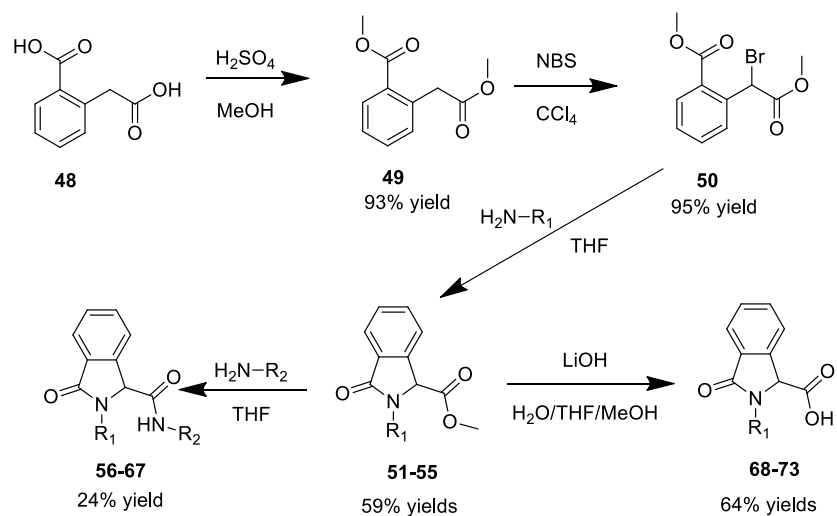
Figure 4.1. Reaction scheme for homophthalic acid multi-step synthesis.
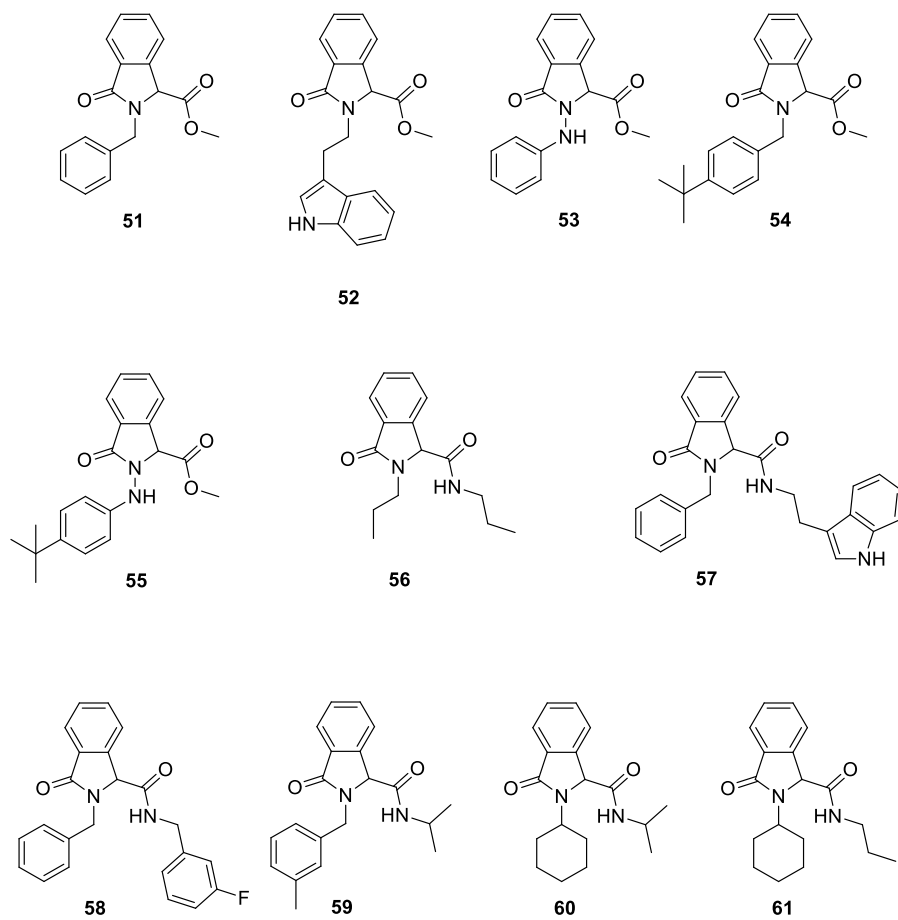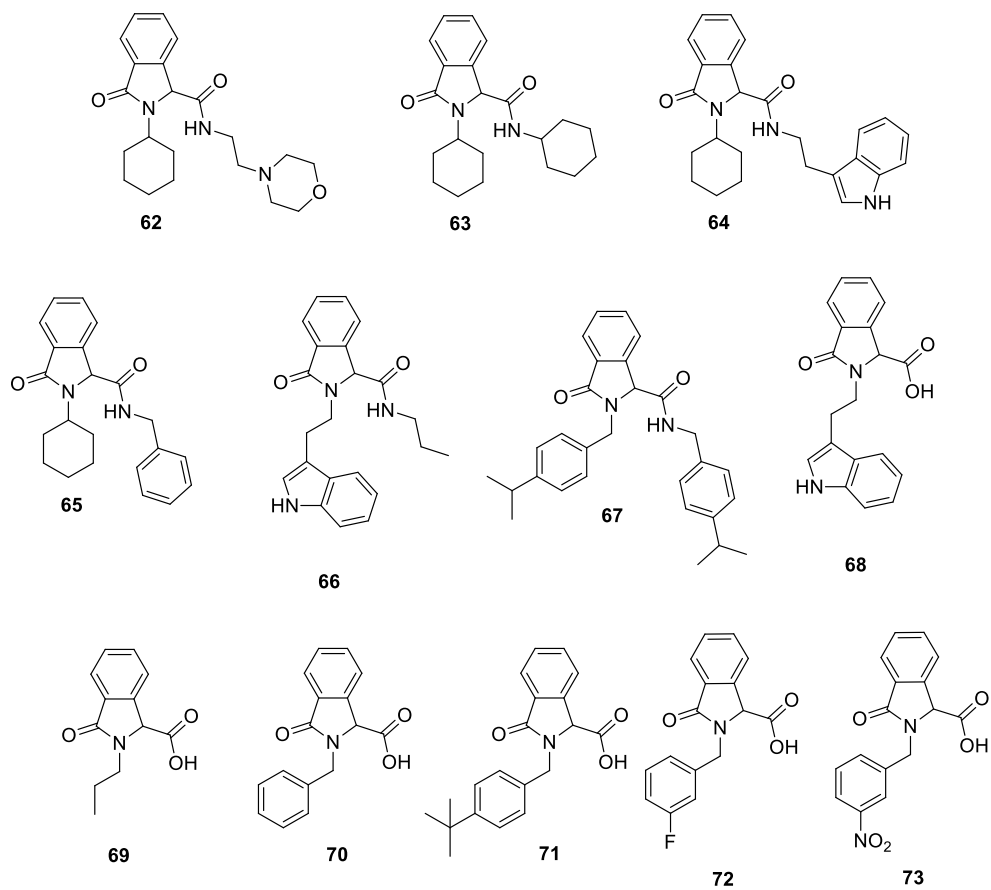
Figure 4.2. Structures of isoindolinone compounds made via scheme shown in Figure 4.1.

4.2 Results and discussion
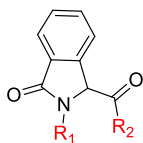
Compound	R$_1$	R$_2$	% DNMT1 Activity		K$_i$' (μM)
8 (RG108)			51.4 ± 5.7		242 ± 55
51 *	benzyl	-OMe	no significant inhibition		-
52 *	-CH$_2$CH$_2$-(3-indoyl)	-OMe	no significant inhibition		-
53 *	-NHPH	-OMe	no significant inhibition		-
54 *	-CH$_2$Ph(4-^{t}Bu)	-OMe	no significant inhibition		-
55 *	-NHPh(4-^{t}Bu)	-OMe	no significant inhibition		-

Table 4.1. Homophthalic acid synthetic route products varying R$_1$ while keeping R$_2$ a methyl ester. '*' next to number indicates no significant inhibition.

Compound	R_1	R_2	% DNMT1 Activity		K_i' (µM)
8 (RG108)			51.4 ± 5.7		242 ± 55
67	-CH$_2$Ph(4-iPr)	-NHCH$_2$Ph(4-^{i}Ph)	58.0 ± 0.59		316 ± 8
66	-CH$_2$CH$_2$-(3-indoyl)	-NHCH$_2$CH$_2$CH$_3$	72.9 ± 4.9		614 ± 151
57	-CH$_2$Ph	-NHCH$_2$CH$_2$-(3-indoyl)	76.3 ± 4.3		736 ± 174
56 *	-CH$_2$CH$_2$CH$_3$	-NHCH$_2$CH$_2$CH$_3$	no significant inhibition		-
58 *	-CH$_2$Ph	-NHCH$_2$Ph(3-F)	no significant inhibition		-
59 *	-CH$_2$Ph(3-Me)	-NHCH(CH$_3$)$_2$	no significant inhibition		-
60 *	Cyclohexane	-NHCH(CH$_3$)$_2$	no significant inhibition		-
61 *	Cyclohexane	-NHCH$_2$CH$_2$CH$_3$	no significant inhibition		-
62 *	Cyclohexane	-NHCH$_2$CH$_2$morpholine	no significant inhibition		-
63 *	Cyclohexane	-NHcyclohexane	no significant inhibition		-
64 *	Cyclohexane	-NHCH$_2$CH$_2$-(3-indoyl)	no significant inhibition		-
65 *	Cyclohexane	-NHCH$_2$Ph	no significant inhibition		-

Table 4.2. Homophthalic acid synthetic route products varying R_1 and R_2. '*' next to number indicates no significant inhibition.

Compound	R_1	R_2	% DNMT1 Activity		$K_i^{'}$ (µM)
70	-CH$_2$Ph	-OH	8.91 ± 0.16		22 ± 0.45
68	-CH$_2$CH$_2$-(3-indoyl)	-OH	10.2 ± 1.7		26 ± 5
73	-CH$_2$Ph(3-NO$_2$)	-OH	24.3 ± 3.4		74 ± 13
72	-CH$_2$Ph(3-F)	-OH	28.3 ± 0.65		90 ± 3
8 (RG108)			51.4 ± 5.7		242 ± 55
69 *	-CH$_2$CH$_2$CH$_3$	-OH	no significant inhibition		-
71 *	-CH$_2$Ph(4-^{t}Bu)	-OH	no significant inhibition		-

Table 4.3. Homophthalic acid synthetic route products varying R_1 and having a carboxylic acid functionality at R_2 site. '*' next to number indicates no significant inhibition.
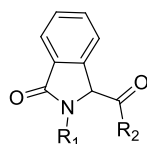
Figure 4.3. Homophthalic acid isoindolinone scaffold.

Table 4.1 shows products of the homophthalic acid route with variability in the R_1 position but keeping the R_2 site a methoxy. These results suggested to us that the methoxy group in the R_2 site is not needed and should be changed.

Compound	R1	R2	% DNMT1 Activity		Ki' (µM)
8 (RG108)			51.4 ± 5.7		242 ± 55
67	-CH2Ph(4-iPr)	-NHCH2Ph(4-iPh)	58.0 ± 0.59		316 ± 8
66	-CH2CH2-(3-indoyl)	-NHCH2CH2CH3	72.9 ± 4.9		614 ± 151
57	-CH2Ph	-NHCH2CH2-(3-indoyl)	76.3 ± 4.3		736 ± 174
56 *	-CH2CH2CH3	-NHCH2CH2CH3	no significant inhibition		-
58 *	-CH2Ph	-NHCH2Ph(3-F)	no significant inhibition		-
59 *	-CH2Ph(3-Me)	-NHCH(CH3)₂	no significant inhibition		-
60 *	Cyclohexane	-NHCH(CH3)₂	no significant inhibition		-
61 *	Cyclohexane	-NHCH2CH2CH3	no significant inhibition		-

62 *	Cyclohexane	-NHCH2CH2morpholine	no significant inhibition		-
63 *	Cyclohexane	-NHcyclohexane	no significant inhibition		-
64 *	Cyclohexane	-NHCH2CH2-(3-indoyl)	no significant inhibition		-
65 *	Cyclohexane	-NHCH2Ph	no significant inhibition		-

Table 4.2 shows the result of changing the R_2 site.

Compounds **56** – **67** were synthesized in order to test the effects of altering both the R_1 and R_2 site. Of the twelve compounds tested, only three of them, compounds **57**, **66,** and **67** showed statistically significant inhibition. Compound **57** has a –CH_2Ph on the R_1 site and a -$NHCH_2CH_2$-(3-indoyl) in the R_2 site. This compound resulted in a DNMT1 activity of 76.3 ± 4.3, which is 24.9 % higher than RG108. The calculated $K_i^{'}$ value is 494 µM larger than RG108, indicating this combination of variables is not the way to go. Compound **66** has a DNMT1 activity of 72.9 ± 4.9, which is 21.5 % higher than RG108 and a calculated $K_i^{'}$ value of 614 ± 151 µM, which is 372 µM higher than RG108. Compound **67** gave a DNMT1 activity of 58.0 ± 0.59, which is 6.6 % higher than RG108. The calculated $K_i^{'}$ value for compound **67** is 316 ± 8 µM, which is 74 µM higher than RG108. It is clear that this series of compounds did not surpass the current RG1008 standard.

The results for the isoindolinones that vary in the R_1 site, but have a hydroxyl group at the R_2 site show that of the six compounds tested, four of them show significant results. (Table

56

4.3) Compound **68** has a DNMT1 activity of 10.2 ± 1.7. This value is 41.2 % lower than RG108.

The calculated $K_i^{'}$ value is 26 ± 5 μM, which is 216 μM lower than RG108. The second

compound in the series with significant results is number **70**. Compound **70** has a DNMT1

activity of 8.91 ± 0.16. This value is 42.5 % lower than RG108. The calculated $K_i^{'}$ value for

compound **70** is 22 ± 0.45 μM, which is 220 μM lower than RG108. Compound **72** has a DNMT1

activity of 28.3 ± 0.65. This value is 23.1 % lower than RG108. The calculated $K_i^{'}$ value is 90 ± 3,

which is 152 μM lower than RG108. Compound **73** has a DNMT1 activity of 24.3 ± 3.4. This

value is 27.1 % lower than RG108. The calculated $K_i^{'}$ value is 74 ± 13, which is 168 μM lower

than RG108. The results for compound **68**, **70**, **72**, and **73** were tested multiple times to insure

the results were not a fluke. Each time the data came to the same conclusion. It is clear from

the results that the carboxylic acid functionality at the R_2 site greatly helps the inhibition

property.

The homophthalic acid synthetic route produced the desired isoindolinone compounds

in good yields. The synthetic route required no isocyanides, providing a way to get around the

issue with the Ugi-IMDAF reaction. The process to isolate and purify the products was much

easier than the Ugi-IMDAF reactions. The main issue with the homophthalic acid reaction is

that it is a multiple step process as there are no reversible steps to overcome. The need to

purify after each step adds time to the isoindolinone creation process. Overall, though, this is a

great synthetic route to create isoindolinone DNMT1 inhibitors.

Chapter 5 **C**ONVERTIBLE ISOCYANIDES SYNTHETIC ROUTE TO PRODUCE ISOINDOLINONES

5.1 Introduction

After showing the capability of the homophthalic acid synthetic route to make isoindolinones (Figure 4.1), we wanted to return to the Ugi-IMDAF reaction. The one-pot Ugi-IMDAF reactions generated the desired isoindolinone structures with overall yields between 54 % and 89%.   The use of the reaction in a true combinatorial sense is limited, as each reaction required individual optimization. Difficulties were observed with the initial Ugi condensation and particularly with the reversibility of the Diels-Alder reaction. That, along with a limited number of isocyanides makes that synthetic route not desirable.   Lindhorst *et al.*, however, showed the synthesis of a new class of convertible isocyanides and use of them in the Ugi-IMDAF reaction (Figure 5.1).[125] A convertible isocyanide can easily be changed into a carboxylic acids and other functionalities. The convertible isocyanide is very simple to make with 4,4-dimethyl-2-oxazoline, **74**, being deprotonated with *n*-BuLi and the resulting lithium alcoholate being captured with an alkyl chloroformate, **75**. This product, **76**, can then be used in the one pot Ugi-IMDAF reaction. This process allows us to use the one pot Ugi-IMDAF reaction, while avoiding the issues of limited commercially available isocyanides. The structures of the products generated are shown below (Figure 5.2).
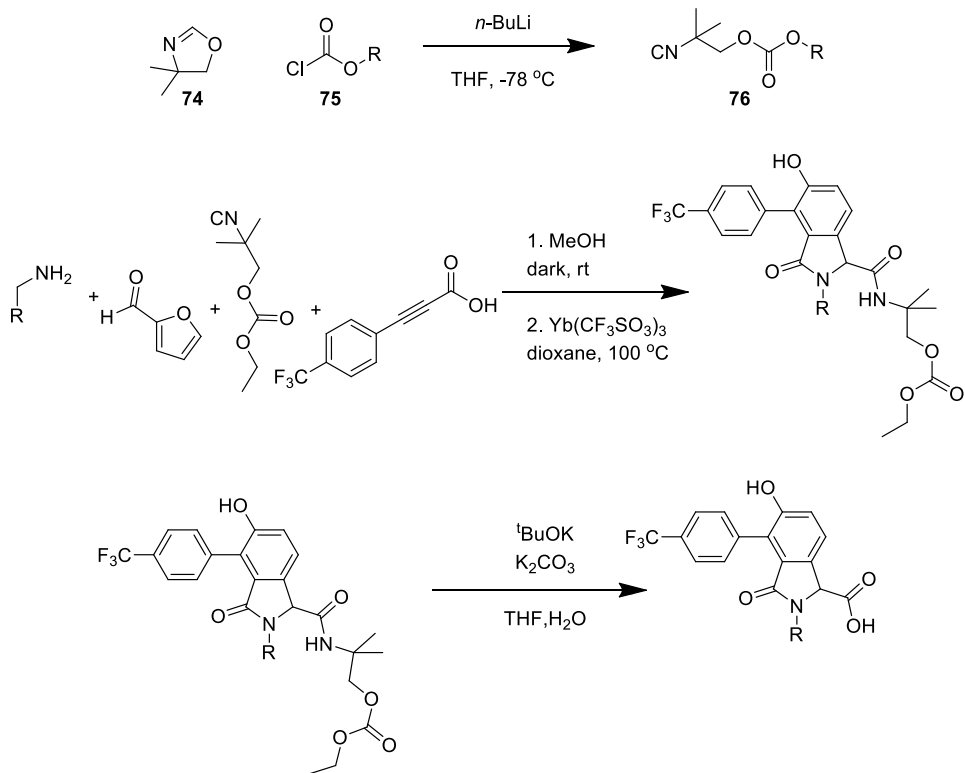
Figure 5.1. Reaction scheme for Ugi-IMDAF reaction using convertible isocyanides.
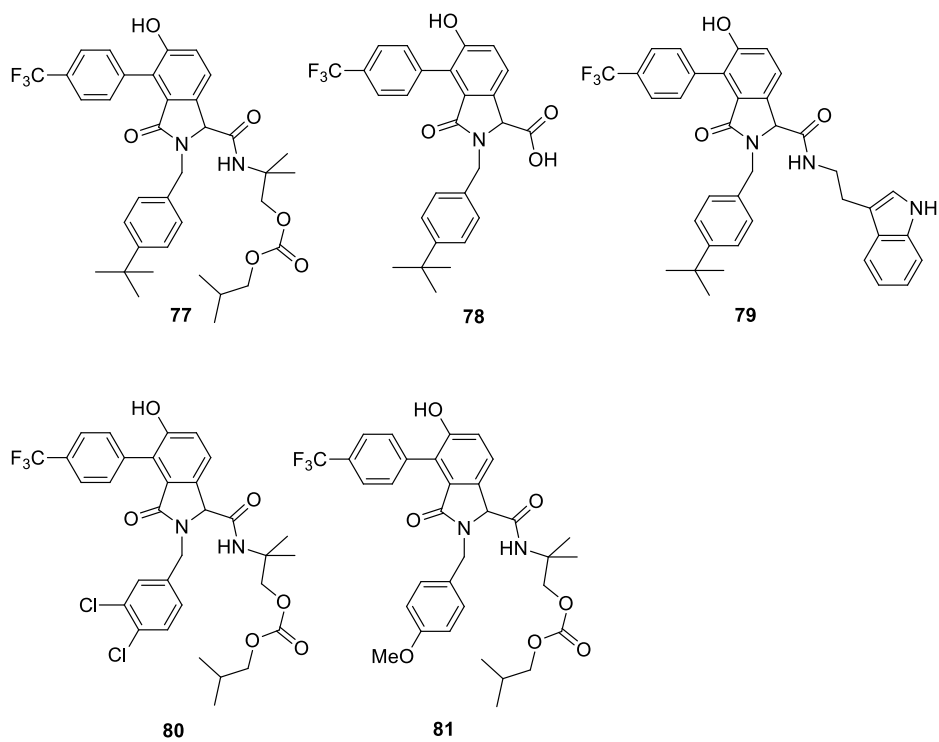
Figure 5.2. Structures of Ugi-IMDAF compounds made via scheme shown in

Figure **5.1.** Reaction scheme for Ugi-IMDAF reaction using convertible isocyanides.

5.2 Results and discussion
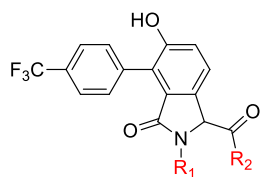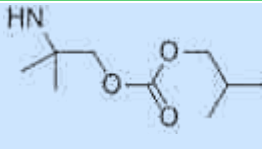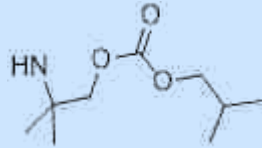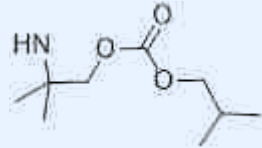
Compound	R$_1$	R$_2$	% DNMT1 Activity		K$_i^{'}$ (μM)
78	-CH$_2$Ph(4-^{t}Bu)	-OH	7.31 ± 0.98		18 ± 3
8 (RG108)			51.4 ± 5.7		242 ± 55
77	-CH$_2$Ph(4-^{t}Bu)		55.7 ± 4.3		287 ± 50
79	-CH$_2$Ph(4-^{t}Bu)	-NHCH$_2$CH$_2$-(3-indolyl)	90.7 ± 3.0		2300 ± 800
80 *	-CH$_2$Ph(3,4-dichloro)		no significant inhibition		-
81 *	-CH$_2$PH(4-methoxy)		no significant inhibition		-

Table 5.1. Convertible isocyanide synthetic route products varying R$_1$ and R$_2$ site. '*' next to number indicates no significant inhibition.
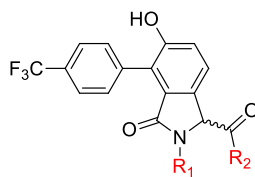
Figure 5.3. Convertible isocyanide isoindolinone scaffold.

Synthesizing our own convertible isocyanides allowed us to create a wider range of Ugi-IMDAF products (Table 5.1). Of the five compounds tested in the series, four of them did not have significant inhibition. Compound **77** has a -CH$_2$Ph(4-^{t}Bu) in the R$_1$ site and one of our synthesized isocyanides at the R$_2$ site. The DNMT1 activity for this compound is 55.7 ± 4.3. This value is 4.3 % higher than RG108. The calculated K$_i^{'}$ value for this compound is 287 ± 50 μM, which is 45 μM higher than RG108. Compound **78** has a -CH$_2$Ph(4-^{t}Bu) in the R$_1$ site and a hydroxyl group at the R$_2$ site. As we saw with the results in Table 4.3, when a carboxylic acid moiety is present on the compound the inhibition property of the compound increases. The DNMT1 activity for compound **78** is 7.31 ± 0.98. This value is 44.1 % lower than RG108. The calculated K$_i^{'}$ value for the compound is 18 ± 3 μM, which is 224 μM lower than RG108. Compound **79** has a -CH$_2$Ph(4-^{t}Bu) on the R$_1$ site and one of our synthesized isocyanides at the R$_2$ site, but failed to perform better than RG108. Compound **79** has a DNMT 1 activity of 90.7 ± 3.0. This value is 39.3 % higher than RG108. The calculated K$_i^{'}$ value for the compound is 2058 μM higher than RG108.

It is clear from the results that a carboxylic acid is needed in order to improve the inhibition of the DNMT1 inhibitors. This was observation was also seen in the homophthalic acid compounds **68**, **70**, **72** and **73**.

Chapter 6 FUTURE DIRECTIONS

6.1 Synthesis

It is clear from looking at all of the results that a carboxylic acid functionality is needed to enhance the inhibition properties of the novel inhibitors. We see the increased inhibition in the Ugi-IMDAF products as well as the homophthalic acid products as long as the carboxylic acid was present. Looking at the docking image for compound **68**, we can see interactions with the nearby conserved amino acids that might help explain the strength of the inhibition (Figure 6.1). The strength of inhibition could be in part due to the interactions that the carboxylic acid has in compound **68** with ALA 1579 in the active site of DNMT1. Or perhaps, compound **68** creates a strong π-π interaction with PRO 1225.
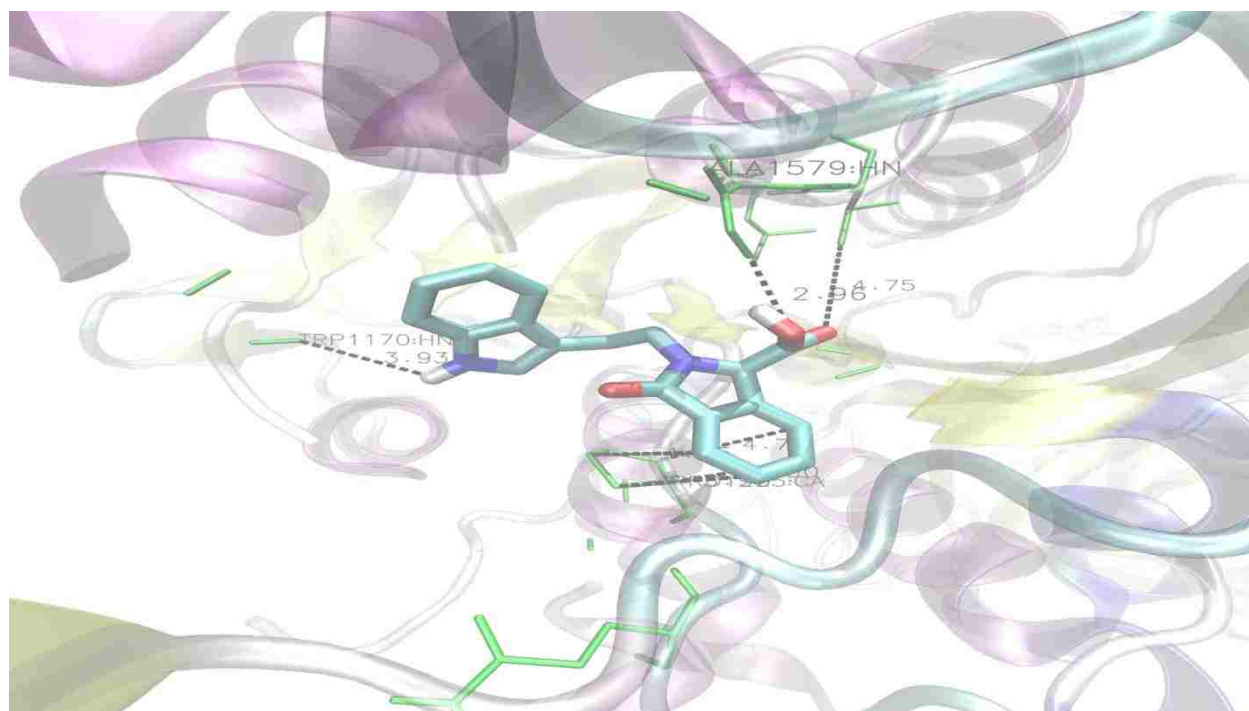
Figure 6.1. Docking image for compound **68** with active site of DNMT1.

The docking image for compound **70** shows that the isoindolinone ring overlaps well with

the PRO 1225 (Figure 6.2). The carboxylic acid functionality also displays interactions with ASN

1578. Analyzing the docking image of compound **75** shows similar interactions with how the

Phenyl(4-CF$_3$) ring overlaps well with PRO 1225 (Figure 6.3). The PRO residue also overlaps well

with the phenyl ring in the ^{t}butyl amine. The carboxylic acid functionality shows an interaction

with TRP 1170 and the OH shows interactions with ASN 1578. These overlaps create strong

interactions that hold the inhibitor in place, thus blocking access to the active site.
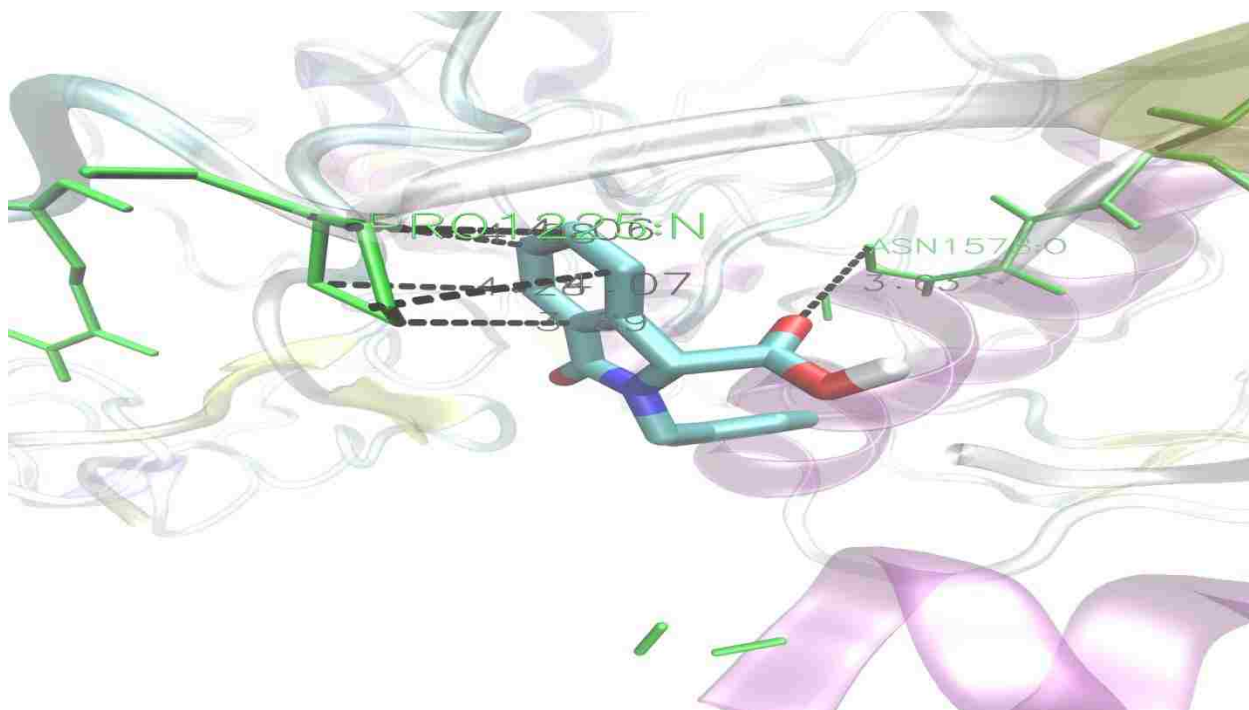
Figure 6.2. Docking image for compound **70** with active site of DNMT1.
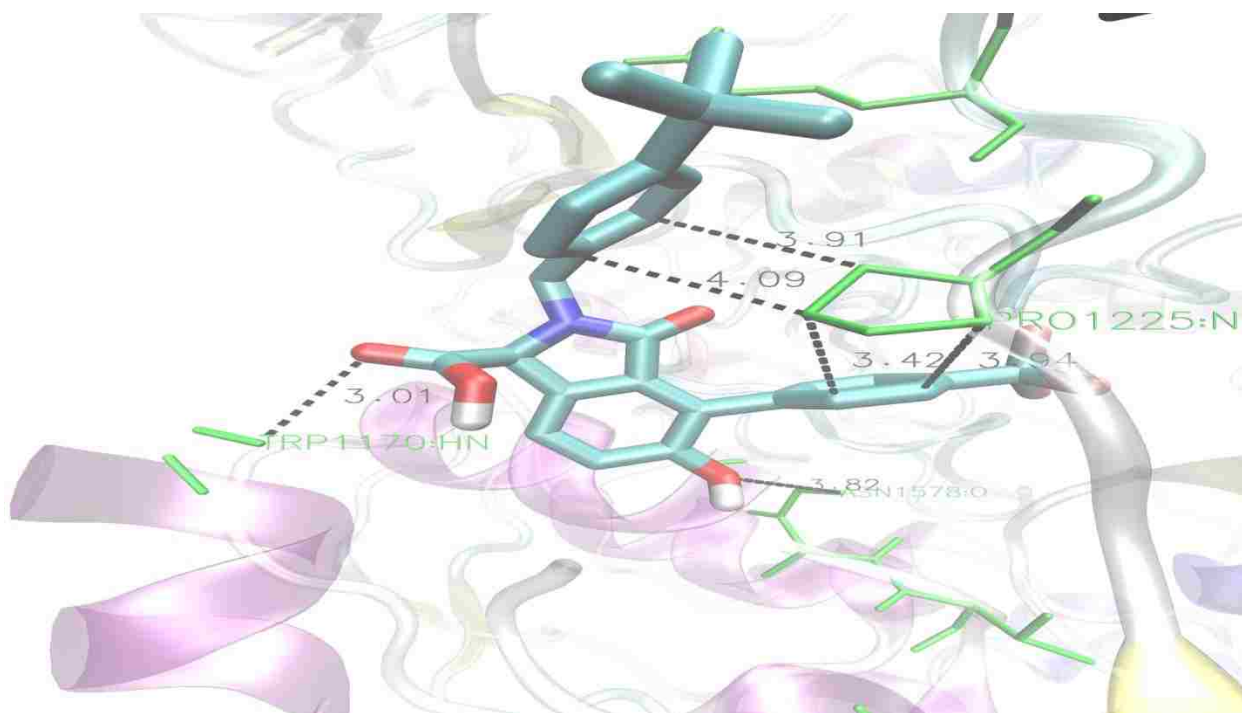
Figure 6.3. Docking image for compound 75 with active site of DNMT1.

The great thing about this research project is that the molecules made are modular and can be altered with ease. One direction this project can go is to create a series of compounds using the homophthalic acid synthetic route with functional groups on the ring (Figure 6.4). The series begins by synthesizing 5-nitrohomophthalic acid **82**, which can be obtained by selective nitration of homophthalic acid **48**.[126] Compound **83** is achieved my reducing the nitro group in **82** to an amine by catalytic hydrogenation on 10% Pd/C.[127] The amine is then protected with phthalic anhydride to make compound **84**.[128] Compound **85**, **A**, and **B** are prepared like their counterparts (Figure 4.1). The amine protecting group is removed to create compound in series **C**. Diazotation using sodium nitrate will give the diazonium salt series **D**. Series **D** can be converted to series **E** by reacting with cuprous halides or by hydrolysis by sulfuring acid. **C** can

be treated with acyl chlorides in a KOH solution to yield the compounds in series **F**. Series **C** can easily be converted to the series **H** by simple esterification techniques. These new series of compounds will allow us to evaluate the importance of different types of functional groups on the ring as well on the R_4 position.

6.2   Competition studies

This dissertation research relied upon computational calculations to extrapolate $K_i^{'}$ values based on one time point and a single concentration. This process was reliable and resulted in the identification of new lead compounds. To take this research a step further, the current lead compounds could be examined in a competition study as outlined by Gros *et al.*[107] In this study, the leads will be tested in a SAM-competition assay and DNA-competition assay.

In the SAM- competition assay, the SAM concentration will be varied, while the DNA concentration will be fixed. For each SAM concentration, the lead compounds concentrations will be adjusted between IC_{10} and its IC_{80}. In the DNA-competition assay, the DNA concentration will be varied, while the SAM concentration will be fixed. For each DNA concentration, the lead compounds concentration will be adjusted between IC_{10} and its IC_{80}.

For each substrate concentrations, the IC_{50} of the tested compound will be calculated by non-linear regression fitting with sigmoidal dose response. For each compound concentration, K_m and V_m of each substrate will be approximated by non-linear fitting of the data with the Michaelis-Menten equation. This study will allow us to confirm if our lead compounds act as competitive inhibitor.
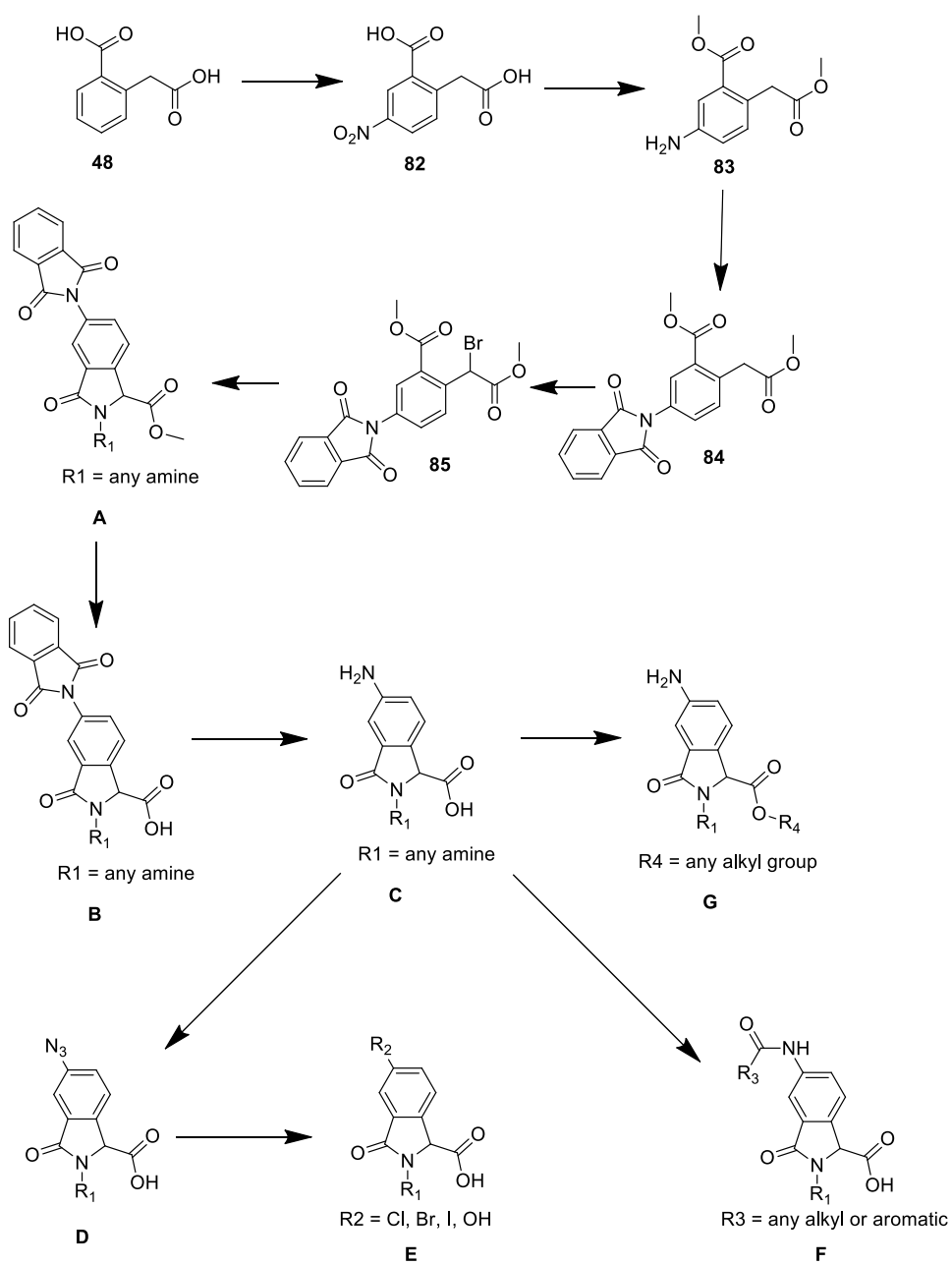
Figure 6.4. Future directions for project.

Chapter 7 **EXPERIMENTAL SECTION**

Experimental Section General Procedures. Solvents were obtained from Fisher Scientific. All

other chemicals, unless noted otherwise, were obtained from the Aldrich Chemical Co.

(Milwaukee, WI). The solvents MeOH (over $Mg(OMe)_2$) and THF (over Na/K-benzophenone)

were dried and distilled prior to use. Solutions were concentrated by evaporation *in vacuo*. All

synthesis procedures, unless noted otherwise, were carried out under a slight positive pressure

of argon gas at ambient temperature (21-25 °C). Column chromatography was performed using

Merck Silica Gel 60. NMR spectra were acquired at 400 MHz (^{1}H) and 100 MHz (^{13}C), were

referenced to the residual solvent, and are reported as follows: chemical shift (δ/ppm), splitting

pattern, coupling constant (*J/Hz*), and intensity.

Radioactivity-based assay procedure

Reagents. A 10X buffer solution (BP1) was prepared (pH = 7.8 ,50.0 mM Tris-HCl, 1.0 mM EDTA,

5% v/v glycerol) and used in the reaction buffer (1X BP1, 0.1 $mg.mL^{-1}$ bovine serum albumin

(BSA) with 3.0 mM dithiothreitol (DTT)).

Radioactivity-based assay. The radioactivity-based gel filtration assay was performed in

triplicate (50 μL total reaction volumes), containing the test compound (250 μM, in 5% v/v

DMSO), [methyl-^{3}H] SAM (0.372 μM in H_2O, PerkinElmer, 15 $Ci.mmol^{-1}$), poly(deoxyinosinic-

deoxycytidylic) acid sodium salt (1.8 μg, Sigma Aldrich), reaction buffer and DNMT1 (25.0 ng,

BPS Bioscience). The reaction was incubated at 37 °C for 1 h, then the tritium labeled DNA

separated by passing through a Micro Bio-Spin® P-30 size exclusion column (Bio-Rad). Both

negative (DMSO carrier with no inhibitor present) and positive controls (*S*-

adenosylhomocysteine, 10 μM, Sigma Aldrich) were also tested in triplicate. The column eluate

was transferred to scintillation vials with Ultima Gold liquid scintillation cocktail (5 mL, PerkinElmer). After thorough mixing, the samples were read on a Beckman 1500 scintillation counter, with a maximum time limit of counting fixed to 1 h. All counts were reported in disintegrations per minute (dpm).
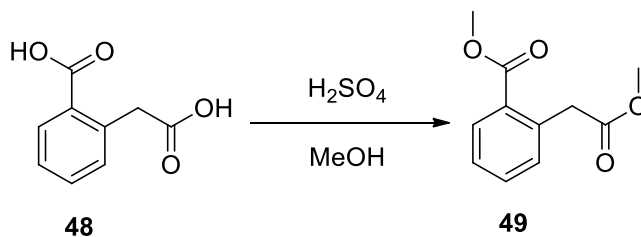
49: **Methyl 2-(2-methoxy-2-oxoethyl)benzoate:** A solution of **48** (10.0 g, 55.5 mmol) in MeOH (100 mL) was heated to 30 °C for 10 minutes. H_2SO_4 (5.0 ml, 5% v/v) was added and the reaction heated to reflux for 2 hours. The progress of the reaction was followed by TLC (EtOAc-hexanes , 1:1). When **48** had been consumed the reaction was allowed to cooled to room temperature and neutralized to pH 7 with aq. sat. $NaHCO_3$ solution (5 mL) and extracted with EtOAc (3 × 5 mL). The organic extracts were combined, dried over anhyd. Na_2SO_4, and concentrated by evaporation *in vacuo* to afford a yellow oil (9.57g, 83%). Compound **49** was used in the subsequent step without further purification. ^{1}H NMR (400 MHz, CDCl$_3$) δ ppm 7.99 (d, *J* =7.8 Hz, 1H), 7.43 (t, *J* = 7.5 Hz, 1H), 7.31 (t, *J* = 7.5 Hz, 1H) 7.22 (d, *J* = 7.5 Hz, 1H), 3.98 (s, 2H), 3.82 (s, 3H), and 3.65 (s, 3H). ^{13}C NMR (100 MHz, CDCl$_3$) δ ppm 171.48, 167.03, 135.67, 131.94, 130.60, 129.24, 127.03, 51.53, 51.43, and 40.04. This known compound was synthesized following the procedure outlined by Wang *et al*.[129]
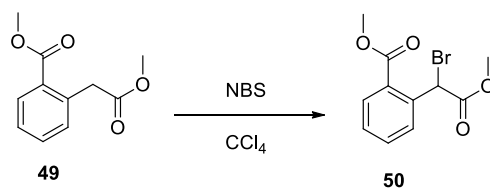
50:   **Methyl 2-(1-bromo-2-methoxy-2-oxoethyl)benzoate:** A solution of **49** (9.57 g, 46.0

mmol) in CCl$_4$ (70 mL) was heated at reflux for 5 min. *N*-Bromosuccinimide (16.50 g,

92.70 mmol) was added followed by AIBN (0.77 g, 4.7 mmol) and two drops of aq. HBr

(45 % w/v), the progress of the reaction followed by TLC (EtOAc-hexanes, 1:1). When

49 had been consumed the reaction was allowed to cool to rt, filtered and the filtrate

concentrated by evaporation *in vacuo* to give an oil. Compound **50** was obtained by

chromatography on silica gel, eluting with EtOAc-hexanes (7-25% gradient) as a yellow

oil (8.10 g, 62%). ^{1}H NMR (400 MHz, CDCl$_3$) δ ppm 7.97 (d, *J* = 6.5 Hz, 1H), 7.88 (d, *J* =

6.9 Hz, 1H), 7.58 (t, *J* = 7.6 Hz, 1H), 7.41, (t, *J* = 7.7 Hz, 1H), 6.59 (s, 1H), 3.92 (s, 3 H),

and 3.79 (s, 3H). ^{13}C NMR (100 MHz, CDCl$_3$) δ ppm 169.04, 166.90, 137.04, 132.75,

131.54, 130.64, 128.72, 128.18, 53.27, 52.36 and 43.97. This known compound was

synthesized following the procedure outlined by Kim *et al.*[130]

50

51
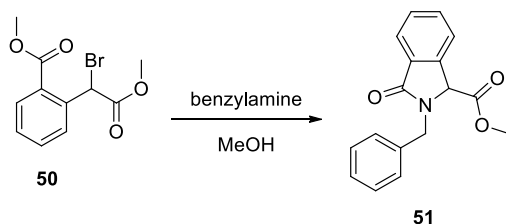
51: **Methyl 2-benzyl-3-oxoisoindoline-1-carboxylate:** A solution of methyl 2-(1-bromo-2-

methoxy-2-oxoethyl)benzoate (308 mg, 1.07 mmol) in MeOH (20 mL) was stirred at

room temperature for 5 minutes. Dropwise addition of 30% benzylamine (588μL, 5.38

mmol) in MeOH was added over 30 minutes and the progress of the reaction followed

by TLC (EtOAc-hexanes, 1:1). When the starting material had been consumed the

reaction was quenched with 2M HCl (10 mL) and extracted with EtOAc (3 × 15 mL). The

organic extracts were combined, dried over anhyd. Na_2SO_4, and concentrated by

evaporation *in vacuo* to afford a brown oil. **51** was obtained by chromatography on

silica gel, eluting with EtOAc-hexanes-triethylamine (75:25:1) as a white solid (117.1

mg, 33.3%). ^{1}H NMR (400 MHz, $CDCl_3$) δ ppm 7.90 - 7.96 (m, 1H), 7.53 - 7.61 (m, 3H),

7.25 - 7.40 (m, 5H), 5.50 (d, *J* = 15.1 Hz, 1H), 4.97 (s, 1H), 4.32 (d, *J* = 15.1 Hz, 1H), and

3.79 (s, 3H). ^{13}C NMR (100 MHz, $CDCl_3$) δ ppm 168.7, 139.2, 136.3, 131.9, 129.3, 128.8,

128.5, 127.8, 124.1, 122.8, 77.3, 77.2, 76.7, 61.2, 52.9, and 45.1. HRMS (ESI-TOF) *m/z*

calcd. for $C_{17}H_{16}NO_3$: 335.1390; found 335.1389 ([M + H]$^+$, Δ ppm 0.23).
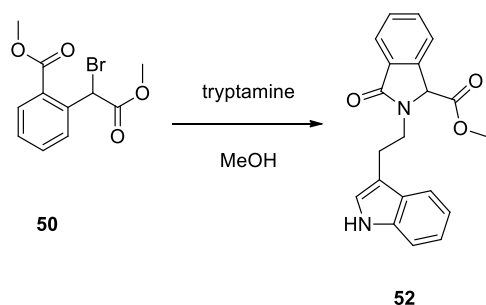
52: **Methyl 2-(2-(1H-indol-2-yl)ethyl)-3-oxoisoindoline-1-carboxylate:** A solution of methyl

2-(1-bromo-2-methoxy-2-oxoethyl)benzoate (2.87 g, 10.0 mmol) in MeOH (200 mL)

was stirred at room temperature for 5 minutes. Dropwise addition of 30% tryptamine

(6.73 g, 50.0 mmol) in MeOH was added over 30 minutes and the progress of the

reaction followed by TLC (EtOAc-hexanes, 1:1). When the starting material had been

consumed the reaction was quenched with 2M HCl (10 mL) and extracted with

methylene chloride (3 × 60 mL). The organic extracts were combined, dried over

anhyd. Na_2SO_4, and concentrated by evaporation *in vacuo* to afford orange oil. **52** was

obtained by chromatography on silica gel, eluting with EtOAc-hexanes-triethylamine

(25:75:1) as a orange solid (2.87 g, 86%). ^{1}H NMR (400 MHz, CDCl$_3$) δ ppm 8.57 (bs, 1H),

7.84 - 7.88 (m, 1H), 7.63 (d, *J* = 8.0 Hz, 1H), 7.63 (d, *J* = 8.0 Hz, 1H), 7.46 - 7.54 (m, 3H),

7.36 (td, *J* = 0.9, 8.03 Hz, 1H), 7.18 (dt, *J* = 1.1, 7.59 Hz, 1H), 7.10 (ddd, *J* = 1.1, 7.0, 7.9

Hz, 1H), 7.01 (d, *J* = 2.5 Hz, 1H), 5.02 (s, 1H), 4.49 (s, 1H), 3.70 (s, 3H), 3.58 - 3.68 (m,

1H), and 3.10 - 3.22 (m, 2H) ^{13}C NMR (100 MHz, CDCl$_3$) δ ppm 168.8, 168.8, 139.4,

136.5, 132.0, 131.9, 129.3, 127.2, 123.8, 122.8, 122.1, 122.1, 119.3, 118.6, 112.5,

111.4, 62.5, 60.4, 52.9, 41.9, 24.2, 21.1, and 14.2. HRMS (ESI-TOF) *m/z* calcd. for

$C_{20}H_{19}N_2O_3$: 282.1125; found 282.1124 ([M + H]$^+$, Δ ppm 0.27).
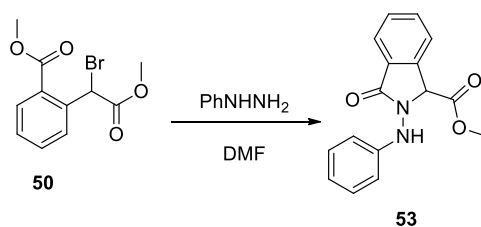
53: **Methyl 3-oxo-2-(phenylamino)isoindoline-1-carboxylate:** A solution of phenyl

hydrazine (0.13 mL, 1.31 mmol) in DMF (0.30 mL) was stirred at room temperature for

5 minutes. Trimethylamine (0.24 mL, 1.74 mmol) followed by a solution of methyl 2-(1-

bromo-2-methoxy-2-oxoethyl)benzoate (0.265 g, 0.92 mmol) in DMF (0.14 mL) was

added and the progress of the reaction followed by TLC (EtOAc-hexanes, 1:1). When

the starting material had been consumed, the reaction was quenched with EtOAc, and

washed with aq. NaHCO$_3$. The organic extracts were combined, dried over anhyd.

Na$_2$SO$_4$, and concentrated by evaporation *in vacuo* to afford a brown oil. **53** was

obtained by chromatography on silica gel, eluting with EtOAc-hexanes (10-35%

gradient) as an orange solid (91.8 mg, 35.2%). ^{1}H NMR (400 MHz, (CD$_3$)$_2$SO) δ ppm 7.96

(d, *J* = 7.5 Hz, 1H), 7.66 (d, *J* = 4.0 Hz, 2H), 7.55 - 7.62 (m, 1H), 7.21 - 7.27 (m, 2H), 6.90 -

6.96 (t, *J* = 7.4 Hz, 1H), 6.75 - 6.80 (m, 2H), 6.40 (s, 1H), 5.45 (s, 1H), and 3.84 (s, 3H). [13]C

NMR (100 MHz, (CD$_3$)$_2$SO) δ 168.5, 166.3, 147.3, 138.3, 132.9, 130.1, 129.5, 128.8,

123.6, 123.3, 119.3, 112.4, 63.4, and 53.0.
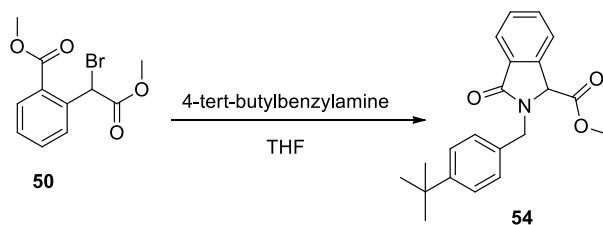
54: **Methyl 2-(4-(tert-butyl)benzyl)-3-oxoisoindoline-1-carboxylate:** A solution of 4-tert-

butylbenzyleamine (1.02 mL, 5.80 mmol) in THF (2.62 mL) was stirred at room

temperature for 5 minutes. Triethylamine (0.88 ml, 6.29 mmol) was added dropwise

and the reaction solution was brought to 0 °C. Methyl 2-(1-bromo-2-methoxy-2-

oxoethyl)benzoate (1.51 g, 5.25 mmol) was added and the progress of the reaction

followed by TLC (EtOAc-hexanes, 1:1). When the starting material had been

consumed, the reaction was quenched with 2M HCl (30 mL) and extracted with EtOAc

(3 × 60 mL). The organic extracts were combined, dried over anhyd. Na_2SO_4, and

concentrated by evaporation *in vacuo* to afford a yellow oil. **54** was obtained by

chromatography on silica gel, eluting with EtOAc-hexanes-triethylamine (25:75:1) as a

clear oil (1.40 g, 79.8%).^{1}H NMR (400 MHz, CDCl₃) δ ppm 7.87 - 7.94 (m, 1H), 7.48 - 7.57

(m, 3H), 7.34 (d, *J* = 8.0 Hz, 2H), 7.20 (d, *J* = 8.2 Hz, 2H), 5.44 (d, *J* = 14.8 Hz, 1H), 4.96 (s,

1H), 4.26 (d, *J* = 14.8 Hz, 1H), 3.77 (s, 3H), and 1.27 - 1.32 (m, 9H). ^{13}C NMR (100 MHz,

CDCl₃) δ ppm 168.7, 168.3, 150.8, 139.2, 133.2, 131.9, 131.8, 129.2, 128.9, 128.2,

127.7, 125.7, 125.6, 125.2, 124.1, 122.8, 61.2, 52.9, 44.7, 34.5, and 31.3.
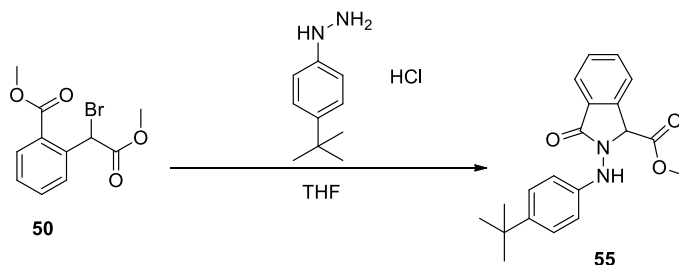
55: **Methyl 2-((4-(tert-butyl)phenyl)amino)-3-oxoisoindoline-1-carboxylate:** A solution of

4-tert-butylphenylhydrazine monohydrochloride (0.40 g, 2.0 mmol) in THF (1.0 mL) was

stirred at room temperature for 5 minutes. Triethylamine (1.23 mL, 8.8 mmol) and

DMF (0.2 mL) was added and the reaction solution brought to 0 °C. A solution of

methyl 2-(1-bromo-2-methoxy-2-oxoethyl)benzoate (0.50 g, 1.7 mmol) in DMF (0.50

mL) was added and the reaction progress followed by TLC (EtOAc-hexanes, 1:1). When

the starting material had been consumed, the reaction was quenched with EtOAc, and

washed with aq. NaHCO$_3$. The organic extracts were combined, dried over anhyd.

Na$_2$SO$_4$, and concentrated by evaporation *in vacuo* to afford a brown oil. **55** was

obtained by chromatography on silica gel, eluting with EtOAc-hexanes (5-25% gradient)

as an orange solid (91.8 mg, 14.2%).^{1}H NMR (400 MHz, CDCl$_3$) δ 8.08 (dd, *J* = 1.3 Hz, 7.8

Hz, 1H), 7.52 (dt, *J* = 1.5 Hz, 7.53 Hz, 1H), 7.45 (m, 2H), 7.29 (m, 1H), 7.24 (m, 2H), 7.00

(m, 2H), 5.45 (s, 1H), 3.80 (s, 3H), and 1.24 (s, 9H). ^{13}C NMR (100 MHz, CDCl$_3$) δ 169.2,

164.6, 146.4, 146.0, 133.9, 133.2, 129.0, 127.5, 127.4, 126.3, 126.2, 116.8, 66.4, 53.1,

34.1, and 31.3. HRMS (ESI-TOF) *m/z* calcd. for C$_{20}$H$_{23}$N$_2$O$_3$: 339.1703; found 339.1711

([M + H]$^+$, Δ ppm 2.43).

56
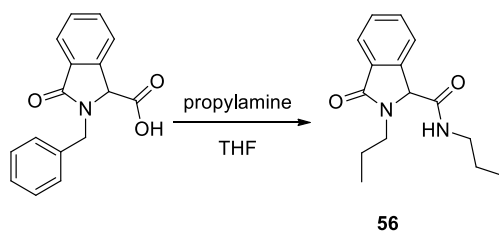
56: **3-Oxo-*N*,2-dipropylisoindoline-1-carboxamide:** A solution of 3-oxo-2-

propylisoindoline-1-carboxylic acid (47.5 mg, 0.216 mmol) in dry THF (1.55 mL) was

chilled to 0 °C. CDI (38.6 mg, 0.238 mmol) was added and the reaction stirred for 2 h.

Propylamine (27.0 μL, 0.325 mmol) was added and the reaction was allowed to reach

rt. The progress of the reaction was followed by TLC (EtOAc-hexanes, 1:1). When the

starting material had been consumed, the reaction was quenched with aq. sat. $NaHCO_3$

and extracted with EtOAc (3 × 5 mL). The organic extracts were combined, dried over

anhyd. Na_2SO_4, and concentrated by evaporation *in vacuo* to afford an oil. **56** was

obtained by chromatography on silica gel, eluting with EtOAc-hexanes-triethylamine

(50:50:1) as a clear oil (24.1 mg, 43%). ^{1}H NMR (400 MHz, $CDCl_3$) δ ppm 7.67 (t, *J* = 7.2

Hz, 2H), 7.56 (t, *J* = 7.7 Hz, 1 H), 7.45 (t, *J* = 7.4 Hz, 1H), 6.23 (bs, 1H), 5.06 (s, 1H), 4.03-

3.96 (m, 1H), 3.30-3.21 (m, 1H), 3.16-3.10 (m, 2H) 1.74-1.62 (m, 2H), 1.50-1.41 (m, 2H),

0.92 (t, *J* = 7.4, 3H), and 0.81 (t, *J* = 7.40, 3H). ^{13}C NMR (100 MHz, $CDCl_3$) δ ppm 169.59,

167.87, 141.24, 132.24, 130.84, 128.99, 123.64, 122.74, 64.56, 43.43, 41.26, 22.58,

21.29, 11.28, and 11.14.   HRMS (ESI-TOF) *m/z* calcd. for $C_{15}H_{21}N_2O_2$: 261.1598; found

261.1594 ([M + H][+], Δ ppm 1.44).
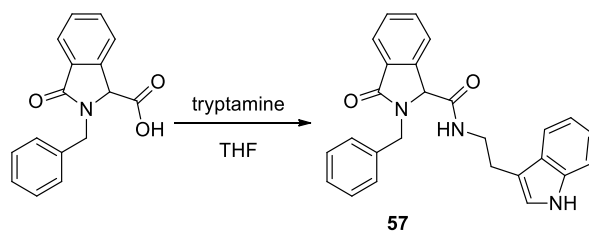
57: ***N*-(2-(1H-indol-3-yl)ethyl)-2-benzyl-3-oxoisoindoline-1-carboxamide:** A solution of 2-benzyl-3-oxo-2,3-dihydro-1H-isonide-1-carboxylic acid (47.4 mg, 0.177 mmol) in dry THF (1.28 mL) was chilled to 0 °C. CDI (31.6 mg, 0.195 mmol) was added and the reaction stirred for 2 h. Tryptamine (42.6 mg, 0.266 mmol) was added and the reaction was allowed to reach rt. The progress of the reaction was followed by TLC (EtOAc-hexanes, 1:1). When the starting material had been consumed, the reaction was quenched with aq. sat. NaHCO$_3$ and extracted with EtOAc (3 × 5 mL). The organic extracts were combined, dried over anhyd. Na$_2$SO$_4$, and concentrated by evaporation *in vacuo* to afford a brown oil. **57** was obtained by chromatography on silica gel, eluting with EtOAc-hexanes-triethylamine (75:25:1) as a clear oil (10.3 mg, 21.8%).^{1}H NMR (400 MHz, CDCl$_3$) δ ppm 8.08 (s, 2H), 7.81 (d, *J* = 7.4 Hz, 2 H), 7.58-7.47 (m, 10 H), 7.35 (d, *J* = 8.2, 1H), 7.24-7.19 (m, 9H), 7.13-7.09 (m, 6H), 6.71 (d, *J* = 2.0 Hz, 2H), 5.97 (t, *J* = 5.7 Hz, 2H) 5.12 (d, J = 14.9 Hz, 2H), 4.79 (s, 2H), 4.13 (q, *J*= 7.2 Hz, 1H), 3.94 (d, *J*= 14.8 Hz, 2H), 3.58-3.45 (m, 5H), 2.95-2.76 (m, 5H), 2.06 (s, 2H), 1.27 (t, *J* = 7.2 Hz, 4H) and 0.95-0.89 (m, 1H). ^{13}C NMR (100 MHz, CDCl$_3$) δ ppm 169.51, 167.39, 141.33, 136.37, 136.04, 132.45, 130.50, 129.06, 128.89, 128.33, 127.95, 127.00, 123.94, 122.89, 122.33, 121.95, 119.62, 118.50, 112.24, 111.32, 64.00, 60.38, 45.52, 39.40, 24.83 and 21.04. HRMS (ESI-TOF) *m/z* calcd. for C$_{26}$H$_{24}$N$_3$O$_2$: 410.1863; found 410.1853

([M + H]$^+$, Δ ppm 2.38).
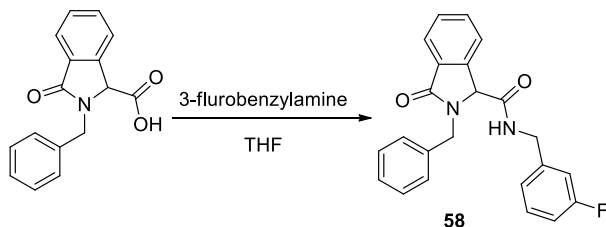
58: **2-Benzyl-*N*-(3-fluorobenzyl)-3-oxoisoindoline-1-carboxamide:** A solution of 2-benzyl-

3-oxoisoindoline-1-carboxylic acid (86.9 mg, 0.325 mmol) in dry THF (2.34 mL) was

chilled to 0 ^{o}C. CDI (58.0 mg, 0.358 mmol) was added and the reaction stirred for 2 h.

3-flurobenzylamine (55.6 μL, 0.488 mmol) was added and the reaction was allowed to

reach rt. The progress of the reaction was followed by TLC (EtOAc-hexanes, 3:2).

When the starting material had been consumed, the reaction was quenched with aq.

sat. NaHCO$_3$ and extracted with EtOAc (3 × 5 mL). The organic extracts were combined,

dried over anhyd. Na$_2$SO$_4$, and concentrated by evaporation *in vacuo* to afford a brown

oil. **58** was obtained by chromatography on silica gel, eluting with EtOAc-hexanes-

triethylamine (60:40:1) as a clear oil (42.3 mg, 34.8%). ^{1}H NMR (400 MHz, CDCl$_3$) δ ppm

7.53 (d, *J* = 7.5 Hz, 1H), 7.45 (td, *J* = 6.9 Hz, 1.38 Hz, 1H) 7.35-7.25 (m, 4H), 7.24-7.17

(m,2H), 7.15-7.09 (m, 3H), 6.84 (dd, *J* = 79 Hz, 1.76 Hz, 2 H) 6.76 (dt, *J* = 9.5 Hz, 1.9 Hz,

1H), 5.16 (d, *J* = 14.9 Hz, 1H), 4.83 (s, 1H), 4.33 (d, *J* = 6.0 Hz, 2H), and 4.13 (d, *J* = 14.9

Hz, 1H). ^{13}C NMR (100 MHz, CDCl$_3$) δ ppm 169.57, 167.77164.09, 161.64, 141.12,

140.53, 140.46, 135.87, 132.43, 130.40, 130.13, 130.04, 129.6, 128.97, 128.41, 128.08,

123.71, 123.19, 122.77, 114.63, 114.48, 114.41, 114.27, 64.16, 45.79, and 42.83.

HRMS (ESI-TOF) *m/z* calcd. for $C_{23}H_{20}FN_2O_2$: 375.1504; found 375.1508 ([M + H]$^+$, Δ ppm 1.13).
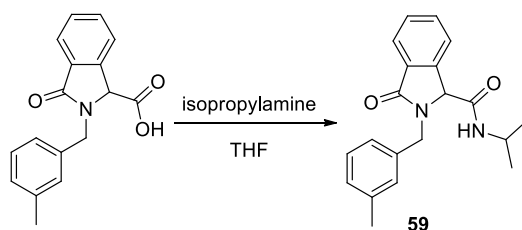
59: ***N*-Isopropyl-2-(3-methylbenzyl)-3-oxoisoindoline-1-carboxamide:** A solution of 2-(3-methyl-benzyl)-3-oxo-2,3-dihydro-1H-isonide-1-carboxylic acid (91.2 mg, 0.320 mmol) in dry THF (2.32 mL) was chilled to 0 °C. CDI (57.8 mg, 0.360 mmol) was added and the reaction stirred for 2 h. Isopropylamine (39 μL, 0.48mmol) was added and the reaction was allowed to reach rt. The progress of the reaction was followed by TLC (EtOAc-hexanes, 1:1). When the starting material had been consumed, the reaction was quenched with aq. sat. NaHCO$_3$ and extracted with EtOAc (3 × 5 mL). The organic extracts were combined, dried over anhyd. Na$_2$SO$_4$, and concentrated by evaporation *in vacuo* to afford a brown oil. **59** was obtained by chromatography on silica gel, eluting with EtOAc-hexanes-triethylamine (75:25:1) as a clear oil (10.3 mg, 17.2%). ^{1}H NMR (400 MHz, CDCl$_3$) δ ppm 7.77 (d, *J* = 7.5 Hz, 1H), 7.62 (d, *J* = 7.5 Hz, 1H), 7.55 (t, *J* = 7.4 Hz, 1H), 7.47 (t, *J* = 7.3 Hz, 1H), 7.21 (t, *J* = 7.5 Hz, 1H), 7.11 (d, *J* = 4.5 Hz, 2H), 7.09 (bs, 1H), 5.91 (d, *J* = 7.5 Hz, 1H), 5.16 (d, *J* = 14.7 Hz, 1H), 4.84 (s, 1H), 4.32 (d, *J* = 14.7 Hz, 1H), 3.96 - 4.05 (m, 1H), 2.31 (s, 3H), 1.07 (d, *J* = 6.53 Hz, 3H), and 0.91 - 0.96 (m,

3H). ^{13}C NMR (100 MHz, CDCl$_3$) δ ppm 169.8, 166.6, 141.5, 138.8, 136.3, 132.4, 130.5, 129.2, 129.0, 128.9, 128.8, 125.6, 123.9, 122.7, 64.5, 46.1, 41.6, 22.3, 22.1, and 21.3. HRMS (ESI-TOF) *m/z* calcd. for C$_{20}$H$_{23}$N$_2$O$_2$: 323.1754; found 323.1752 ([M + H]$^+$, Δ ppm 0.54).

60
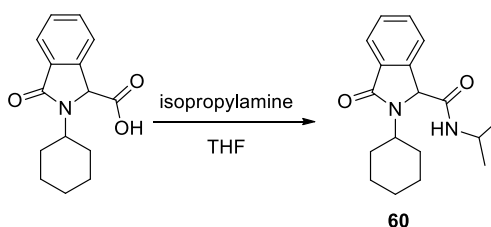
60: **2-Cyclohexyl-*N*-isopropyl-3-oxoisoindoline-1-carboxamide:** A solution of 2-cyclohexyl-3-oxo-2,3-dihydro-1H-isoindole-1-carboxylic acid (62.3 mg, 0.240 mmol) in dry THF (2.73 mL) was chilled to 0 °C. CDI (43.3 mg, 0.267 mmol) was added and the reaction stirred for 2 h. Isopropyl amine (30.0 µL, 0.360 mmol) was added and the reaction was allowed to reach rt. The progress of the reaction was followed by TLC (EtOAc-hexanes, 1:1). When the starting material had been consumed, the reaction was quenched with aq. sat. NaHCO$_3$ and extracted with EtOAc (3 × 5 mL). The organic extracts were combined, dried over anhyd. Na$_2$SO$_4$, and concentrated by evaporation *in vacuo* to afford a brown oil. **60** was obtained by chromatography on silica gel, eluting with EtOAc-hexanes-triethylamine (50:50:1) as a clear oil (8.0 mg, 11.1%). ^{1}H NMR (400 MHz, CDCl$_3$) δ ppm 7.76 (d, *J* = 7.5 Hz, 1H), 7.61 (d, *J*= 7.4 Hz, 1 H), 7.56 (t, *J* = 7.3 Hz, 1H), 7.48 (t, *J* =7.5,1H), 5.69 (d, *J* = 7.9 Hz, 1H), 5.05 (s, 1H), 4.15-3.98 (m, 2H), 2.0 (d, *J* = 11.9 Hz,1H) 1.88-1.80 (m, 3H), 1.71-1.55 (m, 4H), 1.45-1.34 (m, 2H), 1.13 (d, *J* = 6.7

Hz, 3H), and 0.92 (d, J = 6.7Hz, 3H). ^{13}C NMR (100 MHz, CDCl$_3$) δ ppm 170.14, 167.97, 141.73, 132.02, 130.85, 128.62, 123.41, 122.08, 63.23, 53.54, 41.32, 30.62, 30.55, 25.51, 25.39, 24.92, and 21.82. HRMS (ESI-TOF) m/z calcd. for C$_{18}$H$_{25}$N$_2$O$_2$: 301.1911; found 301.1918 ([M + H]$^+$, Δ ppm 2.40).
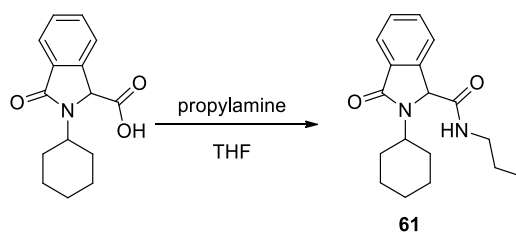
61: **2-Cyclohexyl-3-oxo-N-propylisoindoline-1-carboxamide:** A solution of 2-cyclohexyl-3-oxoisoindoline-1-carboxylic acid (76.3 mg, 0.294 mmol) in dry THF (2.12 mL) was chilled to 0 $^{\circ}$C. CDI (56.0 mg, 0.323 mmol) was added and the reaction stirred for 2 h. Propylamine (26.1 mg, 0.441 mmol) was added and the reaction was allowed to reach rt. The progress of the reaction was followed by TLC (EtOAc-hexanes, 1:1). When the starting material had been consumed, the reaction was quenched with aq. sat. NaHCO$_3$ and extracted with EtOAc (3 × 5 mL). The organic extracts were combined, dried over anhyd. Na$_2$SO$_4$, and concentrated by evaporation *in vacuo* to afford a brown oil. **61** was obtained by chromatography on silica gel, eluting with EtOAc-hexanes-triethylamine (75:25:1) as a clear oil (22.2 mg, 25%). ^{1}H NMR (400 MHz, CDCl$_3$) δ ppm 7.60 (d, J = 7.8 Hz, 1H), 7.63 (d, J = 7.5 Hz, 1H), 7.53 (t, J = 7.3 Hz, 1H), 7.42 (t, J = 7.4 Hz, 1H), 6.28 - 6.37 (m, 1H), 5.07 (s, 1H), 4.07 (tt, J = 3.5, 12.1 Hz, 1H), 3.06 - 3.24 (m, 2H),

1.98 - 2.08 (m, 1H), 1.75 - 1.90 (m, 3H), 1.53 - 1.72 (m, 4H), 1.29 - 1.49 (m, 5H), 1.09 -

1.27 (m, 2H), and 0.78 (t, J = 7.4 Hz, 3H). ^{13}C NMR (100 MHz, CDCl$_3$) δ ppm 170.3, 169.3,

141.5, 132.2, 131.2, 128.8, 123.5, 122.4, 63.6, 53.8, 41.2, 30.8, 30.8, 25.8, 25.7, 25.2,

22.5, and 11.2.   HRMS (ESI-TOF) m/z calcd. for C$_{18}$H$_{25}$N$_2$O$_2$: 301.1911; found 301.1916

([M + H]$^+$, Δ ppm 1.74).

62: **2-Cyclohexyl-*N*-(2-morpholinoethyl)-3-oxoisoindoline-1-carboxamide:** A solution of 2-

cyclohexyl-3-oxo-2,3-dihydro-1H-isoindole-1-carboxylic acid (76.8 mg, 0.296 mmol) in

dry THF (3.50 mL) was chilled to 0 °C. CDI (54.7 mg, 0.337 mmol) was added and the

reaction stirred for 2 h. 4-(2-aminoethyl) morpholine (58.6 mg, 0.450 mmol)) was

added and the reaction was allowed to reach rt. The progress of the reaction was

followed by TLC (EtOAc-hexanes, 1:1). When the starting material had been

consumed, the reaction was quenched with aq. sat. NaHCO$_3$ and extracted with EtOAc

(3 × 5 mL). The organic extracts were combined, dried over anhyd. Na$_2$SO$_4$, and

concentrated by evaporation *in vacuo* to afford a brown oil. **62** was obtained by

chromatography on silica gel, eluting with EtOAc-hexanes-triethylamine (60:40:1) to

MeOH-EtOAc (10:90) as a yellow oil (24.6 mg, 22.4%). ^{1}H NMR (400 MHz, CDCl$_3$) δ ppm

7.70 (d, *J* = 7.4 Hz, 1H), 7.59 (d, *J* = 7.7 Hz, 1 H), 7.52 (t, *J* = 7.4 Hz, 1H), 7.42 (t, *J* = 7.3 Hz, 1H), 6.56 (s,1H), 5.05 (s, 1H), 5.05 (s, 1H), 4.07-3.99 (m,2H) 3.69-3.61 (m, 2H), 3.55 (t, *J* = 4.1 Hz, 4H), 3.41-3.34 (m, 1H), 3.19-3.11 (m,1H), 2.52-2.25 (m, 9H), 2.05 (d, *J* = 11.8 Hz, 1H), 1.81 (d, *J* = 12.67 Hz, 4H), 1.72-1.54 (m,4H), 1.41-1.28 (m, 3H), and 1.23-1.10 (m, 2H). ^{13}C NMR (100 MHz, CDCl$_3$) δ ppm 170.13, 169.19, 141.91, 132.09, 131.29, 128.82, 123.52, 122.46, 66.61, 63.50, 56.55, 53.93, 53.12, 35.68, 30.70, 30.66, 25.79, 25.72, and 25.19. HRMS (ESI-TOF) *m/z* calcd. for C$_{21}$H$_{30}$N$_3$O$_3$: 372.2282; found 372.2267 ([M + H]$^+$, Δ ppm 3.97).
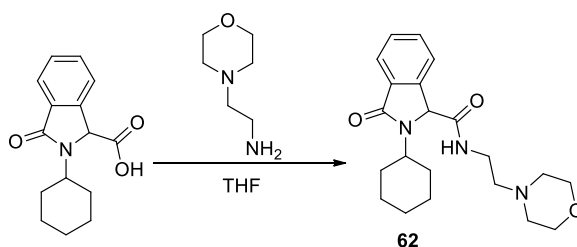

63

63:      ***N*,2-Dicyclohexyl-3-oxoisoindoline-1-carboxamide:** A solution of 2-cyclohexyl-3-oxo-2,3-dihydro-1H-isoindole-1-carboxylic acid (76.7 mg, 0.296 mmol) in dry THF (1.5 mL) was chilled to 0 °C. CDI (53.6 mg, 0.331 mmol) was added and the reaction stirred for 2 h. Cyclohexylamine (51.0 μL, 0.444 mmol) was added and the reaction was allowed to reach rt. The progress of the reaction was followed by TLC (EtOAc-hexanes, 1:1). When the starting material had been consumed, the reaction was quenched with aq. sat. NaHCO$_3$ and extracted with EtOAc (3 × 5 mL). The organic extracts were combined, dried over anhyd. Na$_2$SO$_4$, and concentrated by evaporation *in vacuo* to afford a brown oil. **63** was obtained by chromatography on silica gel, eluting with EtOAc-hexanes-

triethylamine (40:60:1) as a clear oil (6.2 mg, 6.2%). ^{1}H NMR (400 MHz, CDCl$_3$) δ ppm

7.80 (d, J = 7.4 Hz, 1H), 7.61 (d, J = 7.3 Hz, 1 H), 7.55 (t, J = 7.5 Hz, 1H), 7.48 (t, J =

7.4,1H), 5.64 (d, J = 8.0, 1H), 5.05 (s, 1H), 4.15-4.07 (m, 2H), 3.75-3.65 (m,1H) 2.01-1.80

(m, 8H), 1.71-1.57 (m, 11H), 1.45-1.03 (m, 14H), and 0.98-0.77 (m, 2H). ^{13}C NMR (100

MHz, CDCl$_3$) δ ppm 170.49, 168.23, 142.12, 132.35, 131.16, 128.95, 123.74, 122.40,

63.64, 53.93, 48.53, 33.96, 32.67, 32.58, 30.98, 30.88, 25.83, 25.73, 25.26, 24.85, and
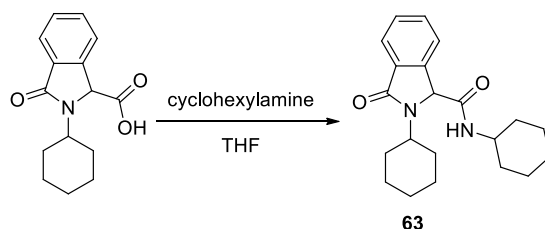
24.68.

64:   ***N*-(2-(1H-indol-3-yl)ethyl)-2-cyclohexyl-3-oxoisoindoline-1-carboxamide:** A solution of

2-cyclohexyl-3-oxo-2,3-dihydro-1H-isoindole-1-carboxylic acid (72.5 mg, 0.280 mmol) in

dry THF (1.5 mL) was chilled to 0 ^{o}C. CDI (67.2 mg, 0.414 mmol) was added and the

reaction stirred for 2 h. Tryptamine (67.1 mg, 0.419 mmol) was added and the reaction

was allowed to reach rt. The progress of the reaction was followed by TLC (EtOAc-

hexanes, 1:1). When the starting material had been consumed, the reaction was

quenched with aq. sat. NaHCO$_3$ and extracted with EtOAc (3 × 5 mL). The organic

extracts were combined, dried over anhyd. Na$_2$SO$_4$, and concentrated by evaporation

in vacuo to afford a brown oil. **64** was obtained by chromatography on silica gel,

eluting with EtOAc-hexanes-triethylamine (60:40:1) to (100:0:1) as a white solid (38.4

mg, 34.2%). ^{1}H NMR (400 MHz, CDCl$_3$) δ ppm 8.26 (bs, 1H), 7.65-7.56 (m, 2H), 7.49-7.39

(m, 3H), 7.35 (d, J = 8.0 Hz, 2H), 7.19 (t, J = 7.0 Hz, 1H), 7.12 (t, J =7.1 Hz, 1H), 7.04 (s,

1H) 6.69-6.54 (m, 2H), 3.72 (t, J = 6.2 Hz, 2H), 3.05 (t, J = 6.5 Hz, 2H), 1.98-1.88 (m, 3H),

1.77-1.66 (m, 3H), 1.65-1.54 (m, 3H), 1.35 (t, J = 13.6 Hz, 4H), 1.29-1.12 (m, 7H), and

0.97-0.84 (m, 2H). ^{13}C NMR (100 MHz, CDCl$_3$) δ ppm 169.40, 168.08,136.37, 134.81,

132.41, 130.03, 128.42, 127.97, 127.15, 122.22, 122.11, 119.40, 118.61, 112.49,

111.25, 48.95, 40.34, 36.61, 32.74, 25.43, 25.15, and 24.67.

65

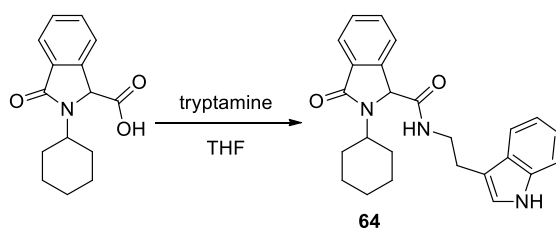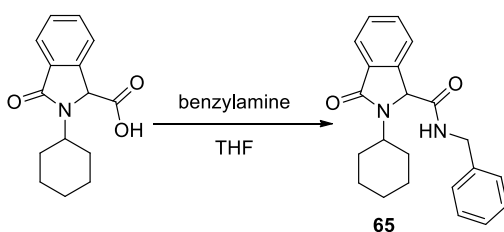65:   ***N*-Benzyl-2-cyclohexyl-3-oxoisoindoline-1-carboxamide:** A solution of 2-cyclohexyl-3-

oxo-2,3-dihydro-1H-isoindole-1-carboxylic acid (76.5 mg, 0.256 mmol) in dry THF (1.5

mL) was chilled to 0 °C. CDI (57.0mg, 0.324 mmol) was added and the reaction stirred

for 2 h. Benzylamine (42.0 μL, 0.384 mmol) was added and the reaction was allowed to

reach rt. The progress of the reaction was followed by TLC (EtOAc-hexanes, 1:1).

When the starting material had been consumed, the reaction was quenched with aq.

sat. NaHCO$_3$ and extracted with EtOAc (3 × 5 mL). The organic extracts were combined,

dried over anhyd. Na$_2$SO$_4$, and concentrated by evaporation *in vacuo* to afford a brown

oil. **65** was obtained by chromatography on silica gel, eluting with EtOAc-hexanes-

triethylamine (50:50:1) as an oil (2.9 mg, 2.8%). ^{1}H NMR (400 MHz, CDCl$_3$) δ ppm 7.64

(d, *J* = 7.5 Hz 1H), 7.57 (t, *J* = 7.4 Hz, 1H), 7.54-7.45 (m, 2H), 7.40-7.31 (m, 1H), 7.26-7.22

(m, 2H), 7.10-7.05 (m, 2H), 6.22 (bs, 1H), 5.13 (s, 1H), 4.46, (dd, *J* = 14.6, 6.3 Hz, 1H),

4.27 (dd, *J* = 14.6, 5.5 Hz, 1H), 1.98-1.55 (m, 10 H), and 1.54-1.02 (m, 11H). ^{13}C NMR

(100 MHz, CDCl$_3$) δ ppm 170.29,169.10, 141.79, 137.20, 132.33, 131.27, 129.08,

128.65, 127.78, 123.82, 122.55, 63.55, 53.85, 43.47, 30.82, 25.68, and 25.18. HRMS

(ESI-TOF) *m/z* calcd. for C$_{22}$H$_{25}$N$_2$O$_2$: 349.1911; found 349.1908 ([M + H]$^+$, Δ ppm 0.79).

66
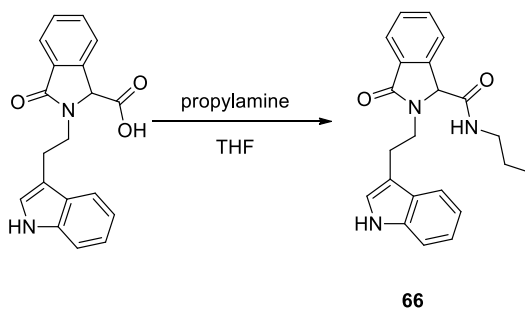
66: **2-(2-(1H-indol-2-yl)ethyl)-3-oxo-*N*-propylisoindoline-1-carboxamide:** A solution of 2-

(2-(1H-indol-3-yl)ethyl)-3-oxoisoindoline-1-carboxylic acid (75.0 mg, 0.250 mmol) in dry

THF (1.5 mL) was chilled to 0 °C. CDI (43.0 mg, 0.270 mmol) was added and the

reaction stirred for 2 h. Propylamine (22.2 mg, 0.377 mmol) was added and the

reaction was allowed to reach rt. The progress of the reaction was followed by TLC

(EtOAc-hexanes, 1:1). When the starting material had been consumed, the reaction

was quenched with aq. sat. NaHCO$_3$ and extracted with EtOAc (3 × 5 mL). The organic

extracts were combined, dried over anhyd. Na$_2$SO$_4$, and concentrated by evaporation

in vacuo to afford a brown oil. **66** was obtained by chromatography on silica gel,

eluting with EtOAc-hexanes-triethylamine (75:25:1) as a clear oil (21.2 mg, 24.9%). ^{1}H

NMR (400 MHz, CD$_3$OD) δ ppm 7.79 (d, J = 7.4 Hz, 1H), 7.45 - 7.62 (m, 4H), 7.32 (d, J = 8.2 Hz, 1H), 7.04 - 7.10 (m, 2H), 6.96 (d, J = 7.2 Hz, 1H), 4.32 (ddd, J = 6.2, 7.9, 14.0 Hz, 1H), 3.38 - 3.46 (m, 1H), 3.03 - 3.24 (m, 5H), 1.43 - 1.54 (m, 2H), and 0.89 (t, J = 7.4 Hz, 4H). ^{13}C NMR (100 MHz, CD$_3$OD) δ ppm 171.5, 169.8, 143.0, 138.4, 133.4, 133.1, 130.3, 128.7, 124.5, 123.7, 123.4, 122.6, 119.9, 119.3, 112.9, 112.5, 43.9, 42.6, 25.2, 23.7, and 11.8.
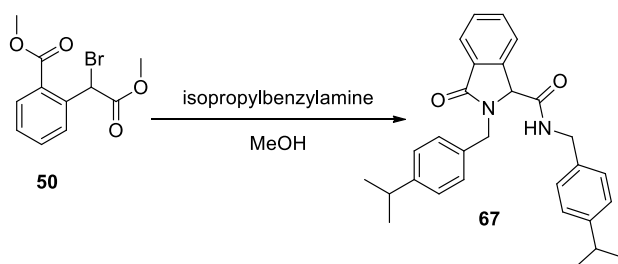
67: ***N*,2-Bis(4-isopropylbenzyl)-3-oxoisoindoline-1-carboxamide:** A solution of **50** (2.1g, 7.1mmol) in MeOH (40 mL) was stirred at rt for 5 minutes. 4-isopropylbenzylamine (5.7mL, 36 mmol) was added slowly over 10 minutes and the progress of the reaction was followed by TLC (EtOAc-hexanes, 30:70). When **50** was consumed the reaction was concentrated in vacuo followed by diluting with 1.2 M HCl and extracting with DCM (3 x 20mL). The organic extracts were combined, dried over anhyd. Na$_2$SO$_4$, and concentrated by evaporation *in vacuo* to afford an orange oil. **67** was obtained by chromatography on silica gel, eluting with EtOAc-hexanes-glacial acetic acid (15:85:1) as a yellow oil (75 mg, 24%). ^{1}H NMR (400 MHz, (CD$_3$)$_2$SO) δ ppm 7.62 (d, J = 8.4 Hz, 2H), 7.54 (t, J = 7.4 Hz, 1H), 7.42 (t, J = 7.5 Hz, 1H), 7.16 (s, 4H), 7.14 (d, J = 8.2 Hz, 2H),

7.05 (d, *J* = 8.2 Hz, 2H), 6.59 (t, *J* = 5.7 Hz, 1H), 5.25 (d, *J* = 14.7 Hz, 1H), 4.91 (s, 1H),

4.40-4.29 (m, 2H), 4.17 (d, *J* = 14.7 Hz, 1H), 2.91-2.84 (m, 2H), 1.22 (d, *J* = 6.9 Hz, 12H).

^{13}C NMR (100 MHz, $(CD_3)_2SO$) δ ppm 169.51, 167.51, 148.77, 148.40, 141.19, 134.82,

133.31, 132.33, 130.59, 129.01, 128.60, 127.68, 127.01, 126.75, 123.92, 122.79, 63.97,

45.51, 43.25, 33.76, and 23.93.

68
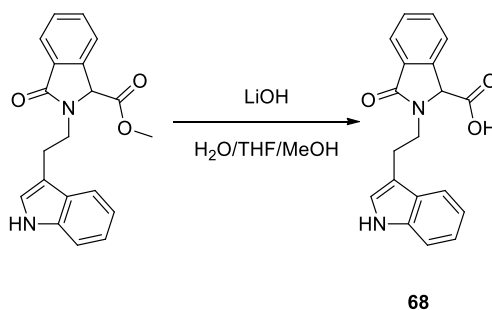
68: **2-(2-(1H-indol-2-yl)ethyl)-3-oxoisoindoline-1-carboxylic acid:** A solution of methyl 2-

(2-(1H-indol-2-yl)ethyl)-3-oxoisoindoline-1-carboxylate (399.0 mg, 1.2 mmol) in a 30 ml

solution of a LiOH (2.5M aq), MeOH, THF (1:2:3 ratio) was stirred at rt and followed by

TLC (EtOAc-hexanes, 1:1). Once the starting material had been consumed, the reaction

was quenched with an acid/base workup. The organic extracts were combined, dried

over anhyd. Na_2SO_4, and concentrated by evaporation *in vacuo* to afford a brown oil.

Dissolving the oil in chloroform and concentrating in vacuo afforded compound **68** as a

yellow oil (253.8 mg, 66.4%). ^{1}H NMR (400 MHz, $(CD_3)_2SO$) δ ppm 10.82 (s, 1H), 7.72 (d,

J = 7.5 Hz, 1H), 7.63 (d, *J* = 3.9 Hz, 2H), 7.56 (dd, *J* = 7.5, 3.5 Hz, 2H) 7.33 (d, *J* = 8.0 Hz,

1H), 7.18 (d, *J* = 2.1 Hz, 1H), 7.07 (t, *J* = 7.7 Hz, 1H), 6.97 (t, *J* = 7.0 Hz, 1H), 5.35 (s, 1H),

4.22-4.12 (m, 1H) 3.50-3.41 (m, 1H), and 3.15-2.93 (m, 2H). ^{13}C NMR (100 MHz,

(CD$_3$)$_2$SO) δ ppm 169.74, 167.45, 140.13, 136.22, 131.92, 131.55, 129.01, 127.02,

122.91, 120.99, 118.29, 118.09, 111.43, 111.16, 62.07, 41.74, and 23.56. HRMS (ESI-

TOF) *m/z* calcd. for C$_{19}$H$_{17}$N$_2$O$_3$: 321.1234; found 321.1242 ([M + H]$^+$, Δ 2.57).

69

69:   **3-Oxo-2-propylisoindoline-1-carboxylic acid:** A solution of methyl 3-oxo-2-

propylisoindoline-1-carboxylate (148.4 mg, 0.6361 mmol) in a 12 ml solution of a LiOH

(2.5M aq), MeOH, THF (1:2:3 ratio) was stirred at rt and followed by TLC (EtOAc-

hexanes, 1:1). Once the starting material had been consumed, the reaction was

quenched with 2M HCl (25 mL) and extracted EtOAc (3 X 25 mL). The organic extracts

were combined, dried over anhyd. Na$_2$SO$_4$, and concentrated by evaporation *in vacuo*

to afford a brown oil. **69** was obtained by chromatography on silica gel, eluting with

EtOAc-hexanes-glacial acetic acid (75:25:1) to (100:0:1) as a yellow solid (86.7 mg,

62.2%). ^{1}H NMR (400 MHz, CD$_3$OD) δ ppm 7.74 (d, *J* = 7.5 Hz, 1H), 7.69 (d, *J* = 7.7 Hz,

1H), 7.59 (t, *J* = 7.4 Hz, 1H), 7.51 (t, *J* = 7.4 Hz, 1H), 5.30 (s, 1H), 3.90 (sex, 2H), and 0.91

(t, *J* = 7.4 Hz, 3H). ^{13}C NMR (100 MHz, CD$_3$OD) δ ppm 172.10, 143.22, 134.25, 133.79,

131.14, 125.23, 125.06, 69.26, 45.43, 23.23, and 12.71. HRMS (ESI-TOF) *m/z* calcd. for

C$_{12}$H$_{14}$NO$_3$: 220.0968; found 220.0967 ([M + H]$^+$, Δ ppm 1.17).

70: **2-Benzyl-3-oxoisoindoline-1-carboxylic acid:** A solution of methyl 3-oxo-2-

propylisoindoline-1-carboxylate (148.4 mg, 0.6361 mmol) in a 12 ml solution of a LiOH

(2.5M aq), MeOH, THF (1:2:3 ratio) was stirred at rt and followed by TLC (EtOAc-

hexanes, 1:1). Once the starting material had been consumed, the reaction was

quenched with 2M HCl (25 mL) and extracted EtOAc (3 X 25 mL). The organic extracts

were combined, dried over anhyd. Na_2SO_4, and concentrated by evaporation *in vacuo*

to afford a brown oil. **69** was obtained by chromatography on silica gel, eluting with

EtOAc-hexanes-glacial acetic acid (75:25:1) to (100:0:1) as a yellow solid (86.7 mg,

62.2%). ^{1}H NMR (400 MHz, CD$_3$OD) δ ppm 7.74 (d, *J* = 7.5 Hz, 1H), 7.69 (d, *J* = 7.7 Hz,

1H), 7.59 (t, *J* = 7.4 Hz, 1H), 7.51 (t, *J* = 7.4 Hz, 1H), 5.30 (s, 1H), 3.90 (sex, 2H), and 0.91

(t, *J* = 7.4 Hz, 3H).   ^{13}C NMR (100 MHz, CD$_3$OD) δ ppm 172.10, 143.22, 134.25, 133.79,

131.14, 125.23, 125.06, 69.26, 45.43, 23.23, and 12.71. HRMS (ESI-TOF) *m/z* calcd. for

$C_{16}H_{14}NO_3$: 268.0968; found 268.0968 ([M + H][+], Δ ppm 0.00).
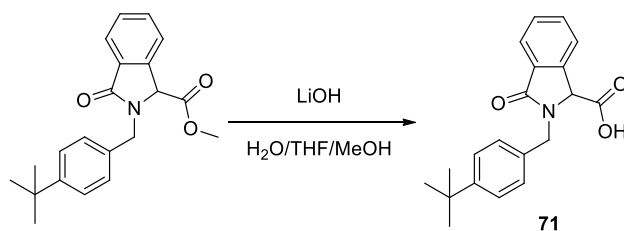
71: **2-(4-(Tert-butyl)benzyl)-3-oxoisoindoline-1-carboxylic acid:** A solution of methyl 2-(4-(tert-butyl)benzyl)-3-oxoisoindoline-1-carboxylate (1.03 mg, 3.05 mmol) in MeOH/THF (2:3, 100 mL) was stirred at room temperature for 5 minutes. 2.5M LiOH (20 mL) was added and the reaction progress was followed by TLC (EtOAc-hexanes, 1:1). Once the starting material had been consumed, the reaction was quenched with 2M HCl (25 mL) and extracted EtOAc (3 X 25 mL). The organic extracts were combined, dried over anhyd. Na_2SO_4, extracted with EtOAc (3 × 15 mL). The aqueous extracts were combined and acidified using 2M HCl and extracted with EtOAc (3 × 15 mL), the organic extracts were combined, dried over Na_2SO_4, and concentrated by evaporation *in vacuo* to afford **71** as a white solid)160 mg, 16.2%). ^{1}H NMR (400 MHz, CD$_3$OD) δ ppm 7.83 (d, *J* = 7.3 Hz, 1H), 7.53 - 7.69 (m, 1H), 7.40 (d, *J* = 8.5 Hz, 2H), 7.21 (s, 2H), 5.36 (d, *J* = 15.3 Hz, 1H), 4.95 (s, 1H), 4.91 - 4.99 (m, 1H), 4.28 (d, *J* = 15.1 Hz, 1H), and 1.29 (s, 9H) ^{13}C NMR (100 MHz, CD$_3$OD) δ ppm 171.2, 170.9, 141.5, 134.7, 133.5, 132.6, 130.6, 130.1, 129.4, 127.1, 124.7, 124.4, 63.3, 45.7, 35.4, and 31.9.
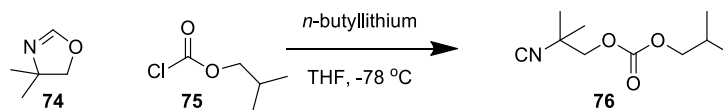
76:   **Isobutyl (2-isocyano-2-methylpropyl) carbonate:** A solution of 4,4-dimethyl-2-

oxazoline (5 mL, 47.4 mmol), **74**, in THF (48 mL) was cooled to -78 $^{\circ}$C in a dry

ice/acetone bath. N-butyl lithium (20 mL, 49.8 mmol) was added drop wise and stirred

for 1 h. Ethyl chloroformate (4.80 mL, 50.1 mmol), **75**, was added and the reaction

progress was followed by TLC (EtOAc-hexanes, 1:1). Once the starting material had

been consumed, the reaction was quenched with DI H_2O, washed with brine, and

extracted with EtOAc. The organic extracts were combined, dried over anhyd. Na_2SO_4,

and concentrated by evaporation *in vacuo* to afford a brown oil. **76** was obtained by

chromatography on silica gel, eluting with EtOAc-hexanes (10 - 50% gradient). **76** was

isolated as a clear oil (5.167 g, 64%). ^{1}H NMR (400 MHz, CDCl$_3$) δ ppm 4.22, (q, *J* = 7.1

Hz, 2H), 4.07 (t, *J* = 1.9 Hz, 2H), 1.45 (t, *J* = 1.9 Hz, 6H), and 1.31 (t, *J* = 7.2 Hz, 3H). ^{13}C

NMR (100 MHz, CDCl$_3$) δ ppm 154.54, 72.31, 64.46, 56.13, 25.69, and 14.07.   This

known compound was synthesized following the procedure outlined by Ugi *et al.*[125]
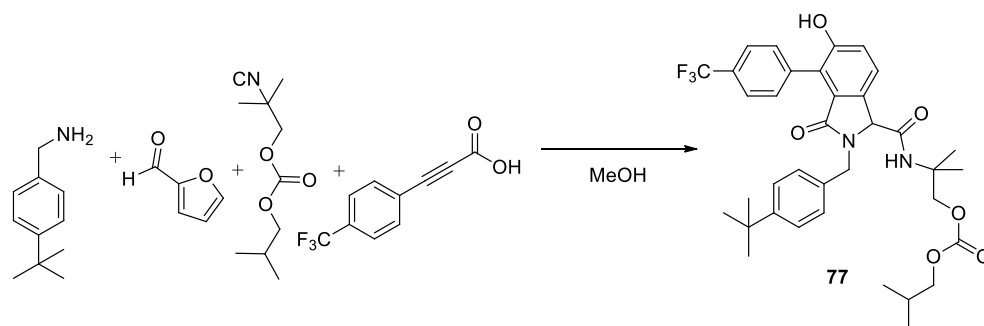
77: **2-(2-(4-(Tert-butyl)benzyl)-5-hydroxy-3-oxo-4-(4-(trifluoromethyl)phenyl)isoindoline-1-carboxamido)-2-methylpropyl isobutyl carbonate:** 4-tert-butyl-benzylamine (1.05 mL, 6.0 mmol) and furfural (0.50 mL, 6.0 mmol) were combined in methanol (6 mL) and stirred at ambient temperature for 20 minutes. Next, a solution of 3-(4-(trifluoromethyl)phenyl)propiolic acid (1.28 g, 6.0 mmol) in methanol (3 mL) was added and stirred for 5 minutes. Next, isobutyl (2-isocyano-2-methylpropyl) carbonate (1.23 g, 6.0 mmol) was added. The reaction flask was then wrapped in foil and stirred at ambient temperature. After 2.5 h, the reaction mixture was concentrated under reduced pressure to near dryness. The crude product was purified by silica gel flash chromatography (10% EtOAc/hexanes - 30% EtOAc/hexanes) yielding a yellow-orange oil which was taken to the next step. To the resultant yellow-orange oil was added dioxane (300 mL) and ytterbium (III) trifluoromethane sulfonate (0.74 g, 1.2 mmol) and stirred at 100°C. After 11 hours, the reaction mixture was cooled to ambient temperature and filtered through Celite and concentrated. The crude product was purified by silica gel flash chromatography (10% EtOAc/hexanes - 40% EtOAc/hexanes) yielding 2-(2-(4-(tert-butyl)benzyl)-5-hydroxy-3-oxo-4-(4-(trifluoromethyl)phenyl)isoindoline-1-carboxamido)-2-methylpropyl isobutyl carbonate

96

(light-yellow solid, 1.60 g, 39.5%). ^{1}H NMR (400 MHz, CDCl$_3$) d 7.77 - 7.84 (d, J = 8.0 Hz, 2H), 7.57 - 7.65 (d, J = 8.0 Hz, 2H), 7.49 (dd, J = 0.6, 8.4 Hz, 1H), 7.30 - 7.37 (m, 2H), 7.20 - 7.26 (m, 2H), 7.18 (d, J = 8.3 Hz, 1H), 5.65 (s, 1H), 5.38 (s, 1H), 5.02 (d, J = 14.8 Hz, 1H), 4.67 (s, 1H), 4.31 (d, J = 14.6 Hz, 1H), 4.18 (s, 2H), 3.88 (d, J= 6.8 Hz, 2H), 1.93 (m, 1H), 1.29 (s, 9H), 1.23 (d, J = 3.0 Hz, 6H), and 0.92 (d, J = 6.8 Hz, 6H).
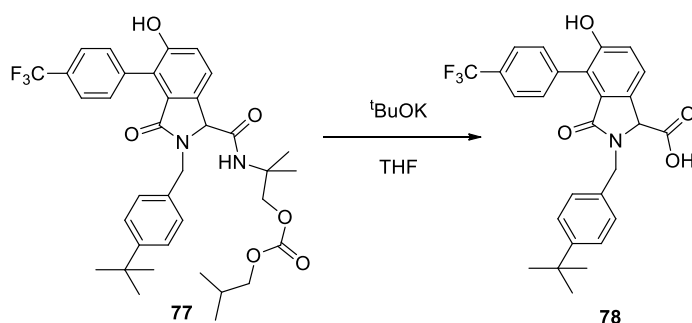
78: **2-(4-(Tert-butyl)benzyl)-5-hydroxy-3-oxo-4-(4-(trifluoromethyl)phenyl)isoindoline-1-carboxylic acid:** A solution of **77** (315.0 mg, 0.50 mmol) in dry THF (1 mL) was stirred at rt for 5 minutes. A solution of ^{t}BuOK (121 mg, 1.01 mmol) in THF (0.5 mL) was added and stirred at ambient temperature for 1 h. A solution of potassium carbonate (78.6 mg, 0.57 mmol) in DI H$_2$O (1.5 mL) was added and the progress of the reaction was followed by TLC (EtOAc-hexanes, 1:1). Once done, the reaction was quenched with aq. HCl (1.2M) and extracted with EtOAc (3 x 5 mL). The organic extracts where combined and washed with brine and dried over anhyd. Na$_2$SO$_4$. The solvent was removed by evaporation *in vacuo* to afford a brown oil. **78** was obtained by chromatography on silica gel gradient eluting with EtOAc-hexanes-1% glacial acetic acid (50:50:1 to

100:0:1) as a yellow oil (85.0 mg, 35%). ^{1}H NMR (400 MHz, CDCl$_3$) δ ppm 11.97 (bs, 2H), 9.89 (bs, 1H), 8.07 (s, 1H), 7.72 (d, J = 8.2 Hz, 2H), 7.54 (d, J = 7.9 Hz, 2H), 7.35 (d, J = 8.3 Hz, 2H) 7.17 (d, J = 8.3 Hz, 1H), 7.12 (d, J = 8.2 Hz, 2H), 4.97 (d, J = 15.2 Hz, 1H), 4.89 (s, 1H), 3.86 (d, J = 15.1 Hz, 1H), and 1.25 (s, 9H). ^{13}C NMR (100 MHz, CDCl$_3$) δ ppm 167.16, 166.41, 154.91, 149.74, 134.12, 133.21, 131.57, 128.91, 127.75, 125.38, 123.92, 123.72, 122.82, 119.16, 54.85, 34.18, and 31.10.

REFERENCES

(1)   Waddington, C. H. The epigenotype. 1942. *International journal of epidemiology* **2012**,
41, 10-13.

(2)   Holliday, R. MECHANISMS FOR THE CONTROL OF GENE ACTIVITY DURING
DEVELOPMENT. *Biological Reviews* **1990**, *65*, 431-471.

(3)   Jablonka, E.; Lamb, M. J. The inheritance of acquired epigenetic variations. *Journal of
Theoretical Biology* **1989**, *139*, 69-83.

(4)   Li, B.; Carey, M.; Workman, J. L. The Role of Chromatin during Transcription. *Cell* **2007**,
128, 707-719.

(5)   Luger, K.; Mader, A. W.; Richmond, R. K.; Sargent, D. F.; Richmond, T. J. Crystal structure
of the nucleosome core particle at 2.8[thinsp]A resolution. *Nature* **1997**, *389*, 251-260.

(6)   Dhanak, D. Cracking the Code: The Promise of Epigenetics. *ACS Medicinal Chemistry
Letters* **2012**, *3*, 521-523.

(7)   Jenuwein, T.; Allis, C. D. Translating the Histone Code. *Science* **2001**, *293*, 1074-1080.

(8)   Lister, R.; Pelizzola, M.; Dowen, R. H.; Hawkins, R. D.; Hon, G.; Tonti-Filippini, J.; Nery, J.
R.; Lee, L.; Ye, Z.; Ngo, Q. M.; Edsall, L.; Antosiewicz-Bourget, J.; Stewart, R.; Ruotti, V.; Millar, A.
H.; Thomson, J. A.; Ren, B.; Ecker, J. R. Human DNA methylomes at base resolution show
widespread epigenomic differences. *Nature* **2009**, *462*, 315-322.

(9)   Hewagama, A.; Richardson, B. The genetics and epigenetics of autoimmune diseases.
Journal of autoimmunity **2009**, *33*, 3-11.

(10)   Liu, L.; van Groen, T.; Kadish, I.; Tollefsbol, T. O. DNA methylation impacts on learning and memory in aging. *Neurobiology of aging* **2009**, *30*, 549-560.

(11)   Ohm, J. E.; McGarvey, K. M.; Yu, X.; Cheng, L.; Schuebel, K. E.; Cope, L.; Mohammad, H. P.; Chen, W.; Daniel, V. C.; Yu, W.; Berman, D. M.; Jenuwein, T.; Pruitt, K.; Sharkis, S. J.; Watkins, D. N.; Herman, J. G.; Baylin, S. B. A stem cell-like chromatin pattern may predispose tumor suppressor genes to DNA hypermethylation and heritable silencing. *Nat Genet* **2007**, *39*, 237-242.

(12)   Wang, Y.; Leung, F. C. C. An evaluation of new criteria for CpG islands in the human genome as gene markers. *Bioinformatics* **2004**, *20*, 1170-1177.

(13)   Delgado, S.; Gómez, M.; Bird, A.; Antequera, F.: *Initiation of DNA replication at CpG islands in mammalian chromosomes*, 1998; Vol. 17.

(14)   Reik, W. Stability and flexibility of epigenetic gene regulation in mammalian development. *Nature* **2007**, *447*, 425-432.

(15)   Watt, F.; Molloy, P. L. Cytosine methylation prevents binding to DNA of a HeLa cell transcription factor required for optimal expression of the adenovirus major late promoter. *Genes & Development* **1988**, *2*, 1136-1143.

(16)   Uribe-Lewis, S.; Stark, R.; Carroll, T.; Dunning, M. J.; Bachman, M.; Ito, Y.; Stojic, L.; Halim, S.; Vowler, S. L.; Lynch, A. G.; Delatte, B.; de Bony, E. J.; Colin, L.; Defrance, M.; Krueger, F.; Silva, A. L.; Ten Hoopen, R.; Ibrahim, A. E.; Fuks, F.; Murrell, A. 5-hydroxymethylcytosine marks promoters in colon that resist DNA hypermethylation in cancer. *Genome biology* **2015**, *16*, 69.

(17)   Sharma, S.; Kelly, T. K.; Jones, P. A. Epigenetics in cancer. *Carcinogenesis* **2010**, *31*, 27-36.

(18)   Jones, P. A.; Baylin, S. B. The epigenomics of cancer. *Cell* **2007**, *128*, 683-692.

(19)   Esteller, M. Epigenetics in cancer. *The New England journal of medicine* **2008**, *358*, 1148-1159.

(20)   Portela, A.; Esteller, M. Epigenetic modifications and human disease. *Nature biotechnology* **2010**, *28*, 1057-1068.

(21)   Bernstein, B. E.; Meissner, A.; Lander, E. S. The mammalian epigenome. *Cell* **2007**, *128*, 669-681.

(22)   Kouzarides, T. Chromatin modifications and their function. *Cell* **2007**, *128*, 693-705.

(23)   Suzuki, M. M.; Bird, A. DNA methylation landscapes: provocative insights from epigenomics. *Nat Rev Genet* **2008**, *9*, 465-476.

(24)   Bird, A. DNA methylation patterns and epigenetic memory. *Genes & Development* **2002**, *16*, 6-21.

(25)   Yoo, C. B.; Jones, P. A. Epigenetic therapy of cancer: past, present and future. *Nature reviews. Drug discovery* **2006**, *5*, 37-50.

(26)   Leppert, S.; Matarazzo, M. R. De novo DNMTs and DNA methylation: novel insights into disease pathogenesis and therapy from epigenomics. *Current pharmaceutical design* **2014**, *20*, 1812-1818.

(27)   Svedruzic, Z. M. Mammalian cytosine DNA methyltransferase Dnmt1: enzymatic mechanism, novel mechanism-based inhibitors, and RNA-directed DNA methylation. *Curr Med Chem* **2008**, *15*, 92-106.

(28)   Jurkowska, R. Z.; Jurkowski, T. P.; Jeltsch, A. Structure and Function of Mammalian DNA Methyltransferases. *ChemBioChem* **2011**, *12*, 206-222.

(29)   Gros, C.; Fahy, J.; Halby, L.; Dufau, I.; Erdmann, A.; Gregoire, J.-M.; Ausseil, F.; Vispé, S.; Arimondo, P. B. DNA methylation inhibitors in cancer: Recent and future approaches. *Biochimie* **2012**, *94*, 2280-2296.

(30)   Svedruzie, Z. M. Mammalian Cytosine DNA Methyltransferase Dnmt1: Enzymatic Mechanism, Novel

Mechanism-Based Inhibitors, and RNA-directed DNA Methylation. *Current Medicinal Chemistry* **2008**, 92-106.

(31)   Pedrali-Noy, G.; Weissbach, A. Mammalian DNA methyltransferases prefer poly(dI-dC) as substrate. *The Journal of biological chemistry* **1986**, *261*, 7600-7602.

(32)   Stein, R.; Gruenbaum, Y.; Pollack, Y.; Razin, A.; Cedar, H. Clonal inheritance of the pattern of DNA methylation in mouse cells. *Proceedings of the National Academy of Sciences of the United States of America* **1982**, *79*, 61-65.

(33)   Tittle, R. K.; Sze, R.; Ng, A.; Nuckels, R. J.; Swartz, M. E.; Anderson, R. M.; Bosch, J.; Stainier, D. Y. R.; Eberhart, J. K.; Gross, J. M. Uhrf1 and Dnmt1 are required for development and maintenance of the zebrafish lens. *Developmental Biology* **2011**, *350*, 50-63.

(34)   Cheng, X.; Blumenthal, R. M. Coordinated Chromatin Control: Structural and Functional Linkage of DNA and Histone Methylation. *Biochemistry* **2010**, *49*, 2999-3008.

(35)   Auclair, G.; Weber, M. Mechanisms of DNA methylation and demethylation in mammals. *Biochimie* **2012**, *94*, 2202-2211.

(36)   Goll, M. G.; Bestor, T. H. Eukaryotic cytosine methyltransferases. *Annual review of biochemistry* **2005**, *74*, 481-514.

(37)   Chen, T.; Hevi, S.; Gay, F.; Tsujimoto, N.; He, T.; Zhang, B.; Ueda, Y.; Li, E. Complete inactivation of DNMT1 leads to mitotic catastrophe in human cancer cells. *Nat Genet* **2007**, *39*, 391-396.

(38)   Bestor, T. H.; Verdine, G. L. DNA methyltransferases. *Current opinion in cell biology* **1994**, *6*, 380-389.

(39)   Bestor, T. H. The DNA methyltransferases of mammals. *Human Molecular Genetics* **2000**, *9*, 2395-2402.

(40)   Pradhan, S.; Estève, P.-O. Allosteric Activator Domain of Maintenance Human DNA (Cytosine-5) Methyltransferase and Its Role in Methylation Spreading. *Biochemistry* **2003**, *42*, 5321-5332.

(41)   Jones, P. A. DNA Methylation Errors and Cancer. *Cancer Research* **1996**, *56*, 2463-2467.

(42)   Jones, P. A.; Liang, G. Rethinking how DNA methylation patterns are maintained. *Nat Rev Genet* **2009**, *10*, 805-811.

(43)   Okano, M.; Bell, D. W.; Haber, D. A.; Li, E. DNA Methyltransferases Dnmt3a and Dnmt3b Are Essential for De Novo Methylation and Mammalian Development. *Cell* **1999**, *99*, 247-257.

(44)   Deplus, R.; Brenner, C.; Burgers, W. A.; Putmans, P.; Kouzarides, T.; Launoit, Y. d.; Fuks, F. Dnmt3L is a transcriptional repressor that recruits histone deacetylase. *Nucleic Acids Research* **2002**, *30*, 3831-3838.

(45)   Herman, J. G.; Baylin, S. B. Gene Silencing in Cancer in Association with Promoter Hypermethylation. *New England Journal of Medicine* **2003**, *349*, 2042-2054.

(46)   Jones, P. A.; Baylin, S. B. The fundamental role of epigenetic events in cancer. *Nat Rev Genet* **2002**, *3*, 415-428.

(47)   Issa, J.-P. J.; Garcia-Manero, G.; Giles, F. J.; Mannari, R.; Thomas, D.; Faderl, S.; Bayar, E.; Lyons, J.; Rosenfeld, C. S.; Cortes, J.; Kantarjian, H. M.: *Phase 1 study of low-dose prolonged exposure schedules of the hypomethylating agent 5-aza-2'-deoxycytidine (decitabine) in hematopoietic malignancies*, 2004; Vol. 103.

(48)   Goffin, J.; Eisenhauer, E. DNA methyltransferase inhibitors-state of the art. *Annals of oncology : official journal of the European Society for Medical Oncology / ESMO* **2002**, *13*, 1699-1716.

(49)   Daniel V.Snti, A. N., Charles Garrett. Covalent bond formation, between a DNA-cytosine methyltransferase and DNA containing 5-azacytosine. *Proc. Natl. Acad. Sci. USA* **1984**, *81*, 6993-6997.

(50)   Sorm, F.; Piskala, A.; Cihak, A.; Vesely, J. 5-Azacytidine, a new, highly effective cancerostatic. *Experientia* **1964**, *20*, 202-203.

(51)   Jones, P. A.; Taylor, S. M. Cellular differentiation, cytidine analogs and DNA methylation. *Cell* **1980**, *20*, 85-93.

(52)   Christman, J. K. 5-Azacytidine and 5-aza-2'-deoxycytidine as inhibitors of DNA methylation: mechanistic studies and their implications for cancer therapy. *Oncogene* **2002**, *21*, 5483-5495.

(53)   Cihak, A. Biological effects of 5-azacytidine in eukaryotes. *Oncology* **1974**, *30*, 405-422.

(54)   Momparler, R. L. A Perspective on the Comparative Antileukemic Activity of 5-Aza-2'-deoxycytidine (Decitabine) and 5-Azacytidine (Vidaza). *Pharmaceuticals* **2012**, *5*, 875-881.

(55)   Santini, V.; Kantarjian, H. M.; Issa, J. P. Changes in DNA methylation in neoplasia: pathophysiology and therapeutic implications. *Annals of internal medicine* **2001**, *134*, 573-586.

(56)   Leone, G.; Voso, M. T.; Teofili, L.; Lubbert, M. Inhibitors of DNA methylation in the treatment of hematological malignancies and MDS. *Clinical immunology (Orlando, Fla.)* **2003**, *109*, 89-102.

(57)   Issa, J. P.; Gharibyan, V.; Cortes, J.; Jelinek, J.; Morris, G.; Verstovsek, S.; Talpaz, M.; Garcia-Manero, G.; Kantarjian, H. M. Phase II study of low-dose decitabine in patients with chronic myelogenous leukemia resistant to imatinib mesylate. *Journal of clinical oncology : official journal of the American Society of Clinical Oncology* **2005**, *23*, 3948-3956.

(58)   Jüttermann, R.; Li, E.; Jaenisch, R. Toxicity of 5-aza-2'-deoxycytidine to mammalian cells is mediated primarily by covalent trapping of DNA methyltransferase rather than DNA demethylation. *Proceedings of the National Academy of Sciences of the United States of America* **1994**, *91*, 11797-11801.

(59)   Cheng, J. C.; Matsen, C. B.; Gonzales, F. A.; Ye, W.; Greer, S.; Marquez, V. E.; Jones, P. A.; Selker, E. U. Inhibition of DNA methylation and reactivation of silenced genes by zebularine. *J Natl Cancer Inst* **2003**, *95*, 399-409.

(60)   Brueckner, B.; Kuck, D.; Lyko, F. DNA methyltransferase inhibitors for cancer therapy. *Cancer journal (Sudbury, Mass.)* **2007**, *13*, 17-22.

(61)   Lyko, F.; Brown, R. DNA Methyltransferase Inhibitors and the Development of Epigenetic Cancer Therapies. *Journal of the National Cancer Institute* **2005**, *97*, 1498-1506.

(62)   Stresemann, C.; Lyko, F. Modes of action of the DNA methyltransferase inhibitors azacytidine and decitabine. *International Journal of Cancer* **2008**, *123*, 8-13.

(63)   Gravina, G. L.; Festuccia, C.; Marampon, F.; Popov, V. M.; Pestell, R. G.; Zani, B. M.; Tombolini, V. Biological rationale for the use of DNA methyltransferase inhibitors as new strategy for modulation of tumor response to chemotherapy and radiation. *Molecular cancer* **2010**, *9*, 305.

(64)   Li, K. K.; Luo, L. F.; Shen, Y.; Xu, J.; Chen, Z.; Chen, S. J. DNA methyltransferases in hematologic malignancies. *Seminars in hematology* **2013**, *50*, 48-60.

(65)   Newell-Price, J.; Clark, A. J.; King, P. DNA methylation and silencing of gene expression. *Trends in endocrinology and metabolism: TEM* **2000**, *11*, 142-148.

(66)   Santi, D. V.; Norment, A.; Garrett, C. E. Covalent bond formation between a DNA-cytosine methyltransferase and DNA containing 5-azacytosine. *Proceedings of the National Academy of Sciences of the United States of America* **1984**, *81*, 6993-6997.

(67)   Castellano, S.; Kuck, D.; Sala, M.; Novellino, E.; Lyko, F.; Sbardella, G. Constrained Analogues of Procaine as Novel Small Molecule Inhibitors of DNA Methyltransferase-1. *Journal of Medicinal Chemistry* **2008**, *51*, 2321-2325.

(68)   Chen, S.; Wang, Y.; Zhou, W.; Li, S.; Peng, J.; Shi, Z.; Hu, J.; Liu, Y.-C.; Ding, H.; Lin, Y.; Li, L.; Cheng, S.; Liu, J.; Lu, T.; Jiang, H.; Liu, B.; Zheng, M.; Luo, C. Identifying Novel Selective Non-Nucleoside DNA Methyltransferase 1 Inhibitors through Docking-Based Virtual Screening. *Journal of Medicinal Chemistry* **2014**.

(69)   Frey, K. M.; Puleo, D. E.; Spasov, K. A.; Bollini, M.; Jorgensen, W. L.; Anderson, K. S. Structure-Based Evaluation of Non-nucleoside Inhibitors with Improved Potency and Solubility That Target HIV Reverse Transcriptase Variants. *J Med Chem* **2015**, *58*, 2737-2745.

(70)   Ceccaldi, A.; Rajavelu, A.; Ragozin, S.; Sénamaud-Beaufort, C.; Bashtrykov, P.; Testa, N.;

Dali-Ali, H.; Maulay-Bailly, C.; Amand, S.; Guianvarc'h, D.; Jeltsch, A.; Arimondo, P. B.

Identification of Novel Inhibitors of DNA Methylation by Screening of a Chemical Library. *ACS

Chemical Biology* **2013**, *8*, 543-548.

(71)   Fahy, J.; Jeltsch, A.; Arimondo, P. B. DNA methyltransferase inhibitors in cancer: a

chemical and therapeutic patent overview and selected clinical studies. *Expert opinion on

therapeutic patents* **2012**, *22*, 1427-1442.

(72)   Gnyszka, A.; Jastrzebski, Z.; Flis, S. DNA methyltransferase inhibitors and their emerging

role in epigenetic therapy of cancer. *Anticancer research* **2013**, *33*, 2989-2996.

(73)   Singh, V.; Sharma, P.; Capalash, N. DNA methyltransferase-1 inhibitors as epigenetic

therapy for cancer. *Current cancer drug targets* **2013**, *13*, 379-399.

(74)   Yang, C. S.; Fang, M.; Lambert, J. D.; Yan, P.; Huang, T. H. M. Reversal of

hypermethylation and reactivation of genes by dietary polyphenolic compounds. *Nutrition

reviews* **2008**, *66*, S18-S20.

(75)   Yoo, C. B.; Cheng, J. C.; Jones, P. A. Zebularine: a new drug for epigenetic therapy.

Biochemical Society transactions **2004**, *32*, 910-912.

(76)   Pina, I. C.; Gautschi, J. T.; Wang, G. Y.; Sanders, M. L.; Schmitz, F. J.; France, D.; Cornell-

Kennon, S.; Sambucetti, L. C.; Remiszewski, S. W.; Perez, L. B.; Bair, K. W.; Crews, P.

Psammaplins from the sponge Pseudoceratina purpurea: inhibition of both histone deacetylase

and DNA methyltransferase. *J Org Chem* **2003**, *68*, 3866-3873.

(77)   Amatori, S.; Bagaloni, I.; Donati, B.; Fanelli, M. DNA Demethylating Antineoplastic

Strategies: A Comparative Point of View. *Genes & Cancer* **2010**, *1*, 197-209.

(78)   Savickiene, J.; Treigyte, G.; Jazdauskaite, A.; Borutinskaite, V. V.; Navakauskiene, R. DNA

methyltransferase inhibitor RG108 and histone deacetylase inhibitors cooperate to enhance

NB4 cell differentiation and E-cadherin re-expression by chromatin remodelling. *Cell biology*

international **2012**, *36*, 1067-1078.

(79)   Brueckner, B.; Garcia Boy, R.; Siedlecki, P.; Musch, T.; Kliem, H. C.; Zielenkiewicz, P.;

Suhai, S.; Wiessler, M.; Lyko, F. Epigenetic reactivation of tumor suppressor genes by a novel

small-molecule inhibitor of human DNA methyltransferases. *Cancer Res* **2005**, *65*, 6305-6311.

(80)   Graca, I.; Sousa, E. J.; Baptista, T.; Almeida, M.; Ramalho-Carvalho, J.; Palmeira, C.;

Henrique, R.; Jeronimo, C. Anti-tumoral effect of the non-nucleoside DNMT inhibitor RG108 in

human prostate cancer cells. *Current pharmaceutical design* **2014**, *20*, 1803-1811.

(81)   Asgatay, S.; Champion, C.; Marloie, G.; Drujon, T.; Senamaud-Beaufort, C.; Ceccaldi, A.;

Erdmann, A.; Rajavelu, A.; Schambel, P.; Jeltsch, A.; Lequin, O.; Karoyan, P.; Arimondo, P. B.;

Guianvarc'h, D. Synthesis and Evaluation of Analogues of N-Phthaloyl-l-tryptophan (RG108) as

Inhibitors of DNA Methyltransferase 1. *Journal of Medicinal Chemistry* **2013**, *57*, 421-434.

(82)   Chavez-Blanco, A.; Perez-Plasencia, C.; Perez-Cardenas, E.; Carrasco-Legleu, C.; Rangel-

Lopez, E.; Segura-Pacheco, B.; Taja-Chayeb, L.; Trejo-Becerril, C.; Gonzalez-Fierro, A.;

Candelaria, M.; Cabrera, G.; Duenas-Gonzalez, A. Antineoplastic effects of the DNA methylation

inhibitor hydralazine and the histone deacetylase inhibitor valproic acid in cancer cell lines.

Cancer Cell International **2006**, *6*, 2-2.

(83)   Issa, J. P.; Vertino, P. M.; Wu, J.; Sazawal, S.; Celano, P.; Nelkin, B. D.; Hamilton, S. R.;

Baylin, S. B. Increased cytosine DNA-methyltransferase activity during colon cancer progression.

J Natl Cancer Inst **1993**, *85*, 1235-1240.

(84)   Mutze, K.; Langer, R.; Schumacher, F.; Becker, K.; Ott, K.; Novotny, A.; Hapfelmeier, A.; Hofler, H.; Keller, G. DNA methyltransferase 1 as a predictive biomarker and potential therapeutic target for chemotherapy in gastric cancer. *European journal of cancer (Oxford, England : 1990)* **2011**, *47*, 1817-1825.

(85)   Belinsky, S. A.; Nikula, K. J.; Baylin, S. B.; Issa, J. P. Increased cytosine DNA-methyltransferase activity is target-cell-specific and an early event in lung cancer. *Proceedings of the National Academy of Sciences of the United States of America* **1996**, *93*, 4045-4050.

(86)   Kobayashi, Y.; Absher, D. M.; Gulzar, Z. G.; Young, S. R.; McKenney, J. K.; Peehl, D. M.; Brooks, J. D.; Myers, R. M.; Sherlock, G. DNA methylation profiling reveals novel biomarkers and important roles for DNA methyltransferases in prostate cancer. *Genome research* **2011**, *21*, 1017-1027.

(87)   Baylin, S. B.; Herman, J. G. DNA hypermethylation in tumorigenesis: epigenetics joins genetics. *Trends in genetics : TIG* **2000**, *16*, 168-174.

(88)   Frigola, J.; Song, J.; Stirzaker, C.; Hinshelwood, R. A.; Peinado, M. A.; Clark, S. J. Epigenetic remodeling in colorectal cancer results in coordinate gene suppression across an entire chromosome band. *Nat Genet* **2006**, *38*, 540-549.

(89)   Choy, J. S.; Wei, S.; Lee, J. Y.; Tan, S.; Chu, S.; Lee, T. H. DNA methylation increases nucleosome compaction and rigidity. *Journal of the American Chemical Society* **2010**, *132*, 1782-1783.

(90)   Rodenhiser, D.; Mann, M. Epigenetics and human disease: translating basic biology into clinical applications. *CMAJ : Canadian Medical Association Journal* **2006**, *174*, 341-348.

(91)   Kurdyukov, S.; Bullock, M. DNA Methylation Analysis: Choosing the Right Method. *Biology* **2016**, *5*, 3.

(92)   Kremer, D.; Metzger, S.; Kolb-Bachofen, V.; Kremer, D. Quantitative measurement of genome-wide DNA methylation by a reliable and cost-efficient enzyme-linked immunosorbent assay technique. *Analytical Biochemistry* **2012**, *422*, 74-78.

(93)   Karaca, B.; Atmaca, H.; Bozkurt, E.; Kisim, A.; Uzunoglu, S.; Karabulut, B.; Sezgin, C.; Sanli, U. A.; Uslu, R. Combination of AT-101/cisplatin overcomes chemoresistance by inducing apoptosis and modulating epigenetics in human ovarian cancer cells. *Molecular biology reports* **2013**, *40*, 3925-3933.

(94)   Park, J. I.; Grant, C. M.; Attfield, P. V.; Dawes, I. W. The freeze-thaw stress response of the yeast Saccharomyces cerevisiae is growth phase specific and is controlled by nutritional state via the RAS-cyclic AMP signal transduction pathway. *Applied and Environmental Microbiology* **1997**, *63*, 3818-3824.

(95)   Hu, J.-P.; Xu, X.-Y.; Huang, L.-Y.; Wang, L.-s.; Fang, N.-Y. Freeze–thaw Caenorhabditis elegans freeze–thaw stress response is regulated by the insulin/IGF-1 receptor daf-2. *BMC Genetics* **2015**, *16*, 1-10.

(96)   Poh, W. J.; Wee, C. P. P.; Gao, Z. DNA Methyltransferase Activity Assays: Advances and Challenges. *Theranostics* **2016**, *6*, 369-391.

(97)   Tyagi, S.; Kramer, F. R. Molecular beacons: probes that fluoresce upon hybridization. *Nature biotechnology* **1996**, *14*, 303-308.

(98)   Wood, R. J.; McKelvie, J. C.; Maynard-Smith, M. D.; Roach, P. L. A real-time assay for CpG-specific cytosine-C5 methyltransferase activity. *Nucleic Acids Res* **2010**, *38*, e107.

(99)   Biggins, J. B.; Prudent, J. R.; Marshall, D. J.; Ruppen, M.; Thorson, J. S. A continuous assay for DNA cleavage: The application of "break lights" to enediynes, iron-dependent agents, and nucleases. *Proceedings of the National Academy of Sciences* **2000**, *97*, 13537-13542.

(100)   Xing, X. W.; Tang, F.; Wu, J.; Chu, J. M.; Feng, Y. Q.; Zhou, X.; Yuan, B. F. Sensitive detection of DNA methyltransferase activity based on exonuclease-mediated target recycling. *Anal Chem* **2014**, *86*, 11269-11274.

(101)   Duan, R.; Zuo, X.; Wang, S.; Quan, X.; Chen, D.; Chen, Z.; Jiang, L.; Fan, C.; Xia, F. Quadratic isothermal amplification for the detection of microRNA. *Nat. Protocols* **2014**, *9*, 597-607.

(102)   Wang, T. S.; Chung, C. H.; Wang, A. S.; Bau, D. T.; Samikkannu, T.; Jan, K. Y.; Cheng, Y. M.; Lee, T. C. Endonuclease III, formamidopyrimidine-DNA glycosylase, and proteinase K additively enhance arsenic-induced DNA strand breaks in human cells. *Chemical research in toxicology* **2002**, *15*, 1254-1258.

(103)   Chen, F.; Zhao, Y. Methylation-blocked enzymatic recycling amplification for highly sensitive fluorescence sensing of DNA methyltransferase activity. *The Analyst* **2013**, *138*, 284-289.

(104)   Halby, L.; Champion, C.; Sénamaud-Beaufort, C.; Ajjan, S.; Drujon, T.; Rajavelu, A.; Ceccaldi, A.; Jurkowska, R.; Lequin, O.; Nelson, W. G.; Guy, A.; Jeltsch, A.; Guianvarc'h, D.; Ferroud, C.; Arimondo, P. B. Rapid Synthesis of New DNMT Inhibitors Derivatives of Procainamide. *ChemBioChem* **2012**, *13*, 157-165.

(105)   Rubin, R. A.; Modrich, P. EcoRI methylase. Physical and catalytic properties of the homogeneous enzyme. *The Journal of biological chemistry* **1977**, *252*, 7265-7272.

(106)   Jeltsch, A.; Friedrich, T.; Roth, M. Kinetics of methylation and binding of DNA by the

EcoRV adenine-N6 methyltransferase1. *Journal of Molecular Biology* **1998**, *275*, 747-758.

(107)   Gros, C.; Chauvigne, L.; Poulet, A.; Menon, Y.; Ausseil, F.; Dufau, I.; Arimondo, P. B.

Development of a universal radioactive DNA methyltransferase inhibition test for high-

throughput screening and mechanistic studies. *Nucleic Acids Res* **2013**, *41*, e185.

(108)   Solapure, S. M.; Raphael, P.; Gayathri, C. N.; Barde, S. P.; Chandrakala, B.; Das, K. S.; De

Sousa, S. M. Development of a microplate-based scintillation proximity assay for MraY using a

modified substrate. *J Biomol Screen* **2005**, *10*, 149-156.

(109)   Berry, J.; Price-Jones, M.; Killian, B. Use of scintillation proximity assay to measure

radioligand binding to immobilized receptors without separation of bound from free ligand.

Methods in molecular biology (Clifton, N.J.) **2012**, *897*, 79-94.

(110)   Michaelis, L.; Menten, M. L.; Johnson, K. A.; Goody, R. S. The original Michaelis constant:

translation of the 1913 Michaelis-Menten paper. *Biochemistry* **2011**, *50*, 8264-8269.

(111)   Khatri, D. K.; Juvekar, A. R. Kinetics of Inhibition of Monoamine Oxidase Using Curcumin

and Ellagic Acid. *Pharmacognosy magazine* **2016**, *12*, S116-120.

(112)   Maldonado-Rojas, W.; Olivero-Verbel, J.; Marrero-Ponce, Y. Computational fishing of

new DNA methyltransferase inhibitors from natural products. *Journal of Molecular Graphics

and Modelling* **2015**, *60*, 43-54.

(113)   Siedlecki, P.; Garcia Boy, R.; Musch, T.; Brueckner, B.; Suhai, S.; Lyko, F.; Zielenkiewicz, P.

Discovery of two novel, small-molecule inhibitors of DNA methylation. *J Med Chem* **2006**, *49*,

678-683.

(114)   Medina-Franco, J. L.; Yoo, J. Docking of a novel DNA methyltransferase inhibitor identified from high-throughput screening: insights to unveil inhibitors in chemical databases. *Molecular diversity* **2013**, *17*, 337-344.

(115)   Singh, N.; Duenas-Gonzalez, A.; Lyko, F.; Medina-Franco, J. L. Molecular modeling and molecular dynamics studies of hydralazine with human DNA methyltransferase 1. *ChemMedChem* **2009**, *4*, 792-799.

(116)   Medina-Franco, J. L.; Caulfield, T. Advances in the computational development of DNA methyltransferase inhibitors. *Drug discovery today* **2011**, *16*, 418-425.

(117)   Datta, J.; Ghoshal, K.; Denny, W. A.; Gamage, S. A.; Brooke, D. G.; Phiasivongsa, P.; Redkar, S.; Jacob, S. T. A new class of quinoline-based DNA hypomethylating agents reactivates tumor suppressor genes by blocking DNA methyltransferase 1 activity and inducing its degradation. *Cancer Res* **2009**, *69*, 4277-4285.

(118)   Yoo, J.; Choi, S.; Medina-Franco, J. L. Molecular modeling studies of the novel inhibitors of DNA methyltransferases SGI-1027 and CBC12: implications for the mechanism of inhibition of DNMTs. *PloS one* **2013**, *8*, e62152.

(119)   Trott, O.; Olson, A. J. AutoDock Vina: Improving the speed and accuracy of docking with a new scoring function, efficient optimization, and multithreading. *Journal of Computational Chemistry* **2010**, *31*, 455-461.

(120)   Rigsby, R. E.; Parker, A. B. Using the PyMOL application to reinforce visual understanding of protein structure. *Biochemistry and molecular biology education : a bimonthly publication of the International Union of Biochemistry and Molecular Biology* **2016**.

(121)   Horiuchi, M.; Ohnishi, K.; Iwase, N.; Nakajima, Y.; Tounai, K.; Yamashita, M.; Yamada, Y. A Novel Isoindoline, Porritoxin Sulfonic Acid, from Alternaria porri and the Structure-phytotoxicity Correlation of Its Related Compounds. *Bioscience, Biotechnology, and Biochemistry* **2003**, *67*, 1580-1583.

(122)   Ayer, W. A.; Miao, S. Secondary metabolites of the aspen fungus Stachybotrys cylindrospora. *Canadian Journal of Chemistry* **1993**, *71*, 487-493.

(123)   Hardcastle, I. R.; Ahmed, S. U.; Atkins, H.; Farnie, G.; Golding, B. T.; Griffin, R. J.; Guyenne, S.; Hutton, C.; Källblad, P.; Kemp, S. J.; Kitching, M. S.; Newell, D. R.; Norbedo, S.; Northen, J. S.; Reid, R. J.; Saravanan, K.; Willems, H. M. G.; Lunec, J. Small-Molecule Inhibitors of the MDM2-p53 Protein–Protein Interaction Based on an Isoindolinone Scaffold. *Journal of Medicinal Chemistry* **2006**, *49*, 6209-6221.

(124)   Alonso, R.; Castedo, L.; Domínguez, D. Synthesis of isoindoloisoquinoline alkaloids. A revision of the structure of (±)-nuevamine. *Tetrahedron Letters* **1985**, *26*, 2925-2928.

(125)   Lindhorst, T.; Bock, H.; Ugi, I. A new class of convertible isocyanides in the Ugi four-component reaction. *Tetrahedron* **1999**, *55*, 7411-7420.

(126)   Billamboz, M.; Bailly, F.; Barreca, M. L.; De Luca, L.; Mouscadet, J.-F.; Calmels, C.; Andréola, M.-L.; Witvrouw, M.; Christ, F.; Debyser, Z.; Cotelle, P. Design, Synthesis, and Biological Evaluation of a Series of 2-Hydroxyisoquinoline-1,3(2H,4H)-diones as Dual Inhibitors of Human Immunodeficiency Virus Type 1 Integrase and the Reverse Transcriptase RNase H Domain. *Journal of Medicinal Chemistry* **2008**, *51*, 7717-7730.

(127)   Karageorge, G. N.; Macor, J. E. Synthesis of novel serotonergics and other N-alkylamines using simple reductive amination using catalytic hydrogenation with Pd/C. *Tetrahedron Letters* **2011**, *52*, 5117-5119.

(128)   Assis, S. P. O.; Araújo, T. G.; Sena, V. L. M.; Catanho, M. T. J. A.; Ramos, M. N.; Srivastava, R. M.; Lima, V. L. M. Synthesis, hypolipidemic, and anti-inflammatory activities of arylphthalimides. *Medicinal Chemistry Research* **2014**, *23*, 708-716.

(129)   Wang, X.; Zhao, G.; Chen, Y.; Xu, X.; Zhong, W.; Wang, L.; Li, S. 1-Oxo-3-substitute-isothiochroman-4-carboxylic acid compounds: synthesis and biological activities of FAS inhibition. *Bioorg Med Chem Lett* **2009**, *19*, 770-772.

(130)   Kim, S. H.; Lee, H. S.; Kim, K. H.; Kim, J. N. An expedient synthesis of poly-substituted 1-arylisoquinolines from δ-ketonitriles via indium-mediated Barbier reaction protocol. *Tetrahedron Letters* **2009**, *50*, 6476-6479.

APPENDIX: SELECTED NMR SPECTRA FOR SYNTHESIZED COMPOUNDS

51

51

52

52

54

56

57

58

59

60

60

61

61

62

63

63

138

64

64

65

65

66

67

67

68

69

70

71